東海大學統計學研究所

碩士論文

指導教授 : 鄭順林 博士

從間斷及連續衰變過程中探究其失效分配

Exploring the Failure Distributions
from Discrete and Continuous Degradation Processes

研究生 : 謝敏雄

中華民國 九十一 年 七 月

Exploring the Failure Distributions from Discrete and Continuous Degradation Processes

Min-Hsiung Hsien

Dept. of Statistics

Tunghai University

Taichung, 40704

Taiwan, R. O. C.

January 21, 2002

Contents

List of Tables

List of Figures

Abstract

It is difficult to asses reliability with traditional life tests for high reliability products that record only time to failure and usually have not many observations. When degradation measures can be taken over time, a relationship between component failure and degradation makes it possible to use degradation models to provide inferences about failure time. In this research, we explore the failure distributions with discrete and continuous degradation process. The mark point process and the Wiener process will be introduced.

For the needs of flexibility of the models to fit the data, three parameter models are considered such as extended generalized gamma (EGENG), exponential Weibull and generalize inverse Gaussian distributions. We employ probability plot and also Anderson-Darling test to identify the proper distribution for the 2024-T351 aluminum data. The data set was produced by the fatigue laboratory in the Department of Mechanical Engineering of National Taiwan University in year 2001. We use bootstrap method to give the confidence intervals of the p-th quantile of the best fitted distribution.

1 Introduction

1.1 Overview

Chapter 1 we give literature review. Chapter 2 introduces discrete degradation process by mark point process and continuous degradation process by Wiener process and some continuous degradation models. About the failure time distribution, we describe the EGENG, GIG and EW distributions. In the last section of this chapter, we

describe some general methods of goodness of fit. Chapter 3 describes the form of estimation of degradation model and failure time distribution. We also describe the bootstrap confidence intervals. Chapter 4 explores failure distributions under degradation models by simulations. Chapter 5 gives a real data example from of the 2024-T351 aluminum data and check by goodness of fit. Chapter 6 includes conclusion and future research.

1.2 Literature Review

1.2.1 Degradation Modeling

Design of high-reliability systems generally requires that the individual system components have extremely high reliability, even after long periods of time. With short product development time, reliability tests must be conducted with severe time constrains. Frequently no or few failures occur during such tests. Thus it is difficult to assess reliability with traditional life tests that record only failure time. Degradation data provide more information from the life test than the failure time data. Lu and Meeker (1993) used a parametric model to describe the degradation measurements. They offered some path models that lead to a closed-form expression for the cdf of the time-to-failure distribution and they also discussed the autocorrelation errors. Meeker and LuValle (1995) described an accelerated life test model based on chemical kinetic models of failure modes. Meeker and Escobar (1998, Ch.13) described the degradation and failure time and showed how to estimate CDF from degradation data. They also used an example to compare degradation analysis with traditional failure-time analysis and presented a simple approximate method for degradation analysis that might be approximated in some applications. In application, Tseng, Hamada and Chiao (1995) used degradation data to improve Fluorescent Lamp reliability.

For some products, however, degradation rates at use conditions are so low that appreciable degradation will not be observed during usual tests. So Meeker and Escobar (1998, Ch.21) described how accelerated degradation tests can be used to assess and improved product reliability and how to analyze accelerated degradation data. Yu and Tseng (1998) described a on line procedure for terminating an accelerated degradation test and used some light-emitting diode (LED) data to demonstrate the proposed procedure. Meeker, Escobar and Lu (1998) also described the accelerated degradation test about that modeling and analysis.

1.2.2 Mark Point Process

Heide-Wendt (1997) described damage processes and resulted in first passage times. He examined a shock model with accumulating damages and the system was suffered from shocks where the shocks happen at time point $(T_n)_{n\geq 1}$ and bring about a gradual damage of the system. Each damage from a shock at random time T_n was described by a scalar non-negative r.v. $X_n, (n = 1, 2, \ldots)$. The damages accumulate so that at any time t the whole damages of the system is given by an r.v. Z_t with $Z_t = \sum_{n=1}^{\infty} I_{(T_n \leq t)} \cdot X_n$. Suppose the existence of a certain wear level h where the system is intact as long as Z_t does not exceed the value h.

The book by Anderson, Borgan, Gill and Keiding (1993) described that a multivariate counting process is a stochastic process which can be thought of as registering the occurrences in time of a number of types of disjoint, discrete events. They supposed that either a filtration is already given, relative to which the processes adapted, or that one constructs the so-called self-exciting filtration generated by the process.

1.2.3 Wiener Process and Inverse Gaussian Distribution

The notion of Brownian motion is applicable in describing the inherent process of many phenomena, particularly in the nature and physical sciences. Because the first passage time of a Brownian motion is distributed as inverse Gaussian (IGAU), it is logical to use it as a lifetime model. The book by Chhikara and Folks (1989) described the inverse Gaussian distribution in detail.

Meeker and Escobar (1998, pp103 - 105) described the properties of IGAU distribution and give a figure of CDF, pdf, quantile and hazard function.

1.2.4 EGENG, EW and GIG Distributions

Many parametric models have been used in the analysis of lifetime data. The most commonly used univariate parametric models in the reliability analysis include the exponential, weibull, gamma, and lognormal distribution. For the needs of flexibility of the models to fit the data, three parameter models are considered such as extended generalized gamma (EGENG), exponential Weibull and generalized inverse Gaussian models.

Shiping Liu (1997) described the generalized gamma model and its maximum likelihood estimation. Early work with the generalized gamma distribution showed that the "natual" parameterization was very unstable. Some authors suggested that hundreds of observation were needed in order to used this distribution. So he developed a reparameterization method that can be used to obtain compuratively stable parameter estimates for the generalized gamma model.

Meeker and Escobar (1998, pp98 - 102) described the properties of GENG distribution and EGENG distribution and give figures of cdf, pdf, quantile and hazard

function.

Mudholkar and Srivastava (1995) described the exponential weibull family. They presented an extension of the weibull family and not only contained distributions with unimodal and bathtub failure rate but also allowed for a broder class of monotone harzard rates and is computationally convenient for censored data.

The book by Brillinger, Gani, Hartigan, Kiefer and Krickeberg (1982) offered the basic properties of the generalized inverse gaussian and given a expressions for moments and cumulants.

Alexandrov and Lacis (2000) described a three-parameter cloud/aerosol size distribution based on the generalized inverse Gaussian density function and explicit expressions for moments, effective radius and variance.

1.2.5 Goodness of Fit

Lawless (1982, Ch. 9) described some general methods of testing hypotheses H_0 : $F(x) = F_0(x)$. The best known procedures for this are the classical goodness of fit tests based on the empirical distribution function (EDF) for continuous unground data and pearson χ^2 or likelihood ratio tests for discrete or grouped data.

Gunes, Dietz, Auclair and Moore (1997) employed Monte Carlo methods to develop and compared modified goodness-of-fit test for the inverse Gaussian model.

Stephens (1974) offered a practical guide to goodness-of-fit tests using statistics based on the empirical distribution function (EDF). Five statistics were examined—those are Kolmogorov statistics D, Cramer-von Mises statistics W^2 , Kuiper statistics V, Watson statistics U^2, Andeson-Darling statistics A^2. Under power comparisons of these statistics, the W^2 and A^2 tests generally have good power against broad ranges

of alternatives.

1.2.6 Real Case Examples

Lu and Meeker (1993) used fatigue-crack-growth data from Bogdanoffand Kozin (1985). There were 21 sample paths (figure 1), one for each of 21 test units and defined a critical crack length of 1.6 inches to be a "failure". They also assumed that testing stopped at 0.12 million cycles. Then, they took the traditional approach of fitting parametric models to the censored time-to-failure data and compared the results with the nonparametric estimate based on the actual failure times of all the 21 units.

Wu and Chen (2001) used the fatigue crack growth of aluminum alloy of the experiment where there were 30 2024-T351 sample paths (figure 2). Since the experimental data that used different fatigue reliability models and then appropriate model to explain the experimental result. It is found that a modified Yang/Manning fatigue reliability model can be adopted for the tested 2024-T351 aluminum alloy specimens. It can then be used as references for the integrity and reliability prediction of aeronautical structures made of 2024-T351 aluminum alloy.

We use these examples to illustrate the procedures we develop in this research.

2 Degradation and Failure Distribution

In this chapter, we describe the discrete degradation by the Marked point process and we also use the result to develop failure time distribution for Gamma and weibull increment. We present the continuous degradation process that relate to failure time distributions. The failure distribution of Inverse Gaussian model can be derived from the Brownian motion as a first passage time distribution we display some properties about the Wiener process. Some failure can be traced to an underlying degradation process which might be linear, convex or concave degradation and some degradation paths that it is possible to write down a closed-form expression. This chapter we also employ some simple degradation paths to derive the failure time distribution. In the lifetime data, the most commonly distributions used to fit the first passtime distribution are location-scale parametric models. For the needs of flexibility of the models to fit the data, we consider the three different failure distributions each having three parameters such as extended generalized gamma, exponential Weibull and generalized inverse Gaussian distributions. In the last section of this chapter, we describe some general methods of goodness of fit.

2.1 Mark Point Process

In connection with the investigation of the reliability of technical systems it is mostly necessary to consider damage processes which are able to occur at these systems. The failure behaviour of technical systems is often influenced by shocks. Wendt (1997) examined a shock model with accumulating damages. Here the system is suffered from shocks where the shocks happened at time points $(T_n)_{n\geq 1}$ and bring about a gradual damage of the system. Each damage from a shock at random time T_n is described by a scalar non-negative r.v. $X_n (n = 1, 2, \ldots)$. The damages accumulate so that at any time t the whole damage of the system is given by an r.v. Z_t with

$Z_t = \sum_{n=1}^{\infty} I_{(T_n \leq t)} X_n$. They supposed the existence of a certain wear level h where the system was intact as long as Z_t does not exceed the value h. The model will be described by marked point processes $\Phi = ((T_n, X_n))_{n \geq 1}$.

System Failure Time of Independent Marking

The following formulation is given by Wendt (1997). Let (X_n^*) be a sequence of i.i.d **X**-valued random elements with distribution G independent of an arbitrary point process (T_n) . $\Phi = ((T_n, X_n))_{n \geq 1}$ is called an independent G-marking of (T_n) if $X_n = X_n^*$ in the case $T_n < \infty$ and else $X_n = x_\infty$. Then the (P, F_t) -compensator of Φ is given as follows

$$\nu(w, t, B) = \nu(w, (0, t] \times B) = \nu(w, t, \mathbf{X}) \cdot \int_B G(\mathrm{d}x) \quad B \in \chi$$

So that the distribution of an independent G-marking is uniquely determined by G and the distribution of (T_n).

1. Let the sequence (T_n) is the jump times and corresponding counting process denoted by N, i.e $N_t = \Phi((0, t] \times \mathbf{X}) = card(n \geq 1 : T_n \leq t)$. Now assumed the existence of the (P, F_t) -stochastic intensity $\tilde{\lambda}$ of the point process (T_n) , i.e. $\nu(w, t, \mathbf{X}) = \int_0^t \tilde{\lambda}(w, s) ds$ where λ is an $\{F_t\}$ -predictable function. A heuristic equation is given as

$$P(\Phi(dt \times \mathbf{X}) > 0 \mid F_t -) = \tilde{\lambda}(w, t) \mathrm{d}t$$

Let $F_t = F_t^N \bigvee \sigma(\Lambda)$ be a history of (T_n) where $F_t^N = \sigma(\Phi((0, t] \times \mathbf{X}))$ is the internal history of (T_n) and Λ -generating F_0 - is non-negative random element of any measurable space. The (P, F_t) -stochastic intensity $\tilde{\lambda}(w, t)$ is assumed to be given by

$$\tilde{\lambda}(w, t) = \Lambda(w) \cdot a(t)$$

Where $a(t)$ denotes a deterministic function. If $a(t)$ is left-continuous with right-hand limits then $\tilde{\lambda}$ will be $\{F_t\}$ - predictable. Usually Λ and $a(t)$ will depend on

unknown parameters. Then obtain for $N_t = card\{n \geq 1 : T_n \leq t\}$ and $j \in Z^+$

$$p(N_t = j) = E\left[\frac{(\Lambda \int_0^t a(s)\mathrm{d}s)^j}{j!} \exp\left(-\Lambda \int_0^t a(s)\mathrm{d}s\right)\right] \tag{2.1.1}$$

2. The system failure time Z_h^* can be written as

$$Z_h^* = inf\left\{t : \sum_{n=0}^{\infty} I_{(T_n \leq t)} \cdot X_n \geq h\right\}$$

And

$$P(Z_h^*) = \sum_{n=0}^{\infty} P(N_t = n) \cdot P(X_0 + X_1 + \ldots + X_n < h | T_n \leq t < T_{n+1}) \tag{2.1.2}$$

And in the special case of independent marking we can get

$$P(Z_h^*) = \sum_{n=0}^{\infty} P(N_t = n) \cdot P(X_0 + X_1 + \ldots + X_n < h) \tag{2.1.3}$$

Now we give three examples for the distributions of Z_h^* by independent marking. The first one was given by Wendt (1997). We use the result to develop failure time distribution for Gamma and weibull increment. First we assume continue random variables X_n where the event $\{X_n = 0\}$ does not occur $(n \geq 1)$.

Example 1. Let X_n have an exponential distribution with parameter p and assume T_n is given as mixed poisson process with $\tilde{\lambda}(w, t) = \Lambda \sim Exp(c)$. i.e. the distribution function of Λ has the density

$$c \cdot \exp^{-c\lambda} I_{(\lambda \geq 0)}$$

And since $\tilde{\lambda}(w,t) = \Lambda(w) \cdot a(t)$ and $n \in Z^+$

$$\begin{aligned} p(N_t = n) &= E\left[\frac{\left(\Lambda \int_0^t a(s)ds\right)^n}{n!} \exp\left(-\Lambda \int_0^t a(s)\mathrm{d}s\right)\right] \\ &= \int_0^\infty \frac{(\lambda t)^n}{n!} \exp^{-\lambda t} \cdot c \exp^{-\lambda c} \mathrm{d}\lambda \\ &= c \cdot \int_0^\infty \frac{\lambda^n t^n}{n!} \exp^{-\lambda(c+t)} \mathrm{d}\lambda \\ &= \frac{c \cdot t^n}{(c+t)^{n+1}} \int_0^\infty \frac{(c+t)^{n+1}}{\Gamma(n+1)} \lambda^n \exp^{-\lambda(c+t)} \mathrm{d}\lambda \\ &= \left(\frac{c}{c+t}\right)\left(\frac{t}{c+t}\right)^n \end{aligned}$$

Let $X_0 = x_0 = const. < h$, then we determine the survival distribution of Z_h^* as follows

$$\begin{aligned} P(Z_h^* > t) &= P(N_t = 0) + \sum_{n=1}^\infty \int_0^{h-x_0} p^n \frac{X^{n-1}}{(n-1)!} \exp^{-px} \mathrm{d}x \cdot \frac{c}{c+t}\left(\frac{t}{c+t}\right)^n \\ &= \frac{c}{c+t} + \frac{c}{c+t} \int_0^{h-x_0} \exp^{-px} \left[\sum_{n=1}^\infty p^n \left(\frac{t}{c+t}\right)^n x^{n-1} \frac{1}{(n-1)!}\right] \mathrm{d}x \\ &= \frac{c}{c+t} + \frac{c}{c+t} \cdot \frac{pt}{c+t} \int_0^{h-x_0} \exp\left[-x\left(p - \frac{pt}{c+t}\right)\right] \mathrm{d}x \\ &= 1 - \frac{c}{c+t} \cdot \exp\left[-(h-x_0)p \cdot \left(\frac{c}{c+t}\right)\right] \end{aligned}$$

The density $f_{Z_h^*}$ of Z_h^* is given, for $t \geq 0$

$$\begin{aligned} f_{Z_h^*}(t) &= \frac{\partial\left[1 - P(Z_h^* > t)\right]}{\partial t} \\ &= \exp\left[-(h-x_0)p \cdot \left(\frac{c}{c+t}\right)\right] \cdot \left[\frac{c}{(c+t)^2} + (h-x_0)\frac{pct}{(c+t)^3}\right] \end{aligned}$$

Example 2. Let X_n have a Gamma distribution with parameters $(\alpha,\ \beta)$. In the case of independent marking, the sum $X_1 + X_2 + \ldots + X_n$ has the density

$$\frac{1}{\Gamma(n\alpha)\beta^{n\alpha}} X^{n\alpha-1} \exp - \left(\frac{X}{\beta}\right) I_{(X>0)}, \quad \alpha > 0,\ \beta > 0$$

Now, we assume $\tilde{\lambda}(w,t) = \Lambda(w) \sim Uni[a,b]$, with $[a,b] \in B^+$ and has the density

$$\frac{1}{b-a} \cdot I_{\lambda \in [a,b]}$$

It follows that

$$\begin{aligned} P(N_t = n) &= \int_b^a \frac{(\lambda t)^n}{n!} \cdot \exp^{-\lambda t} \cdot \frac{1}{b-a} \mathrm{d}\lambda \\ &= \frac{t^{n-1}}{b-a} \int_a^b \frac{\lambda^n}{n!} \mathrm{d} \exp^{-\lambda t} \end{aligned}$$

After repeat partial integration

$$P(N_t = n) = \frac{1}{t(b-a)} \sum_{i=0}^{n} \left(\frac{(at)^i}{i!} \cdot \exp^{-at} - \frac{(bt)^i}{i!} \cdot \exp^{-bt} \right)$$

And we assume $X_0 = x_0 = const < h$.

$$\begin{aligned} P(Z_h^* > t) &= P(N_t = 0) + \sum_{n=1}^{\infty} \int_0^{h-x_0} \frac{1}{\Gamma(n\alpha)\beta^{n\alpha}} X^{n\alpha-1} \exp - \left(\frac{X}{\beta} \right) \cdot P(N_t = n) dX \\ &= P(N_t = 0) + \sum_{n=1}^{\infty} P(N_t = n) \cdot \Phi_{Gam}(h - x_0) \\ &= \frac{1}{t(b-a)} \left[(\exp^{-at} - \exp^{-bt}) \right] \\ &\quad + \sum_{n=1}^{\infty} \sum_{i=0}^{n} \left[\Phi_{Gam}(h - x_0) \cdot \left(\frac{(at)^i}{i!} \cdot \exp^{-at} - \frac{(bt)^i}{i!} \cdot \exp^{-bt} \right) \right] \end{aligned}$$

where $\Phi_{Gam}(\cdot)$ is the distribution function of Gamma.

$$\Phi_{Gam}(h - x_0) = \int_0^{h-x_0} \frac{1}{\Gamma(n\alpha)\beta^{n\alpha}} X^{n\alpha-1} \exp - \left(\frac{X}{\beta} \right) \mathrm{d}X$$

Example 3. Let X_n has a weibull distribution with parameters $(\eta,\ \beta)$. As in Example 1 we assume that $P(N_t = n) = \frac{c}{c+t} \cdot \left(\frac{t}{c+t} \right)^n$ and $X_0 = x_0 = const. < h$. The density of X_n is

$$f(x;\ \eta,\ \beta) = \frac{\beta}{\eta} \left(\frac{x}{\eta} \right)^{\beta-1} \exp \left[- \left(\frac{x}{\eta} \right)^{\beta} \right], \quad x > 0,\ \eta > 0,\ \beta > 0$$

In the case of independent marking,

$$f(x_1, x_2, \ldots, x_n,\ \eta,\ \beta) = \left(\frac{\beta}{\eta}\right)^n \left(\frac{x}{\eta}\right)^{n\beta-n} \exp\ \Big[-\sum_{i=1}^{n} \left(\frac{x_i}{\eta}\right)^{\beta} \Big]$$

$$P(x_1 + x_2 + \ldots + x_n < h - x_0) = \int \ldots \int_{x_1+\ldots+x_n<h-x_0} f(x_1, \ldots, x_n,\ \eta,\ \beta)\ \mathrm{d}x_1 \ldots \mathrm{d}x_n$$

By the form so that we can write

$$\begin{aligned} P(Z_h^* > t) = P(N_t = 0) + \sum_{n=1}^{\infty} \int \ldots \int_{x_1+\ldots+x_n<h-x_0} \left(\frac{\beta}{\eta}\right)^n \left(\frac{x}{\eta}\right)^{n\beta-n} \\ \exp\ \left[-\sum_{i=1}^{n} \left(\frac{x_i}{\eta}\right)^{\beta} \right] \cdot \frac{c}{c+t} \left(\frac{t}{c+t}\right)^n \mathrm{d}x_1 \ldots \mathrm{d}x_n \\ = \frac{c}{c+t} \Bigg\{ 1 + \sum_{n=1}^{\infty} \int \ldots \int_{x_1+\ldots+x_n<h-x_0} \left(\frac{\beta t}{\eta(c+t)}\right)^n \left(\frac{x}{\eta}\right)^{n\beta-n} \\ \exp\ \left[-\sum_{i=1}^{n} \left(\frac{x_i}{\eta}\right)^{\beta} \right] \mathrm{d}x_1 \ldots \mathrm{d}x_n \Bigg\} \end{aligned}$$

where the expression of n integrals can be solved by numerical method.

2.2 Wiener Process and Inverse Gaussian Distribution

This section presents the distribution of Inverse Gaussian (IGAU), which is derived from the Brownian motion as a first passage time distribution. IGAU distribution can be used to describe the failure distribution under conditions that will be described below. The Brownian motion process is sometimes called the Wiener process and there are two parameters, drift ν and diffusion σ^2. Now we describe the Wiener process properties below:

1. The nonoverlay differences of W(t) are independent. That is, when $0 \leq t_1 < t_2 \ldots t_i < t_{i+1} \leq \infty$. $W(t_2) - W(t_1), \ldots, W(t_{i+1}) - W(t_i)$ are independent.

2. $W(t_{i+1}) - W(t_i) \sim N(\nu(t_{i+1} - t_i), \sigma^2(t_{i+1} - t_i))$, for $t_{i+1} > t_i$.

If $\nu = 0$ and $\sigma = 1$, the process is called the standard Brownian motion B_t. The form of Wiener process can be obtained as $W(t) = \nu t + \sigma B_t$.

When the process reaches a critical quality, the first passage time T follows distribution of IG (Chhikara and Folks, 1989, Chapter 3). Now we describe the arguments to obtain the relationship between (ν, σ^2) and (μ, ϕ) where (μ, ϕ) are the parameters of IG. Let $Q(t|s_0)$ be the quality of detected object in the stress s_0 which may be temperature or voltage or others. Let D_Q denote the lower critical value of the quality. When Q reaches D_Q, the product could be claimed as failed. Suppose we can find a transformable function φ by character of product, such that $\varphi(Q(t|s_0))$ satisfy the Wiener process with drift ν and σ^2. So the first passage time T is defined as $T = \inf\{t|\varphi\left(Q(t|s_0)\right) \leq \varphi\left(D_Q\right)\}$.

The form of CDF of IG distribution is:

$$F(t;\mu,\phi) = \Phi\left[\sqrt{\frac{\mu\phi}{t}}(\frac{t}{\mu} - 1)\right] + e^{2\phi}\Phi\left[-\sqrt{\frac{\mu\phi}{t}}(\frac{t}{\mu} + 1)\right]$$

where $\Phi(\cdot)$ is the CDF of standard normal.

The pdf of IG distribution is:

$$f(t;\mu,\phi) = \sqrt{\frac{\mu\phi}{2\pi}}t^{-\frac{3}{2}}\exp\left[-\frac{\phi(t-\mu)^2}{2\mu t}\right], \quad for\ all \ \ t > 0.$$

where $\mu = \varphi(D_Q)/\nu$ and $\phi = \nu\varphi(D_Q)/\sigma^2$.

The reliability function of IGAU distribution is:

$$R(t) = 1 - F(t) = \Phi\left[\sqrt{\frac{\lambda}{t}}(1-\frac{t}{\mu})\right] - \exp^{(2\lambda/\mu)}\Phi\left[-\sqrt{\frac{\lambda}{t}}(1+\frac{t}{\mu})\right]$$

The character of product $Q(t|s_0)$ often is not expressed in numeric form or the prim-

itive data are hard to analysis. It is important for analysis to identify the dataset which determined by a professional with specialized knowledge in order to obtain φ.

Suppose $Q(t|s)$ be the quality of product in the stress s, denote ξ as a transformation between s_0 and s. Consider:

$$Q(t|s) = Q(e^{A\xi}t|s_0)$$

, hence

$$\begin{aligned}\varphi(Q(t|s)) &= \nu(e^{A\xi}t) + \sigma B_{e^{A\xi}t} \\ &= (e^{A\xi}\nu)t + (e^{\frac{A\xi}{2}}\sigma)B_t\end{aligned}$$

where $A > 0$, then $\varphi((Q(t|s))$ be a Wiener process with drift $e^{A\xi}\nu$ and diffusion $e^{A\xi}\sigma^2$. As defined above we have random variates following $IG(\mu(\xi), \phi(\xi))$ at the stress s, where

$$\begin{aligned}\mu(\xi) &= \frac{\varphi(D_Q)}{e^{A\xi}\nu} = \frac{\mu}{e^{A\xi}} \\ \phi(\xi) &= \frac{e^{A\xi}\nu\varphi(D_Q)}{e^{A\xi}\sigma^2} = \phi\end{aligned}$$

Take logarithm for first equation, and consider $\beta_0 = \ln(\mu)$; $\beta_1 = -A$, then we can obtain below:

$$\ln \mu(\xi) = \beta_0 + \beta_1\xi$$

By results above, we assume the criteria below:

1. The failure time of the every experiment units follow IG distribution with mean μ and shape ϕ.

2. There is a relation between the mean μ and the transformable function ξ such that

$$\ln \mu(\xi) = \beta_0 + \beta_1\xi.$$

3. The shape ϕ is a constant.

The IGAU distribution has some useful properties, including the following (Chhikara and Folks,1989):

1. The family of IGAU distributions is closed under a change of scale. that is, for any IGAU random variable T and any number $c > 0$, cT is IGAU distributed with parameters $c\mu$ and $c\lambda$.

2. For a linear combination $\sum c_i T_i$, $c_i > 0$, of IGAU random variables has an IGAU distribution with parameters $\mu = \sum c_i \mu_i$ and $\lambda = \xi(\sum c_i \mu_i)^2$ if $\lambda/(\mu_i^2 c_i) = \xi \; \forall i$.

3. The family of inverse Gaussian distributions is complete.

4. The sample mean $\bar{X}$ from a sample of iid IGAU random variables has an IGAU distribution.

2.3 General Continuous Degradation Path Model

Following the description of Meeker and Escobar (1998, Ch. 11). Let the notation by the actual degradation path of a particular unit over time be denoted $D(t)$, $t > 0$. In applications, values of $D(t)$ are sampled at discrete points in time $t_1, t_2, t_3, \ldots$. The observed sample degradation y_{ij} of unit i at time t_{ij} is

$$y_{ij} = D_{ij} + \varepsilon_{ij}, \; i = 1, \ldots, n, \; j = 1, \ldots, m_i, \tag{2.3.1}$$

where $D_{ij} = D(t_{ij}, \beta_{1i}, \ldots, \beta_{ki})$ is the actual path of the unit i at time t_{ij} (the times need not be the same for all units) and $\varepsilon_{ij} \sim N(0, \sigma_\varepsilon)$ is a residual deviation for unit i at time t_{ij}. The total number of inspections on unit i is denoted by m_i. Time t could be real-time, operating time, or some other appropriate measure of use like

miles for automobile tires or cycles in fatigue tests. The parameters $\beta_1, \ldots, \beta_k$ could be modeled as common across all units.

Degradation model choice requires not only specification of the form of the $D(t_{ij})$ function, but also specification of which of the $\beta_1, \ldots, \beta_k$ are random (differing from unit to unit) and which are fixed (common to all units). For some cases deviations ε_{ij} can be ignored. Because in many practical applications involving inference on the degradation of units from a population or process, the correlation is weak and dominated by unit-to-unit variability in the $\beta_1, \ldots, \beta_k$ values. But in situations where autocorrelation cannot be ignored, one can use time series model for the residual term.

2.3.1 Continuous Degradation Models

Most failures can be traced to an underlying degradation process, and degradation paths might be linear, convex or concave degradations (e.g. Figure 3). In some applications, there may be more than one degradation variable or more than one underlying degradation process. Usually models start with a deterministic description of the degradation process — often in the form of a differential equation or system of differential equations. Then randomness can be introduced, as appropriate, using probability distributions to describe variability in initial conditions and model parameters like rate constants or material properties. The following three cases, we describe some general degradation path models.

Case 1. *Linear Degradation.*
Linear degradation arises in some simple wear processes (e.g., automobile tire wear). If $D(t)$ is the amount of automobile tire tread wear at time t and wear rate is $dD(t)/dt = C$, then

$$D(t) = D(0) + C \times t$$

where the parameters $D(0)$ and C could be taken as constant for individual units, but random from unit-to-unit (Meeker and Escobar, 1998, Ch.13)

Tseng, Hamada and Chiao (1995) use degradation model to improve fluorescent lamp reliability. The model for luminous flux $D(t)$ at time t is

$$\ln D(t) = \theta + \lambda t$$

where the parameters θ and λ are the initial luminous flux and rate of degradation, and the fluorescent lamp industry defined the lamp failure when a lamp's luminous flux $D(t)$ falls below 60% of its luminous flux after 100 hours of use.

Case 2. *Convex Degradation.*
Let $a(t)$ denote the size of a crack at time t. A simple deterministic Pairs-rule model

$$\frac{da(t)}{dt} = C \times [\triangle K(a)]^m$$

provides a useful model for cracks within a certain size range, where C and m are material properties and $\triangle K(a)$ is a function of crack size a (Meeker and Escobar 1998, Ch. 13). For example, to model a two-dimensional edge-crack in a plate with a crack that is small relative to the width of the plate, $\triangle K(a) = \text{Stress}\ \sqrt{\pi a}$. The deterministic solution to the resulting differential equation is

$$a(t) = \begin{cases} \left\{[a(0)]^{1-m/2} + (1-m/2) \times C \times (Stress\sqrt{\pi})^m \times t\right\}^{2/(2-m)} & m \neq 2 \\ a(0) \times \exp\left\{C \times (Stress\sqrt{\pi})^2 \times t\right\} & m = 2 \end{cases}$$

Case 3. *Concave Degradation*

$$D(t_{ij}) = \beta_0 + \beta_{i1} \times \sqrt{t_{ij}}.$$

Figure 14 display the simple concave degradation.

2.3.2 Model Relating to Continuous Degradation and Failure Distribution

A fixed value of D_f will be used to denote the critical level for the degradation path above (or below) which failure is assumed to have occurred. The failure time T is defined as the time when the actual path $D(t)$ crosses the critical degradation level D_f and use t_c denote the planned stopping time in the experiment which is called censor time. Since a specific degradation model $D(t)$ and specific fail level D_f can define a failure-time distribution. In general, this distribution can be written as a function of the degradation model parameters. Suppose that a unit fails at time t if the degradation level first reaches D_f at time t. Then

$$P(T \leq t) = F(t) = F(t;\ \theta_\beta) = P\left(\ D(t, \beta_1, \beta_2, \ldots, \beta_k) \geq D_f\ \right) \tag{2.3.3}$$

In some simple degradation models, it is possible to write down a closed-form expression for $F(t)$ by the (2.3.3) and the failure distribution of T depends on the parameters $(\beta_1, \beta_2, \ldots, \beta_k)$, which are the degradation path parameters.

Here we display some simple path models which $F(t)$ can be expressed as a function of the basic path parameters in a closed form. The following example 1 to example 3 are given by Meeker, Luvalle and Michael (1995).

Example 1. Suppose the degradation path of a particular unit is given by

$$D(t) = \beta_1 + \beta_2 t$$

where β_1 is fixed and β_2 varies from unit to unit according to a $LOGNOR(\mu, \sigma)$ distribution. The parameter β_1 represents the common initial amount of degradation of all the test units at time 0 and β_2 represents the degradation rate, random from

unit to unit. Then

$$F_T(t;\beta_1,\mu,\sigma) = \Pr(D(t) > D_f)$$
$$= \Phi_{nor}\left[\frac{\log t - [\log(D_f-\beta_1)-\mu]}{\sigma}\right], \qquad t>0.$$

This shows that T has a lognormal distribution with parameters that depend on the path parameters (β_1,μ,σ) and D_f. So that path model can be a close form for failure-time distribution.

Example 2. With *example 1*, let β_1 has a Normal distribution with parameters (μ_1,σ_1) and β_2 also has a Normal distribution with parameters (μ_2,σ_2). $\beta_1>0,\ \beta_2>0,\ \beta_1$ and β_2 are independent. In practice, both $P(\beta_1<0)$ and $P(\beta_2\le 0)$ would be negligible. Then, $D(t)\sim N(\mu_1+\mu_2 t,\ \sigma_1^2+\sigma_2^2t^2)$ and the density is

$$F_T(t) = \Pr(D(t) > D_f)$$
$$\approx 1-\Phi_{nor}\left[\frac{D_f-(\mu_1+\mu_2 t)}{\sqrt{\sigma_1^2+\sigma_2^2t^2}}\right]$$
$$\approx 1-\Phi_{nor}\left[\frac{t-(D_f-\mu_1)/\mu_2}{\sqrt{(\sigma_1^2+\sigma_2^2t^2)/\mu_2^2}}\right], \qquad t>0.$$

Example 3. Similarly, in the *Example 1.* If β_1 is fixed and β_2 follows a exponential distribution with parameter θ; that is,

$$G_{\beta_2}(y) = 1-\exp(-y/\theta), \quad y>0,\ \theta>0$$

For the critical level D_f, $D_f=\beta_1+\beta_2\cdot T$ and $T=(D_f-\beta_1)/\beta_2$. The distribution function of T is

$$F_T(t) = P(T\le t) = P(\frac{D_f-\beta_1}{\beta_2}\le t) = P(\beta_2\ge\frac{D_f-\beta_1}{t})$$
$$= 1-P(\beta_2\le\frac{D_f-\beta_1}{t}) = exp\Big[-(\frac{D_f-\beta_1}{\theta t})\Big], \quad t>0.$$

So the distribution $F_T(t)$ depends on $D_f,\ \beta_1,\ \theta$, and distribution parameter θ. The distribution of T is known as the reciprocal exponential because $1/T$ follows a exponential distribution.

Example 4. Suppose that a unit path is given by

$$D(t) = \phi_1 + \psi \cdot \exp(\phi_2 t),\ \phi_2 > 0$$

where $\phi = (\phi_1, \phi_2)'$ are fixed and ψ has a Weibull distribution with parameters (η, β). In particular, $log(\psi) \sim SEV(\mu, \sigma)$, where $\sigma = 1/\beta$ and $\mu = log(\eta)$. So

$$F_\psi(x) = \Phi_{sev}\left[\frac{\log(x) - \mu}{\sigma}\right]$$

where $\Phi_{sev}(z) = 1 - exp\Big[-exp(z)\Big]$. Then T can be expressed as follows:

$$T = \frac{\log(D_f - \phi_1) - \log\psi}{\phi_2}$$

The distribution function of T for the critical level D_f is

$$\begin{aligned}
F_T(t) = P(T \le t) &= P\left[\ \frac{\log(D_f - \phi_1) - \log(\psi)}{\phi_2} \le t\ \right] \\
&= P\left[\ -\log(\psi) \le t\phi_2 - \log(D_f - \phi_1)\ \right] \\
&= P\left[\ \log(\psi) \ge \log(D_f - \phi_1) - t\phi_2\ \right] \\
&= 1 - \Phi_{sev}\left[\ \frac{\log(D_f - \phi_1) - t\phi_2 - \mu}{\sigma}\ \right] \\
&= 1 - \Phi_{sev}\left\{\ \frac{-\Big[t - \Big(\log(D_f - \phi_1) - \mu\Big)\Big/\phi_2\Big]}{\sigma/\phi_2}\ \right\}
\end{aligned}$$

The possibility of negative T arises because, if $\psi > D_f - \phi_1,\ \psi + \phi > D_f$, then $D(0) > D_f$ which $D(t)$ crosses D_f before time 0.

2.4 Failure Distributions

Many parametric models have been used in the analysis of lifetime data. The most commonly used location-scale parametric models in the reliability analysis include exponential, weibull, normal, and lognormal distribution. For the needs of flexibility of the models to fit the data, we consider three parameter models such as extend generalized gamma, exponential Weibull and generalized inverse Gaussian distributions. This section we will describe the properties of extend generalized gamma, exponential Weibull and generalized inverse Gaussian distributions.

2.4.1 Generalized Gamma Distribution

The Generalized Gamma Model

Meeker and Escobar (1998, Ch.5) described that generalized gamma distribution contains the exponential, gamma, weibull, and lognormal distributions as special cases. When T has a generalized gamma distribution we indicate that by $T \sim GENG(\theta, \beta, k)$.

The cdf and pdf for the generalized gamma distribution are

$$F(t;\theta,\beta,k) = \Gamma_I\left[\left(\frac{t}{\theta}\right)^{\beta};k\right],$$

$$f(t;\theta,\beta,k) = \frac{\beta}{\Gamma(k)\theta}\left(\frac{t}{\theta}\right)^{k\theta-1}\exp\left[-\left(\frac{t}{\theta}\right)^{\beta}\right],\ t>0.$$

Where $\theta > 0$ is a scale parameter, $\beta > 0$ and $k > 0$ are shape parameters, and $\Gamma_I(\nu, k)$ is the incomplete gamma distribution and is given as follows

$$\Gamma_I(\nu,k) = \frac{\int_0^{\nu} x^{k-1}\exp(-x)dx}{\Gamma(k)},\ \nu>0.$$

Generalized Gamma Moments and Quantiles

For $m \geq 0,\ E(T^m) = \theta^m \cdot \Gamma(m/\beta + k)/\Gamma(k)$. From this

$$E(T) = \frac{\theta\Gamma(1/\beta + k)}{\Gamma(k)}\ ,$$
$$Var(T) = \theta^2[\frac{\Gamma(2/\beta + k)}{\Gamma(k)} - \frac{\Gamma^2(1/\beta + k)}{\Gamma^2(k)}]\ ,$$
$$t_p = \theta[\Gamma^{-}1_I(p;k)]^{1/\beta}\ .$$

Special Cases of the Generalized Gamma Distribution

Here we show the relationship between the $GENG(\theta, \beta, k)$ and the well-known distributions that special cases:

1. When $\beta = 1,\ T \sim GAM(\theta, k)$.

2. When $k = 1,\ T \sim WEI(\theta, \beta)$.

3. When $(\beta, k) = (1, 1),\ T \sim EXP(\theta)$.

4. As $k \to \infty,\ T \sim LOGNOR(\log(\theta) + \log(k)/\beta, 1/(\beta\sqrt{k}))$.

Generalized Gamma Reparameterization for Numerical Calculation

The parameterization in terms of (θ, β, k) is generally numerically unstable for fitting the distribution to data. Farewell and Prentice (1977) recommend the alternative parameterization

$$\mu = \log(\theta) + \frac{1}{\beta}\log(\lambda^{-2}), \quad \sigma = \frac{1}{\beta\sqrt{k}}, \quad \lambda = \frac{1}{\sqrt{k}}.$$

This parameterization is numerically stable if there is little or no censoring. By considering the transformation of $w = [\log(t) - \mu]/\sigma$ the pdf, cdf and p quantile of T

can be written

$$\begin{aligned} F(t;\theta,\beta,k) &= \Gamma_I[\lambda^{-2}\exp(\lambda w);\lambda^{-2}] \\ &= \Phi_{lg}[\lambda w + \log(\lambda^{-2});\lambda^{-2}] \ , \\ f(t;\theta,\beta,k) &= \frac{\lambda}{\sigma t}\phi_{lg}[\lambda w + \log(\lambda^{-2});\lambda^{-2}],\ t>0 \\ t_p &= \exp\{\mu + \frac{\sigma}{\lambda}\log[\lambda^2\Gamma_I^{-1}(p;\frac{1}{\lambda^2})]\} \ , \end{aligned}$$

where $-\infty < \mu < \infty,\ \sigma > 0,\ and\ \lambda > 0$

and

$$\begin{aligned} \Phi_{lg}(s;k) &= \Gamma_I[exp(s);k] \ , \\ \phi_{lg}(s;k) &= \frac{1}{\Gamma(k)}\exp[ks - \exp(s)] \ , \end{aligned}$$

are the cdf and pdf for the standardized loggamma variable $S = \log(T/\theta) = \log(T) - \mu,\ T \sim GAM(\theta,k)$ (Meeker and Escobar, 1998).

Extended Generalized Gamma Distribution

Using the alternative stable parameterization and allowing λ to become negative, Meeker and Escobar (1998, pp 101-102) called it the extended generalized gamma distribution, which enlarges the family to include other distributions as special cases. Let T have an $EGENG(\mu,\sigma,\lambda)$ distribution, the form of the cdf and pdf are given as follows.

$$F(t;\mu,\sigma,\lambda) = \begin{cases} \Phi_{lg}[\lambda w + \log(\lambda^{-2});\lambda^{-2}] & \text{if } \lambda > 0, \\ \Phi_{nor}(w) & \text{if } \lambda = 0, \\ 1 - \Phi_{lg}[\lambda w + \log(\lambda^{-2});\lambda^{-2}] & \text{if } \lambda < 0. \end{cases} \tag{2.4.1}$$

$$f(t;\mu,\sigma,\lambda) = \begin{cases} \frac{|\lambda|}{\sigma t}\phi_{lg}[\lambda w + \log\lambda^{-2};\lambda^{-2}] & \text{if } \lambda \neq 0, \\ \frac{1}{\sigma t}\phi_{nor}(w) & \text{if } \lambda = 0, \end{cases} \tag{2.4.2}$$

where $t > 0,\ w = [\log(t) - \mu]/\sigma,\ -\infty < \mu < \infty,\ and\ \sigma > 0,\ \Phi_{lg},\ \phi_{lg}$ as defined in previous distribution.

And the form of the p quantile

$$t_p = \exp[\mu + \sigma w(p; \lambda)],$$

where $w(p; \lambda)$ is the p quantile of $[\log(T) - \mu]/\sigma$ given by

$$w(p;\lambda) = \begin{cases} (1/\lambda)\log[\lambda^2\Gamma_I^{-1}(p;\lambda^{-2})] & \text{if } \lambda > 0, \\ \phi_{nor}^{-1}(p) & \text{if } \lambda = 0, \\ (1/\lambda)\log[\lambda^2\Gamma_I^{-1}(1-p;\lambda^{-2})] & \text{if } \lambda < 0. \end{cases}$$

Some properties of the $EGENG$ distribution

• If $T \sim EGENG(\mu, \sigma, \lambda)\ and\ c > 0\ \Rightarrow cT \sim EGENG(\mu + \log(c), \sigma, \lambda)$.

• $\exp(\mu)$ is a scale parameter and σ and λ are shape parameters.

• If λ is fixed, the $EGENG$ distribution is a log-location-scale distribution.

Special Case of the EGENG Distribution

1. If $\lambda > 0$, then $EGENG(\mu, \sigma, \lambda) = GENG(\mu, \sigma, \lambda)$.

2. If $\lambda = 1,\ T \sim WEIB(\mu, \sigma)$.

3. If $\lambda = 0,\ T \sim LOGNOR(\mu, \sigma)$.

4. If $\lambda = -1,\ 1/T \sim WEIB(-\mu, \sigma)$.

5. If $\lambda = \sigma,\ T \sim GAM(\theta, k)$, where $\theta = \lambda^2 \exp(\mu)$ and $k = \lambda^{-2}$.

6. If $\lambda = \sigma = 1,\ T \sim EXP(\theta)$, where $\theta = \exp(\mu)$.

2.4.2 Exponential Weibull Family

The Weibull distribution is commonly used for analyzing lifetime data. The Weibull family accommodates increasing and decreasing failure rate. But it is not allow non-monotone failure rates, which are common in practice and on occasion. The most

common nonmonotone failure rate situation involves bathtub shapes. The exponential weibull family not only contains distribution with unimodal and bathtub failure rates (Figure 4) but also allows for a broader class of monotone hazard rates and is computationally convenient for censor data (Mudholkar and Srivastava, 1995).

The form of the cdf, pdf, p quantile and hazard function are

$$
\begin{aligned}
F(t;\alpha,\theta,\sigma) &= [1-\exp(-(\frac{t}{\sigma}))^{\alpha}]^{\theta}, \\
f(t;\alpha,\theta,\sigma) &= \frac{\alpha\theta}{\sigma}[1-\exp(-(t/\sigma)^{\alpha})]^{\theta-1}\times\exp(-(t/\sigma)^{\alpha})(t/\sigma)^{\alpha-1}, \\
t_p &= \sigma[-\log(1-p^{1/\theta})]^{1/\alpha}, \\
h(t;\alpha,\theta,\sigma) &= \frac{\alpha\theta[1-\exp(-(t/\sigma)^{\alpha})]^{\theta-1}\exp(-(t/\sigma)^{\alpha})(t/\sigma)^{\alpha-1}}{\sigma[1-(1-\exp(-(t\sigma)^{\alpha}))^{\theta}]},
\end{aligned}
$$

where $\alpha>0,\ \theta>0,\ \sigma>0$ and $t>0$.

Note when $\theta=1$, the exponential weibull family corresponds to the weibull distribution.

2.4.3 Generalized Inverse Gaussian

Let T has a generalized inverse Gaussian which $T\sim GIG(t;\lambda,\chi,\psi)$ (Jorgensen, 1982). The probability density function of the generalized inverse Gaussian is

$$
\frac{(\psi/\chi)^{\lambda/2}}{2K_{\lambda}(\sqrt{\chi\psi})}t^{\lambda-1}\exp[-1/2(\chi t^{-1}+\psi t)], \qquad t>0, \tag{2.4.3}
$$

where K_{λ} is the modified Bessel function of the third kind of order λ.

Special cases of the Generalized Inverse Gaussian

- If $\chi=0,\ \lambda>0, T\sim$ the Gamma distribution.

- If $\psi = 0,\ \lambda < 0, T \sim$ the inverted Gamma distribution.
- If $\lambda = -\frac{1}{2}, T \sim$ the inverse Gaussian distribution.
- If $\lambda = \frac{1}{2}, T \sim$ the inverted inverse Gaussian distribution.
- If $\lambda = 0, T \sim$ the hyperbola distribution

Basic properties of the Generalized Inverse Gaussian

The domain of variation for the parameters is given by

$$\lambda \in \mathbf{R}, \qquad (\chi, \psi) \in \mathbf{\Theta}_\lambda.$$

Where

$$\mathbf{\Theta}_\lambda = \begin{cases} \{(\chi,\psi) :\ \chi \geq 0,\ \psi > 0\} & \text{if } \lambda > 0, \\ \{(\chi,\psi) :\ \chi > 0,\ \psi > 0\} & \text{if } \lambda = 0, \\ \{(\chi,\psi) :\ \chi > 0,\ \psi \geq 0\} & \text{if } \lambda < 0. \end{cases}$$

In the case $\chi = 0$ and $\psi = 0$ the norming constant in (2.4.3) is found using (A.2) and the asymptotic relation (A.8).

Now we introduce the parameters w and η which are given by

$$w = \sqrt{\chi\psi}, \qquad \eta = \sqrt{\frac{\chi}{\psi}}.$$

Thus $w > 0$ denotes the case where both χ and ψ are positive and where the density(2.4.1) takes the alternatives form

$$\frac{\eta^{-\lambda}}{2K_\lambda(w)} t^{\lambda-1} \exp -\frac{w}{2}(\eta t^{-1} + \eta^{-1} t). \tag{2.4.4}$$

If the random variable T has distribution $GIG(\lambda, \chi, \psi)$, let $Y = T^{-1}$ and by the

transformation and (2.4.3). We can derive that

$$\begin{aligned} f(y;\lambda,\chi,\psi) &= \frac{(\psi/\chi)^{\lambda/2}}{2K_\lambda(\sqrt{\chi\psi})}(1/y)^{\lambda-1}\exp\left[-\frac{1}{2}(\chi y+\psi/y)\right](1/y)^2 \\ &= \frac{(\chi/\psi)^{-\lambda/2}}{2K_\lambda(\sqrt{\chi\psi})}y^{-\lambda-1}\exp\left[-\frac{1}{2}(\chi y+\psi/y)\right] \\ &= \frac{(\chi/\psi)^{-\lambda/2}}{2K_{-\lambda}(\sqrt{\chi\psi})}y^{-\lambda-1}\exp\left[-\frac{1}{2}(\chi y+\psi/y)\right], \quad \text{(By the A.2).} \end{aligned}$$

So we can get that $T^{-1} \sim GIG(-\lambda,\psi,\chi)$.

Similarly if $c>0$ we can also derive that

$$cT \sim GIG(\lambda, c\chi, c^{-1}\psi).$$

The density (2.4.1) is unimodal and the mode point is given by

$$m = \begin{cases} \frac{\lambda-1+\sqrt{(\lambda-1)^2+\chi\psi}}{\psi} & \text{if } \psi>0, \\ \frac{\chi}{2(1-\lambda)} & \text{if } \psi=0. \end{cases}$$

Some convolution formulas from the density (2.4.3) :

$$\begin{aligned} GIG(-1/2,\chi_1,\psi)+GIG(-1/2,\chi_2,\psi) &= GIG(-1/2,(\sqrt{\chi_1}+\sqrt{\chi_2})^2,\psi), \\ GIG(-\lambda,\chi,\psi)+GIG(\lambda,0,\psi) &= GIG(\lambda,\chi,\psi) \qquad (\lambda>0), \\ GIG(-1/2,\chi_1,\psi)+GIG(1/2,\chi_2,\psi) &= GIG(1/2,(\sqrt{\chi_1}+\sqrt{\chi_2})^2,\psi). \end{aligned}$$

Moments of the Generalized Inverse Gaussian

Let T be a random variables with distribution (2.4.3). The Moments $u_k^{'} = E(T^k)$ are given by

$$u_k^{'} = \frac{K_{\lambda+k}(w)}{K_\lambda(w)}\eta^k, \qquad k \in R. \tag{2.4.5}$$

In the case $\chi=0, \quad \lambda>0$, we have by (A.8)

$$u_k^{'} = \begin{cases} \frac{\Gamma(\lambda+k)}{\Gamma(\lambda)}(\frac{2}{\psi})^k & \text{if } k>-\lambda, \\ \infty & \text{if } k\le-\lambda. \end{cases} \tag{2.4.6}$$

And in the case $\psi = 0, \quad \lambda < 0$, we have by (A.8) and (A.2)

$$u_k^{'} = \begin{cases} \frac{\Gamma(-\lambda-k)}{\Gamma(-\lambda)}(\frac{\chi}{2})^k & \text{if } k < -\lambda, \\ \infty & \text{if } k \geq -\lambda. \end{cases} \tag{2.4.7}$$

Let the formulas are simplified by using the functions R_λ and D_λ defined by

$$R_\lambda(w) = \frac{K_{\lambda+1}(w)}{K_\lambda(w)},$$
$$D_\lambda(w) = \frac{K_{\lambda+1}(w)K_{\lambda-1}(w)}{K_\lambda^2(w)}.$$

From (2.4.5), (2.4.6) and (2.4.7), we have

$$E(T) = \begin{cases} R_\lambda(w)\eta & \text{if } w > 0, \\ \frac{2\lambda}{\psi} & \text{if } \chi = 0, \quad \lambda > 0, \\ \frac{\chi}{2(-\lambda-1)} & \text{if } \psi = 0, \quad \lambda < -1, \\ \infty & \text{if } \psi = 0, \quad -1 \leq \lambda < 0. \end{cases} \tag{2.4.8}$$

And

$$E(T^{-1}) = \begin{cases} R_{-\lambda}(w)\eta^{-1} & \text{if } w > 0, \\ \frac{\psi}{2(\lambda-1)} & \text{if } \chi = 0, \quad \lambda > 1, \\ \infty & \text{if } \chi = 0, \quad 0 < \lambda \leq 1, \\ \frac{-2\lambda}{\chi} & \text{if } \psi, \quad \lambda < 0. \end{cases} \tag{2.4.9}$$

From the (2.4.3) that the variance of the distribution is given by

$$V(T) = \eta^2(\frac{K_{\lambda+2}(w)}{K_\lambda(w)} - \frac{K_{\lambda+1}^2(w)}{K_\lambda^2(w)}). \tag{2.4.10}$$

Using the definitions of R_λ and D_λ, we have

$$V(T) = \eta^2 R_\lambda^2(w)(D_{\lambda+1}(w) - 1). \tag{2.4.11}$$

2.5 Goodness-of-Fit

Some general methods of testing fit

Some general methods of testing hypotheses $H_0 : \ F(x) = F_0(x)$, where $F_0(x)$ is a specified family of models. The best known procedures for this are the classical goodness of fit tests based on the empirical distribution function (EDF) for continuous ungrouped data and the pearson χ^2 or likelihood ratio tests for discrete or grouped data. The following are given by Lawless (1982, ch 9).

2.5.1 Tests of Fit Based on Grouped Data

Uncensored grouped data. With grouped uncensored data, tests of fit can be based on the multinomial model, the best-known procedures being the classical Pearson (χ^2) test and the likelihood ratio test. Let the observations can fall into $k+1$ classes $I_j = [a_j - 1, a_j),\ j = 1, 2, \ldots, k+1$, with $a_0 = 0,\ a_{k+1} = \infty,$ and $a_k = T$ as an upper limit of observations. Let d_j represent the number of observations in a random sample of size n that fall into I_j, let p_j be the probability of an observation falling into I_j, and consider the hypothesis

$$H_0 : p_j = p_{j0}, \qquad j = 1, 2, \ldots, k+1,$$

where the p_{j0} are specified but may involve unknown parameters. Let $\tilde{p}_{j0}$ be the m.l.e. of p_j under H_0, or some other asymptotically fully efficient estimator, and let $e_j = n\tilde{p}_{j0}$. The Pearson statistic for testing H_0 is

$$X^2 = \sum_{j=1}^{k+1} \frac{(d_j - e_j)^2}{e_j}.$$

When the p_{jo} are known constants, $e_j = np_{j0}$ and the limiting distribution of X^2 is $\chi^2_{(k)}$. When the P_{jo} involve s unknown parameters, the limiting distribution is $\chi^2_{(k-s)}$.

The likelihood ratio test is an alternative test of H_0. The likelihood function for $p_1, p_2, \ldots, p_k$ is multinomial,

$$L(p_1, p_2, \ldots, p_k) \propto \prod_{j=1}^{k+1} p_j^{d_j}.$$

where $p_{k+1} = 1 - p_1 - p_2 - \ldots - p_k$. The likelihood ratio statistic for testing H_0 against the alternative that the p_j's satisfy only $p_j \geq 0$, $\sum p_j = 1$, is easily seen to be

$$\begin{aligned}\Lambda &= 2\sum_{j=1}^{k=1} d_j \log(\frac{d_j}{n}) - 2\sum_{j=1}^{k+1} d_j \log \tilde{p}_{j0} \\ &= 2\sum_{j=1}^{k+1} d_j \log(\frac{d_j}{e_j}).\end{aligned}$$

The limiting distribution of Λ under H_0 is $\chi^2_{(k-s)}$ when the p_{j0}'s involve s unknown parameters. When testing a hypothesis $H_0 : F(t) = F_0(t)$ about a continuous model, the X^2 and likelihood ratio tests have the advantages of easy computation and the ability to accommodate unknown parameters. They are less powerful than based on the EDF in some situation, but are not appreciably less so in most situations of practical importance, provided that intervals are chosen appropriately. In general, the X^2 and likelihood ratio statistics provide good omnibus tests of fit.

2.5.2 Tests Based on the EDF

Case 1: *Uncensored data.* Let T be a random variables with continuous distribution function (d.f.) $F(t)$ and the hypotheses $H_0 : F(t) = F_0(t)$, where $F_0(t)$ is some family of d.f.'s and is completely specified (i.e. does not contain any unknown parameters). Give a random sample $t_1, t_2, \ldots, t_n$ from the distribution for T,

$$\tilde{F}_n(t) = \frac{Number\ of\ t_i's \leq t}{n}$$

is the empirical d.f. (EDF) for the sample. A great many statistics that have been proposed for testing H_0 are based on the notion of measuring "distance" between $\tilde{F}_n(t)$ and $F_0(t)$ (e.g. Stephens, 1974). Two statistics are discussed here, large values of the statistics are indicative of evidence against the hypothesized model. The statistics are

1. The Kolmogorov-Smirnov statistics:

$$\begin{aligned} D_n^+ &= \sup_t [\tilde{F}_n(t) - F_0(t)], \\ D_n^- &= \sup_t [F_0(t) - \tilde{F}_n(t)], \\ D_n &= \sup_t |\tilde{F}_n(t) - F_0(t)| = \max(D_n^+, D_n^-). \end{aligned} \tag{2.5.1}$$

2. The Anderson-Darling statistic:

$$A_n^2 = n \int_{-\infty}^{\infty} \frac{[\tilde{F}_n(t) - F_0(t)]^2}{F_0(t)[1 - F_0(t)]} dF_0(t). \tag{2.5.2}$$

$\tilde{F}_n(t)$ is a step function with jumps at the order statistics $t_{(1)} < t_{(2)} < \ldots < t_{(n)}$ and the EDF satisfies that

$$\begin{aligned} \tilde{F}_n(t) &= 0 \qquad t < t_{(1)}, \\ \tilde{F}_n(t) &= i/n \qquad t_{(i)} \le t < t_{(i+1)}, \quad i = 1, 2, \ldots, n-1, \\ \tilde{F}_n(t) &= 1 \qquad t_{(n)} \le t. \end{aligned}$$

For computational purposes the expressions (2.5.1) and (2.5.2) can be expressed by

$$D_n^+ = \max_{1 \le i \le n} (\frac{i}{n} - F_0(t_{(i)})), \qquad D_n^- = \max_{1 \le i \le n} (F_0(t_{(i)}) - \frac{i-1}{n}),$$

$$D_n = \max(D_n^+, D_n^-), \tag{2.5.3}$$

$$A_n^2 = -\sum_{i=1}^{n} \frac{2i-1}{n} \{ \log[F_0(t_{(i)})] + \log[1 - F_0(t_{(n+1-i)})] \} - n. \tag{2.5.4}$$

Case 2: *Censored data.* When data are Type II or singly Type I censored, simple modifications can be made to the EDF goodness of fit statistics, and distribution theory becomes only slightly more complicated than in the corresponding uncensored situation.

Single Type I or Type II Censoring

If the data are Type II censored at t_r, the r smallest observation in a random sample of n, then D_n and A_n^2 can be modified as

$$D_{n,\,r} = \sup_{-\infty < t \le t_{(r)}} |\tilde{F}_n(t) - F_0(t)|, \tag{2.5.5}$$

$$A^2_{n,\,r} = n \int_{-\infty}^{t_{(r)}} \frac{[\ \tilde{F}_n(t) - F_0(t)\ ]^2}{F_0(t)[\ 1 - F_0(t)\ ]}\, \mathrm{d}F_0(t). \tag{2.5.6}$$

For single Type I censoring at the point t_c analogous statistics are defined

$$D_{n,\,p} = \sup_{-\infty < t \le L} |\tilde{F}_n(t) - F_0(t)|, \tag{2.5.7}$$

$$A^2_{n,\,p} = n \int_{-\infty}^{L} \frac{[\ \tilde{F}_n(t) - F_0(t)\ ]^2}{F_0(t)[\ 1 - F_0(t)\ ]}\, \mathrm{d}F_0(t), \tag{2.5.8}$$

where $p = F_0(L)$.

Alternate forms of (2.5.6) and (2.5.8) are convenient for computation. It can be expressed by

$$\begin{aligned} A^2_{n,\,r} = &-\sum_{i=1}^{r} \Big(\frac{2i-1}{n} \log F_0(t_{(i)}) - \frac{2n-2i+1}{n} \log[\ 1 - F_0(t_{(i)})\ ] \Big) \\ &+ \frac{r^2}{n} \log F_0(t_{(r)}) - \frac{(n-r)^2}{n} \log[\ 1 - F_0(t_{(r)})\ ] - nF_0(t_{(r)}), \end{aligned} \tag{2.5.9}$$

$$\begin{aligned} A^2_{n,\,p} = &-\sum_{i=1}^{r} \Big(\frac{2i-1}{n} \log F_0(t_{(i)}) + \frac{2n-2i+1}{n} \log[\ 1 - F_0(t_{(i)})\ ] \Big) \\ &+ \frac{r^2}{n} \log F_0(t_c) - \frac{(n-r)^2}{n} \log[\ 1 - F_0(t_c)\ ] - nF_0(t_c). \end{aligned} \tag{2.5.10}$$

Note that in $A^2_{n,r}$, r is fixed. However in $A^2_{n,p}$, r is random.

2.5.3 Simulate Quantiles for Functions of A^2 with Failure Distribution

(1). Pseudorandom Observations from Continuous Distributions

Suppose $U_1, U_2, \ldots, U_n$ is a pseudorandom sample from a $Unif(0,1)$. If $t_p = F_T^{-1}(p)$ is the quantile function for the distribution of the random variable T, then $T_1 = F_T^{-1}(U_1), \ldots, T_n = F_T^{-1}(U_n)$ is a pseudorandom sample from F_T. For example, to generate a pseudorandom sample from EGENG distribution for specified parameters (μ, σ, λ) (see section 2.4). First we obtain the $Unif(0,1)$ pseudorandom sample $U_1, U_2, \ldots, U_n$ and then compute $T_1 = \exp[\mu + \sigma w(U_1; \lambda)], \ldots, T_n = \exp[\mu + \sigma w(U_n; \lambda)]$. Similarly, for the Exponential Weibull Family and Generalized Inverse Gaussian distribution.

(2). Quantiles for Anderson-Darling Statistic with Exact Failure Time Data

Let $T_{(i)}$ be the ith order statistic from $T_1, T_2, \ldots, T_n$ and since (2.5.4)

$$A_n^2 = -\sum_{i=1}^{n} \frac{2i-1}{n} \{ \log[F_0(t_{(i)})] + \log[1 - F_0(t_{(n+1-i)})] \} - n,$$

where $F_0(\cdot)$ is specified as needed.

By the process in (1) and (2) that we can obtain a value of A^2. We repeat the process m times to obtain m values of A^2 and use it to approximate the distribution of A^2 under specified model parameters. Then quantiles of the distribution of A^2 can be easily approximated.

(3). Quantiles for Anderson-Darling Statistic with Type I Censoring Data

Let t_c denote the censoring time and by the $T_{(1)}, \ldots, T_{(n)}$, if $T_{(i)} > t_c$ which the sample consists of the failure time $T_{(1)}, \ldots, T_{(i-1)}$ and $(n - i + 1)$ censored observations. However from the (2.5.10) and the process as in (1) and (2), we can obtain a value of $A_{n,p}^2$. Then we repeat the process m times which it will obtain m values of $A_{n,p}^2$ and use it to approximate the distribution of $A_{n,p}^2$ under specified model parameters.

Then quantiles of the distribution of $A^2_{n,p}$ can be easily approximated.

3 Inference

3.1 Estimation of Degradation Model Parameters

Considering the degradation model (2.3.1), let the parameters $\beta_1, \beta_2, \ldots, \beta_k$ be a multivariate normal distribution with mean vector μ_β and covariance matrix $\mathbf{\Sigma}_\beta$ and use the $\theta_\beta = (\mu_\beta, \mathbf{\Sigma}_\beta)$ to denote the overall population process parameters.

The likelihood for the random parameter degradation model can be expressed as

$$L(\theta_\beta,\ \sigma_\varepsilon \mid data) = \prod_{i=1}^{n} \int_{-\infty}^{\infty} \cdots \int_{-\infty}^{\infty} \left[\prod_{j=1}^{m_i} \frac{1}{\sigma_\varepsilon}\, \phi_{nor}(\xi_{ij}) \right] \times f_\beta(\beta_{1i}, \ldots, \beta_{ki}; \theta_\beta) d\beta_{1i}, \ldots, d\beta_{ki} \quad , \tag{3.1.1}$$

where $\xi_{ij} = [y_{ij} - D(t_{ij}, \beta_{1i}, \ldots, \beta_{ki})]/\sigma_\varepsilon$ and $f_\beta(\beta_{1i}, \ldots, \beta_{ki}; \theta_\beta)$ is the multivariate normal distribution density function. Maximizing (3.1.1) with respect to $(\mu_\beta, \mathbf{\Sigma}_\beta, \sigma_\varepsilon)$ directly, even with today's computational capabilities, is extremely difficult unless $D(t)$ is a linear function. (Meeker and Escobar, 1998, Ch.13)

With the same degradation model in (2.3.1) and following the expression (3.1.1), we can extend to three parameters distributions. For example the EGENG distribution, suppose $\varepsilon_{ij} \sim EGENG(0, \sigma, \lambda)$ as in (2.4.2), we can give the expression as belowing:

$$L(\theta_\beta,\ \sigma, \lambda \mid data) = = \prod_{i=1}^{n} \int_{-\infty}^{\infty} \cdots \int_{-\infty}^{\infty} \left[\prod_{j=1}^{m_i} f(w_{ij};\ \sigma, \lambda) \right] \times f_\beta(\beta_{1i}, \ldots, \beta_{ki}; \theta_\beta) d\beta_{1i}, \ldots, d\beta_{ki},$$

where $w_{ij} = [log\,(y_{ij} - D(t_{ij}, \beta_{1i}, \ldots, \beta_{ki}))]\,/\sigma$.

3.2 Likelihood Function for Failures Distributions

The likelihood for a sample $t_1, t_2, \ldots, t_n$ from a location-scale distribution for a random variable $-\infty < T < \infty$, consisting of exact (i.e., not censored) and right-censored observations, can be written as

$$L(\theta) = \prod_{i=1}^{n} L_i(\theta;\ \text{data}_i) = \prod_{i=1}^{n} \Big[f(t_i;\ \theta)\Big]^{\delta_i} \Big[1 - F(t_i;\ \theta)\Big]^{1-\delta_i},$$

where

$$\delta_i = \begin{cases} 1 & \text{if } t_i \text{ is an exact observation,} \\ 0 & \text{if } t_i \text{ is a right-censored observation.} \end{cases}$$

3.3 Bootstrap Confidence Intervals of percentiles

The following is given by Efron and Tibshirani (1993). This method "Parametric Bootstrap" that simulates each sample of size n from the assumed parametric distribution, using the ML estimates computed from the actual data to replace the unknown parameters. That is, sampling is from $F(t;\hat{\theta})$ which is defined to be a random sample of size n draw from $F(t;\hat{\theta})$, say $X^* = (x_1^*, x_2^*, \ldots, x_n^*)$,

$$F(t;\hat{\theta}) \rightarrow (x_1^*, x_2^*, \ldots, x_n^*).$$

On the other hand, the "nonparametric bootstrap" data points $X^* = (x_1^*, x_2^*, \ldots, x_n^*)$ are a random sample of size n drawn with replacement from the population of n objects $(x_1, x_2, \ldots, x_n)$. Thus the bootstrap data set $X^* = (x_1^*, x_2^*, \ldots, x_n^*)$ consists of members of the original data set $(x_1, x_2, \ldots, x_n)$.

Corresponding to a bootstrap data set X^* is a bootstrap replication of $\hat{t}_p$,

$$\hat{t}_p^* = S(X^*)$$

That is, we must use some finite number of B of replications. To proceed, we generate B independent bootstrap data sets $X^{*1}, X^{*2}, \ldots, X^{*B}$ and compute the bootstrap replications $\hat{t}_p^*(b) = S(X^{*b}),\ b = 1, 2, \ldots, B$. Let $\hat{t}_{pB}^{*(\alpha)}$ be the $100 \cdot \alpha$th empirical percentile of the $\hat{t}_p^*(b)$ values, that is the $B \cdot \alpha$th value in the order list of the B replications of $\hat{t}_p^*$. So the $\hat{t}_{pB}^{*(\alpha)}$ be the $100 \cdot \alpha$th empirical percentile and the $\hat{t}_{pB}^{*(1-\alpha)}$ be the $100 \cdot (1-\alpha)$th empirical percentile. The approximate $1 - 2\alpha$ percentile interval is

$$\left[\ \hat{t}_{p(lower)}\ ,\ \hat{t}_{p(upper)}\ \right] \approx \left[\ \hat{t}_{pB}^{*(\alpha)}\ ,\ \hat{t}_{pB}^{*(1-\alpha)}\ \right].$$

4 Exploring Failure Distributions under Degradation Models

Because the close forms of failure distributions that be difficult to obtain for most degradation models except some simple degradation ones (e.g. section 2.3.2 examples). So in this chapter, we employ the computer to simulate some degradation data from several interesting degradation models that contain both the "Type I censoring" data and exact failure data. From the data, we can find the firstpass times on different failure levels and employ the lognormal probability plot to fit some parametric distributions such as EGENG, EW and GIG distributions.

4.1 Linear Models

Case 1. Consider the degradation model

$$D(t_{ij}) = \beta_0 + \beta_{i1} \times t_{ij}, \quad i = 1, \ldots, 50,\ j = 1, \ldots, 60, \tag{4.1.1}$$

where i is the experiment unit, j is the experiment time. We let β_0 equal 50 to indicate the initial level of degradation. β_{i1} has a normal distribution with parameters $\mu = 3,\ \sigma = 0.3$ that indicates the variability from unit-to-unit. Let the degradation paths be linear in time t. Figure 5 shows this linear degradation model (4.1.1). To illustrate a complete failure data set, we define the failure levels at 130 and 150, where we can obtain the firstpass time. Figure 6 and Figure 7 show the lognormal probability plot of the firstpass time data, comparing ML estimates of the EGENG, exponential Weibull,GIG and lognormal distributions. We find that the EGENG and exponential Weibull distributions can fit better than others.

Case 2. Consider the degradation model

$$D(t_{ij}) = \beta_{i0} + \beta_{i1} \times t_{ij}, \quad i = 1, \ldots, 50,\ j = 1, \ldots, 60, \tag{4.1.2}$$

where β_{i0} has a exponential distribution with parameter rate equal to 1 that indicates the initial level with a little variability, β_{i1} has a weibull distribution with shape parameter equal to 3 and scale parameter equal to 1. Here we assume that β_{i0} is independent with β_{i1}. Figure 8 shows the (4.1.2) model and we can see that the variation is increasing from unit-to-unit. Here we define that the failure levels are equal to 30 and 50, censor time is equal to 5.9. From Figure 8 we can see that the data of the firstpass time are censored. Figure 9 and Figure 10 show the lognormal probability plot of the firstpass time data, comparing ML estimates of the EGENG, lognormal, generalized inverse Gaussian and exponential Weibull distributions. We find that EGENG distribution can fit well. Additionally, generalized inverse Gaussian and exponential Weibull distributions also fit well except for early failures.

4.2 Nonlinear Models

Case 3. Consider the degradation model

$$D(t_{ij}) = \beta_{i0}+\exp\left(|\beta_{i1}| \times t_{ij}\right), \quad i = 1, 2, \ldots, 150,\ j = 1, \ldots, 60, \tag{4.1.3}$$

where β_{i0} has a Normal distribution with parameters $\mu = 4,\ \sigma^2 = 0.001$ and β_{i1} has a Normal distribution with parameters $\mu = 0,\ \sigma^2 = 0.01$. β_{i0} is independent with β_{i1}. Figure 11 shows this degradation model (4.1.3). Here we define that failure levels at 5.025 and 5.04, censor time is equal to 59. The data of the firstpass time are right censored. Figure 12 and Figure 13 show the lognormal probability plot of the firstpass time data, comparing ML estimates of the EGENG, lognormal, generalized inverse Gaussian and exponential Weibull distributions. We see that EGENG and generalized inverse Gaussian distributions fit well.

Case 4. Consider the degradation model

$$D(t_{ij}) = \beta_0 + \beta_{i1} \times \sqrt{t_{ij}}, \quad i = 1, \ldots, 100,\ j = 1, \ldots, 60, \tag{4.1.4}$$

where β_0 is fixed and is equal to 20, β_{i1} has a normal distribution with parameters $\mu = 3,\ \sigma = 0.3$. Figure 14 shows that model (4.1.4) is a concave degradation path model. Here we define the failure levels at 32 and 36, censor time is equal to 59. Figure 15 and Figure 16 show the lognormal probability plot of the firstpass time data, comparing ML estimates of the EGENG, exponential Weibull, lognormal and generalized inverse Gaussian distributions. We see that EGENG and EW distributions fit well and the lognormal distribution can also fit well except for early failure.

4.3 Random Error Models

Case 5. Consider the degradation model

$$D(t_{ij}) = \beta + |\eta_i| \times t_{ij} + \varepsilon_{ij}, \quad i = 1, \ldots, 50,\ j = 1, \ldots, 60, \tag{4.1.5}$$

where β is fixed and is equal to 20, η_i has a normal distribution with parameters $\mu = 5,\ \sigma = 2$ and ε_{ij} has a uniform distribution with $(0, t_{ij})$. Figure 17 shows that model (4.1.5) with degradation rate varying due to variations in time. Here we define the failure levels at 35 and 40, censor time is equal to 5.9. The data of the firstpass time are the right censored. Figure 18 and Figure 19 show the lognormal probability plot of the firstpass time data, comparing ML estimates of the EGENG, lognormal, generalized inverse Gaussian and exponential Weibull distributions. We see that the only EGENG distribution fits better than others.

Case 6. Consider the degradation model is

$$D(t_{ij}) = \beta_0 + |\eta_{i0}| \times t_{ij} + \varepsilon_{ij}, \quad i = 1, \ldots, 100,\ j = 1, \ldots, 60, \tag{4.1.6}$$

where β_0 is fixed and is equal to 20, η_{i0} has a normal distribution with parameters $\mu = 5,\ \sigma = 2$ and ε_{ij} has a exponential distribution with mean equal to $t_{ij}/2$. Figure 20 shows the model (4.1.6). Here we define the failure levels at 32 and 34, censor time is equal to 5.9. The data of the firstpass time are right censored. Figure 21 and

Figure **??** show the lognormal probability plot of the firstpass time data, comparing ML estimates of the EGENG, exponential Weibull, lognormal and generalized inverse Gaussian distributions. We see that EGENG and generalized inverse Gaussian distributions fit well. Additionally, the lognormal and exponential Weibull distributions also fit well except for early failure.

Case 7. Consider the degradation model

$$D(t_{ij}) = |\beta_{i0}| + |\eta_{i0}| \times t_{ij} + |\gamma_{i0}| \times t_{ij}^2 + \varepsilon_{ij}, \quad i = 1, \ldots, 100,\ j = 1, \ldots, 60, \tag{4.1.7}$$

where β_{i0} has a normal distribution with parameters $\mu = 0,\ \sigma = 3$, η_{i0} has a normal distribution with parameters $\mu = 5,\ \sigma = 2$, γ_{i0} has a normal distribution with parameters $\mu = 2,\ \sigma = 1$ and ε_{ij} has a uniform distribution with $(0, 2t + 0.1)$. Figure 23 shows the model (4.1.7). Here we define the failure levels at 45 and 50, censor time is equal to 5.9. The data of the firstpass time are right censored. Figure 24 and Figure 25 show the lognormal probability plot of the firstpass time data, comparing ML estimates of the EGENG, exponential Weibull, lognormal and generalized inverse Gaussian distributions. We see that EGENG distribution fits well.

4.4 First Order Autocorrelated Models

Case 8. Consider the degradation model

$$D(t_{ij}) = \theta_{ij} + D(t_{ij-1}), \quad i = 1, \ldots, 100,\ j = 1, \ldots, 65, \tag{4.1.8}$$

where θ_{ij} has a uniform distribution with (0, 2). Model (4.1.8) indicates that $D(t_{ij}) - D(t_{ij-1})$ is independent with $D(t_{ij-1}) - D(t_{ij-2})$ that has a uniform distributions. Figure 26 shows the model (4.1.8). Here we define the failure levels at 30 and 40, censor time is equal to 600. Figure 27 and Figure 28 show the lognormal probability plot of the firstpass time data, comparing ML estimates of the EGENG, exponential

Weibull, lognormal and generalized inverse Gaussian distributions. We see that all of the four parametric distributions fit well.

Case 9. Consider the degradation model

$$D(t_{ij}) = \beta_{ij} + D(t_{ij-1}), \quad i = 1, \ldots, 100, \ j = 1, \ldots, 65, \tag{4.1.9}$$

where β_{ij} has a exponential distribution with parameter $\lambda = 4$. Model (4.1.9) is similar to model (4.1.8) on that the increment between t_{ij} and t_{ij-1} has an exponential distribution and every increment is independent. Figure 29 shows the model (4.1.9). Here we define the failure levels at 7 and 11, censor time is equal to 600. Figure 30 and Figure 31 show the lognormal probability plot of the firstpass time data, comparing ML estimates of the EGENG, exponential Weibull, lognormal and generalized inverse Gaussian distributions. We see that EGENG and exponential Weibull distributions fit well and the GIG distribution also fit well except the later period failures.

5 Real Data Example

The 2024-T351 aluminum data was produced by the fatigue laboratory in the Department of Mechanical Engineering of National Taiwan University in year 2001 (Wu and Chen). There are 30 sample paths (figure 2).

Here we consider several specified failure levels (D_f) and different censor times. We use probability plot and Anderson-Darling test to identify the proper failure distribution for the 2024-T351 aluminum data. First we will discuss the case of complete failures, then discuss the case of right censoring.

Case 1. Complete Failure Case

We consider the specified failure level D_f at crack size 23, 24, 25 and 26 mm. Figure 32, 33, 34 and 35 show the lognormal probability plot of the complete failure data for 2024-T351 aluminum, comparing ML estimates of the EGENG, lognormal, generalize inverse Gaussian and exponential Weibull distributions. The ML estimates of EGENG, GIG and exponential Weibull distributions are in Table 1.

The fitting result is not very convincing for all four distributions. By our experience in chapter 4, EGENG is very flexible for different degradation models. We use Anderson-Darling test to check the goodness of fits for EGENG, GIG and EW distributions. Table 2 is the quantile of Anderson-Darling statistic obtained by 5000 simulations for those distributions with parameters in table 1. Using the MLE of EGENG, GIG, EW and the expression (2.5.4), we can find the Anderson-Darling statistic A^2_{30} in Table 3. From Table 2 and Table 3, there are no evidence against the hypothesis of EGENG and GIG from that test.

For simplicity of computation we will use the parametric way to generate data and nonparametric way to generate bootstrap samples which to give the confidence intervals of the p-th quantile of the EGENG distribution in Table 4, 5, 6 and 7 by

10000 replications. The result will be similar to pure parametric bootstrap when sample size is large.

Table 1: ML estimates of EGENG, GIG and EW Distributions with Complete 2024-T351 Aluminum Data

MLE of the EGENG Distribution

	μ	σ	λ
Fail level 23	10.4518	0.1598	-0.818
Fail level 24	10.5414	0.1515	-0.982
Fail level 25	10.6332	0.1557	-0.840
Fail level 26	10.6830	0.1506	-0.943

MLE of the GIG Distribution

	w	η	λ
Fail level 23	14.91	9999.99	26.16
Fail level 24	13.73	10000.01	27.09
Fail level 25	13.20	9999.98	28.41
Fail level 26	12.61	9999.96	28.93

MLE of the EW Distribution

	θ	α	σ
Fail level 23	12.69	1.26	10000.5
Fail level 24	160.47	1.21	10000.5
Fail level 25	203.44	1.17	10000.9
Fail level 26	239.13	1.15	10000.9

Table 2: Quantiles of Anderson-Darling Statistics from Complete 2024-T351 Aluminum Data with EGENG, GIG and EW Distributions.

Percentage	0.01	0.05	0.1	0.80	0.85	0.90	0.95	0.99
αth-Quantile	0.2018	0.2780	0.3463	1.4031	1.6190	1.9442	2.4875	3.8025

Table 3: The Anderson-Darling statistic A^2_{30} from Complete 2024-T351 Aluminum Data

A^2_{30}	EGENG	GIG	EW
Fail level 23	0.4437	0.6841	4.1908
Fail level 24	0.4885	0.7785	4.1100
Fail level 25	0.5243	0.7829	6.4527
Fail level 26	0.5361	0.8184	3.7193

Table 4: The Confidence Intervals of the $\hat{t_p}$ by Bootstrap method with fail level equal to 23.

	$\hat{t_p}$	2.5%	5%	95%	97.5%
5%	28614	28614	28650	28879	28888
10%	29907	29907	29924	30151	30177
20%	31649	31649	31678	31874	31880

Table 5: The Confidence Intervals of the $\hat{t_p}$ by Bootstrap method with fail level equal to 24.

	$\hat{t_p}$	2.5%	5%	95%	97.5%
5%	32100	31979	31998	32236	32258
10%	33406	33266	33282	33520	33542
20%	35254	35145	35157	35351	35368

Table 6: The Confidence Intervals of the $\hat{t_p}$ by Bootstrap method with fail level equal to 25.

	$\hat{t_p}$	2.5%	5%	95%	97.5%
5%	34527	34376	34410	34705	34722
10%	36178	36015	36034	36299	36326
20%	38278	38136	38154	38401	38435

Table 7: The Confidence Intervals of the $\hat{t_p}$ by Bootstrap method with fail level equal to 26.

	$\hat{t_p}$	2.5%	5%	95%	97.5%
5%	36831	36705	36719	36935	36972
10%	38188	38032	38053	38324	38347
20%	40334	40194	40215	40463	40494

Case 2. Right Censored

In field applications and experimental processes, life test may stop earlier because of time restrictions. We mimic the situation by setting the possible censor time at 52000, 57500, and 60500 cycles. We consider the specified failure level D_f equal to 24, 25, 26 mm. Figure 36, 37 and 38 show the lognormal probability plot of the 2024-T351 aluminum data, comparing ML estimates of the EGENG, lognormal, generalize inverse Gaussian and exponential Weibull distributions. The EGENG distribution fits better than others. The ML estimates of EGENG are in Table 8.

The fitting is well in the probability plot for EGENG distribution. We also use Anderson-Darling test to check the goodness of fit. Table 9 is the quantile of Anderson-Darling statistic obtained by 10000 simulations for EGENG distribution with parameters in Table 8. Using the MLE of EGENG and the expression (2.5.10), we can obtain the Anderson-Darling statistic $A^2_{30,p}$ in Table 10. Since Table 9 and Table 10, there are no evidence against the hypothesis of EGENG from that test. The EGENG distribution can be used to estimate the quantile before the censor time. It is quite useful because most fild problems are interested in the early failure time. With the same method in last case, we also obtain the confidence intervals of the p-th quantile of EGENG distribution in Table 11, 12 and 13.

Table 8: MLE of EGENG Distribution of Censor 2024-T351 Aluminum Data

Parameters	μ	σ	λ
Fail level 24	10.39	0.058	-5.881
Fail level 25	10.56	0.124	-1.886
Fail level 26	10.587	0.101	-2.684

Table 9: Quantiles of Anderson-Darling Statistics from Censor 2024-T351 Aluminum Data with EGENG Distribution.

Percentage	0.01	0.05	0.1	0.80	0.85	0.90	0.95	0.99
Fail level 24	0.1185	0.1734	0.2188	1.1032	1.2870	1.5539	2.0546	3.3605
Fail level 25	0.1439	0.2072	0.2550	1.2212	1.4197	1.7210	2.2427	3.6373
Fail level 26	0.1368	0.1968	0.2458	1.1896	1.3811	1.6794	2.1733	3.5505

Table 10: The Anderson-Darling statistic $A^2_{30,p}$ from Censor 2024-T351 Aluminum Data of EGENG Distribution

$A^2_{30,p}$	EGENG
Fail level 24	0.1616
Fail level 25	0.2081
Fail level 26	0.1957

Table 11: The Confidence Intervals of the $\hat{t_p}$ by Bootstrap method with fail level equal to 24 mm and censor time equal to 52000 cycles.

	$\hat{t_p}$	2.5%	5%	95%	97.5%
5%	32126	32067	32075	32177	32189
10%	32752	32690	32696	32825	32832
20%	34149	34027	34039	34250	34268

Table 12: The Confidence Intervals of the $\hat{t_p}$ by Bootstrap method with fail level equal to 25 mm and censor time equal to 57500 cycles.

	$\hat{t_p}$	2.5%	5%	95%	97.5%
5%37105	37018	37024	37197	37205	
10%	38073	37976	37996	38143	38165
20%	39601	39487	39511	39721	39740

Table 13: The Confidence Intervals of the $\hat{t_p}$ by Bootstrap method with fail level equal to 26 mm and censor time equal to 60500 cycles.

	$\hat{t_p}$	2.5%	5%	95%	97.5%
5%	37122	37019	37035	37210	37219
10%	38026	37948	37962	38117	38133
20%	39673	39555	39576	39764	39782

6 Conclusion and Future Research

6.1 Conclusion

In considering degradation problems, we explore the discrete and continuous degradation process. In discrete degradation process that is defined by the mark point process, we describe the property of the mark point process that leads to the failure distribution. So we extend the result of Wendt (1997) to develop failure time distribution with Gamma and Weibull increment. In the case of continuous degradation process as a special random process of Wiener process, the failure distribution of inverse Gaussian model can be derived from the Wiener process as a first passage time distribution. We show the relation between a simple degradation model and the Wiener process.

On the other hand, some failure distributions can be traced down from an underlying degradation process which might be linear, convex or concave. It is possible for some simple degradation paths to be written down with a closed-form expression. In this thesis we consider 9 different degradation paths and fit the failure time distributions.

Many parametric models have been used in the analysis of lifetime data. The most commom distributions used to fit the first passtime distribution are location-scale parametric models. For the needs of flexibility of the models to fit the data, we consider the three different failure distributions each having three parameters such as extended generalized gamma, exponential Weibull and generalized inverse Gaussian distributions.

Because the close forms for failure distributions are difficult to obtain for most continuous degradation models except some simple ones or a Wiener process. We employ

the computer to simulate some degradation data from several interesting degradation models such as linear, nonlinear, random error and first order autocorrelated models that result in both complete failure data and the right censored data. From the simulated data, we define the firstpass times on different failure levels and employ the lognormal probability plot to fit four parametric distributions such as EGENG, EW, GIG and lognormal distributions. We find that, EGENG distribution can fit better than others in those the degradation model we consider.

In this thesis, we also investigate a real data set of the 2024-T351 aluminum crack size. First we discuss the case of complete failures, then discuss the case of right censoring. In the complete case, we consider the specified failure level D_f at crack size 23, 24, 25 and 26 mm. We employ the lognormal probability plot, comparing the EGENG, GIG, EW and lognormal distributions. The fitting results are not very convincing for the four distributions from the probability plots. So we also use Anderson-Darling statistic to check the goodness-of-fit. We calculate the quantiles of Anderson-Darling statistic by 5000 simulations for EGENG, GIG and EW distributions. In the result, there are no evidence to against the hypothesis of EGENG and GIG from that test. By our experience in chapter 4, EGENG distribution is very flexible for different degradation models. So we employ the bootstrap method to estimate the confidence interval of quantile by using EGENG distribution.

In field applications and experimental processes, life test may stop earlier because of time restrictions. We mimic the situation by setting the possible censor time at 52000, 57500, and 60500 cycles for the 2024-T351 aluminum crack test. We consider the specified failure level D_f equal to 24, 25, 26 mm. We also employ the lognormal probability plot, comparing the EGENG, GIG, EW and lognormal distributions. We find that only EGENG distribution fits better than others. So we also check the goodness-of-fit of EGENG distribution. There is no evidence against the hypothesis of EGENG from the test. The EGENG distribution can use to estimate the quantile

before the censor time. The better fitted models for right censoring such as EGENG are quite useful because most fild problems are interested in the early failure times.

6.2 Future Research

There are several directions that could use for future research.

- Further research on Mark point process to estimate the increment parameters. For the different qualities of products, we may employ different degradation paths and together with mark point process to derive the failure distributions.

- Use parametric model as GIG, EW and EGENG to fit the failure distributions form from Mark point process.

  In mark point processes, we derive the failure distributions by using the Wendt (1997) forms (2.1.1) and (2.1.3) with different distribution of increment. The numerical calculation is not carried out yet. One comparison is to fit the parametric models as GIG, EW and EGENG.

- Fit the 2024-T351 aluminum data from degradation model using physical model. Figure 2 displays the degradation paths of 2024-T351 aluminum data. If we obtain more knowledge on the material fatigue properties, we could employ a physical model to fit the degradation paths and comparing with failure fitting by the qualities of 2024-T351 aluminum.

- Search a distribution model to have a better fitting for the 2024-T351 aluminum data. In chapter 5 we employ some parametric distributions to fit 2024-T351 aluminum but the result is not very convincing. So we could extend our search of distribution models to have a better fitting for the 2024-T351 aluminum data.

- Consider the time series models on the degradation processes. The degradation process are taken serially on units, hence, there is some potential for autocorrelation and the crack growth depends on previous status (e.g. 2.3.1). Especially if there are many closely spaced readings. In situations where the autocorrelation cannot be ignored, one can use a time series model to describe the data.

Appendix

Some properties of the modified Bessel function

(1). The modified Bessel function of the third kind and index $\lambda \in \mathbf{R}$ is denoted by $K_\lambda(\cdot)$. And $K_\lambda(w),\ w > 0$ is given by

$$K_\lambda(w) = \frac{1}{2}\int_0^\infty t^{\lambda-1}\exp^{-\frac{1}{2}w(t+t^{-1})}\,dt \tag{A.1}$$

And the Bessel functions $K_\lambda,\ \lambda \in \mathbf{R}$, satisfy the relations

$$K_\lambda(w) = K_{-\lambda}(w) \tag{A.2}$$

$$K_{\lambda+1}(w) = \frac{2\lambda}{w}K_\lambda(w) + K_{\lambda-1}(w) \tag{A.3}$$

$$K_{\lambda-1}(w) + K_{\lambda+1}(w) = -2K_\lambda^{'}(w) \tag{A.4}$$

(2). For $\lambda = n + \frac{1}{2}$ and $n = 0, 1, 2, \ldots$ one has

$$K_{n+\frac{1}{2}}(w) = \sqrt{\frac{\pi}{2}}w^{-1/2}\exp^{-w}(1+\sum_{i=1}^{n}\frac{(n+1)!}{(n-i)!(i!)}(2w)^{-i}) \tag{A.5}$$

(3). The connection between K_λ and the modified Bessel function of the first kind I_v can be expressed by

$$K_\lambda(w) = \frac{\pi}{2}\frac{1}{\sin(\pi\lambda)}(I_{-\lambda}(w) - I_\lambda(w)) \tag{A.6}$$

where the right hand side is to be interpreted in the limiting sense in case λ is an integer. Since

$$I_\lambda(w) = \sum_{m=0}^{\infty}\frac{(w/2)^{2m\lambda}}{m!\Gamma(m+\lambda+1)} \tag{A.7}$$

(4). As $w \to 0$, in particular one has the first order approximation

$$K_\lambda(w) \simeq \Gamma(\lambda)2^{\lambda-1}w^{-\lambda}, \qquad (\lambda > 0) \tag{A.8}$$

For $\lambda = 0$,

$$K_0(w) \simeq -\ln w$$

(5). For large w , the asymptotic expansion of $K_\lambda(w)$ is

$$K_\lambda(w) = \sqrt{\frac{\pi}{2}} w^{-1/2} \exp^{-w} (1 + \frac{u^{-1}}{8w} + \frac{(u-1)(u-9)}{2!(8w)^2} + \frac{(u-1)(u-9)(u-25)}{3!(8w)^3} + \ldots) \tag{A.9}$$

where $u = 4\lambda^2$.

References

[1] Alexandrov, M. D. and Lacis A. A. (2000), *A new three-parameter cloud/aerosol particle size distribution based on the Generalized Inverse Gaussian density function*, *Applied Mathematics and Computation*, **116**, *153-165.*

[2] Anderson, per K., Borgan, O., Gill, R. D. and Keiding, N. (1992), *Statistical Models based on Counting Processes*, *Springer Verlag New York*, INC.

[3] Bogdanoff, J. L. and Kozin, F. (1985), *Probabilistic Models of Cumulative Damage*, *New York*: *John Wiley & Sons.*

[4] Brillinger, D., Fienberg, J. G., Hartigan, J., Kiefer J. and Krickeberg K. (1982), *Lecture Notes in Statistics*, *Springer-Verlag New York*, INC.

[5] Chhikara, R. S. and Folks, J. L. (1989), *The Inverse Gaussian Distribution*, *New York: Marcel Dekker*, INC.

[6] Efron, B. and Tibshirani, R. J. (1993), *An Introduction to the Bootstrap*, *Chapman and Hall*, INC.

[7] Farewell, V. T. and Prentice, R. L. (1977), *A study of distributional shape in life testing*, *Technometrics*, **19**, *69-75.*

[8] Gunes, H., Dietz, D. C., Auclair, P. F. and Moore, A. H. (1997), *Modified goodness-of-fit tests for the Inverse Gaussian distribution*, *Computational Statistics and Data Analysis*, **24**, *63-77.*

[9] Kuo, M. H. (2001), *The Optimum Plan Accurate Inference for Accelerated Life test under Inverse Gaussian Distribution*, *Dept. of Statistics Tunghai University.*

[10] Lawless, J. F. (1982), *Statistical Models and Methods for lifetime data*, *John Wiley.*

[11] Liu, S. (1997), *The Generalized Gamma Model and Its Maximum likelihood Estimation*, *Thesis, Department of Statistics, Iowa State University.*

[12] Lu, C. J. and Meeker, W. Q. (1993), *Using Degradation Measures to estimate a Time-to-Failure Distribution*, *Technometrics*, **35**, **2**, *161-173.*

[13] Meeker, W. Q. and Escobar, L. A. (1998), *Statistical Methods for Reliability Data*, *John Wiley & Sons.*

[14] Meeker, W. Q., Escobar, L. A. and Lu, C. J. (1998), *Accelerated Degradation Tests: Modeling and Analysis*, *Technometrics*, **40**, **2**, *89-99.*

[15] Meeker, W. Q. and Luvalle, M. J. (1995), *An Accelerated Life Test model based on Reliability Kinetics*, *Technometrics*, **37**, **2**, *133-145.*

[16] Mudholkar, G. S. and Srivastava, D. K. (1995), *The Exponentiated Weibull Family: A Reanalysis of the Bus-Motor-Failure Data*, *Techmetrics*, **37**, **4**, *436-445.*

[17] Nobile, A. G., Ricciardi, L. M. and Sacerdote, L. (1985), *A Note on First Passage Time and Some Related Problems*, *Applied Probability Trust*, **22**, *346-359.*

[18] Stephens, M. A. (1974), *EDF Statistics for Goodness of fit and Some Comparisons*, *Journal of the American Statistical Association*, **69**, *347.*

[19] Tseng, S. T., Hamada, M. and Chiao, C. H. (1995), *Using Degradation Data to Improve Fluorescent Lamp Reliability*, *Journal of Quality Technology*, **27**, **4**, *363-369.*

[20] Wendt, H. (1997), *Some Models describing Damage processes and Resulting First Passage Times*, *Advance in Statistic Models for Reliability, Quality and Safety*, *Birkhauser.*

[21] Wu, W. F. and Chen, C. Z. (2001), *Reliability research on crack growth of Aluminum Alloy*, *National Taiwan University.*

[22] Yu, H. F. and Tseng, S. T. (1998), *On Line Procedure for Terminating an Accelerated Degradation Test*, *Statistica Sinica*, **8**, *207-220.*

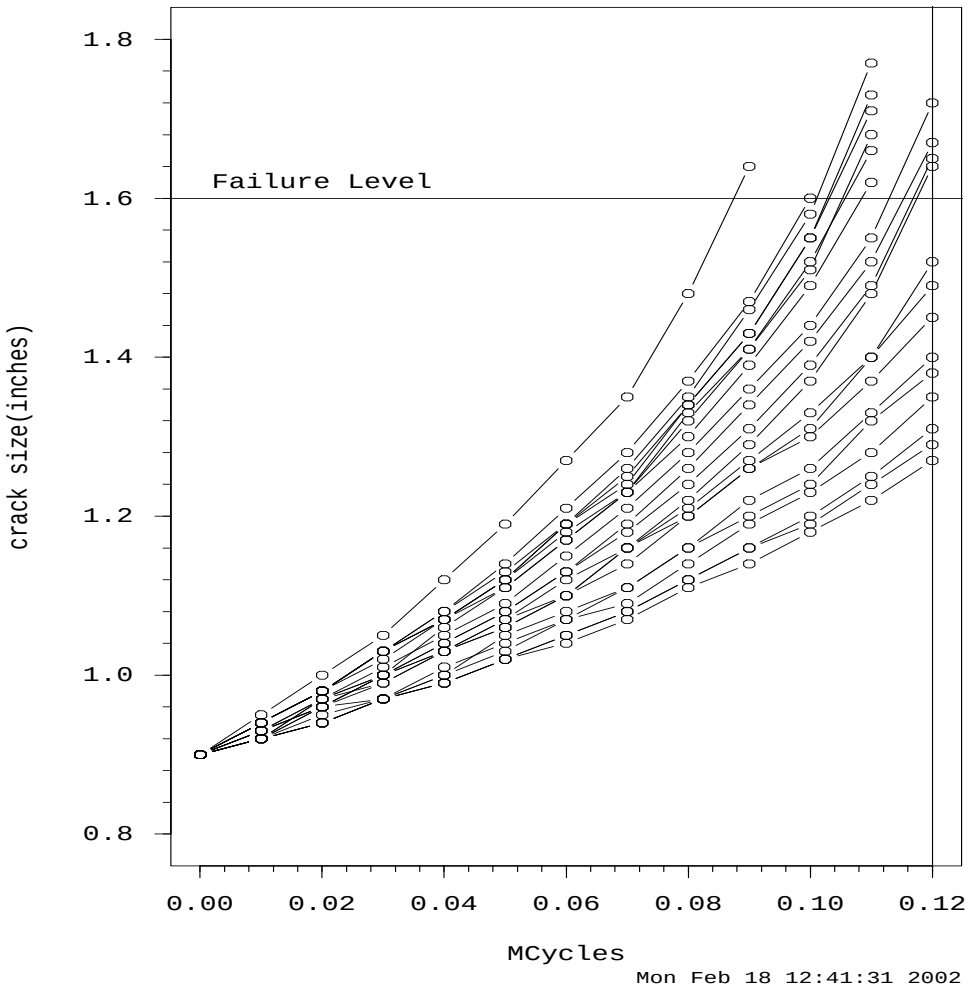

Figure 1: Fatigue-Crack-Growth Data from Bogdanoff and Kozin (1985).

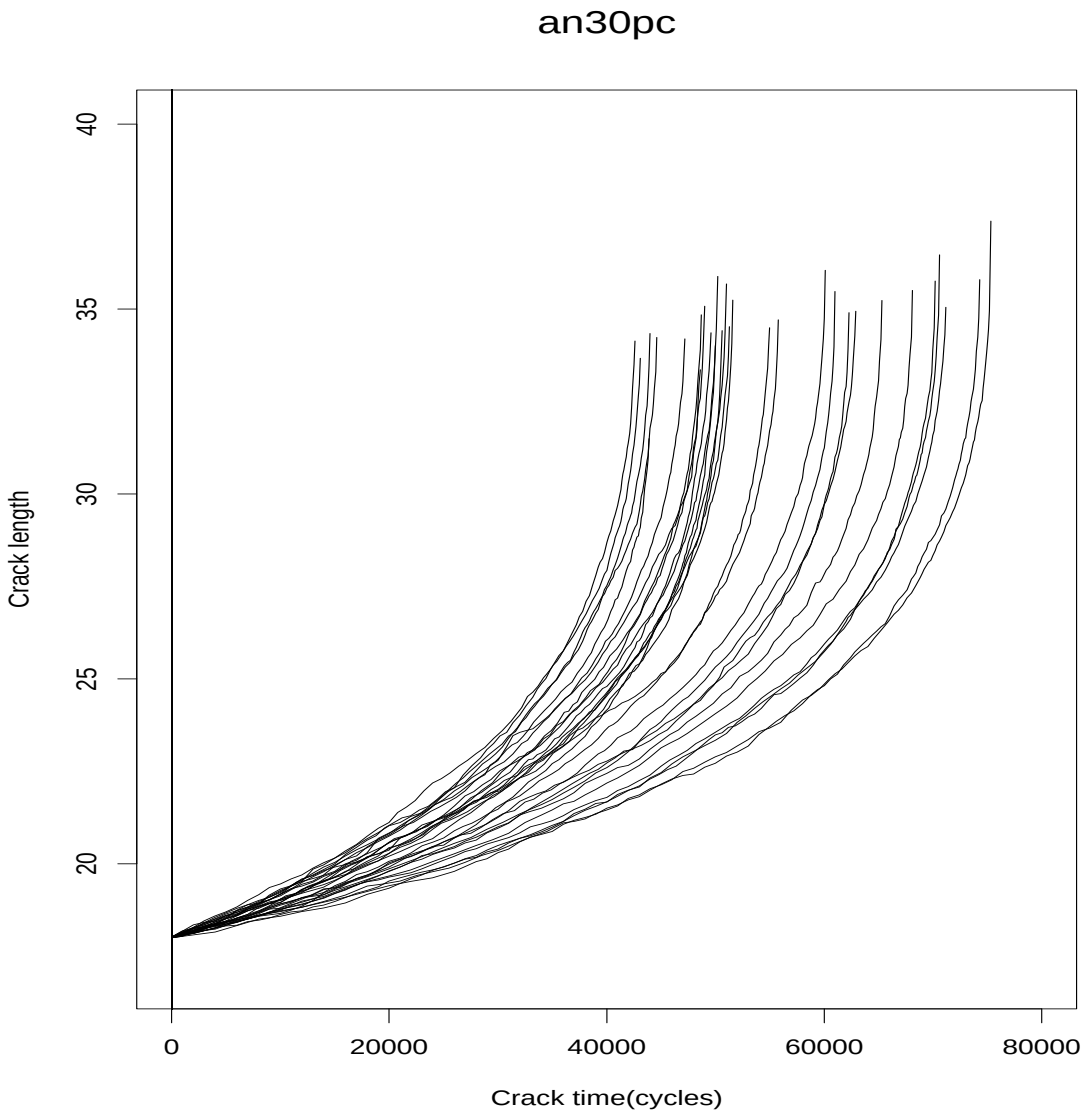

Figure 2: Plot the 30 degradation paths of 2024-T351 Aluminum Alloy.

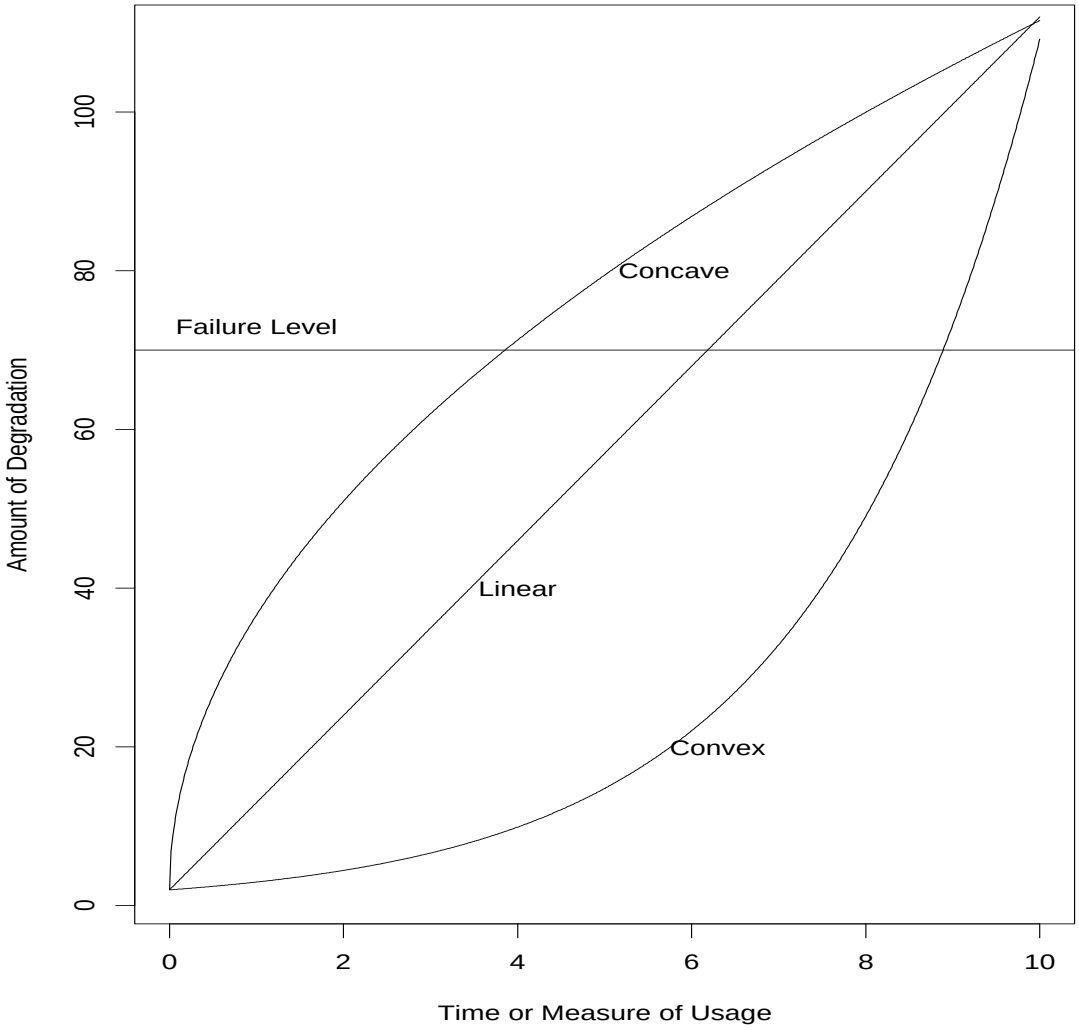

Figure 3: Possible shapes for univariate degradation curves.

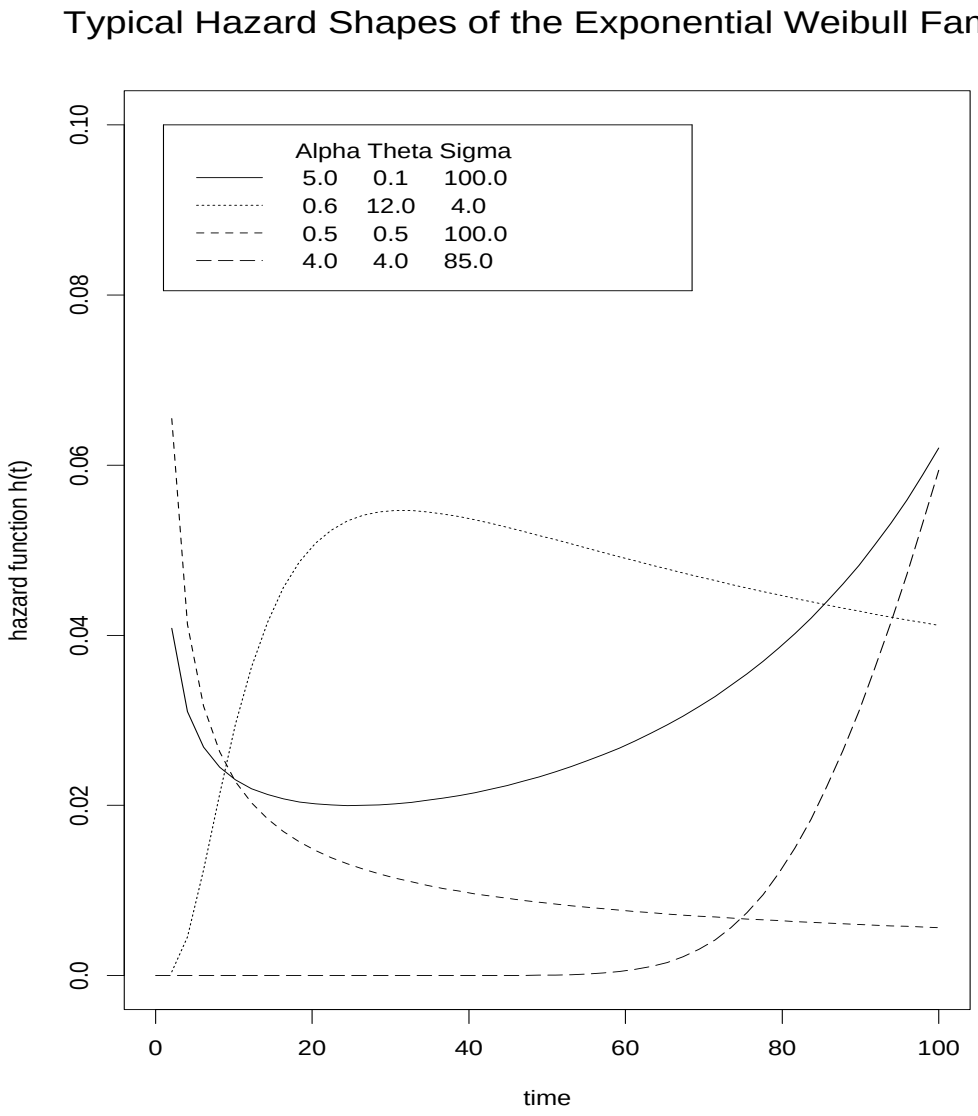

Figure 4: Hazard function of Exponential Weibull Family.

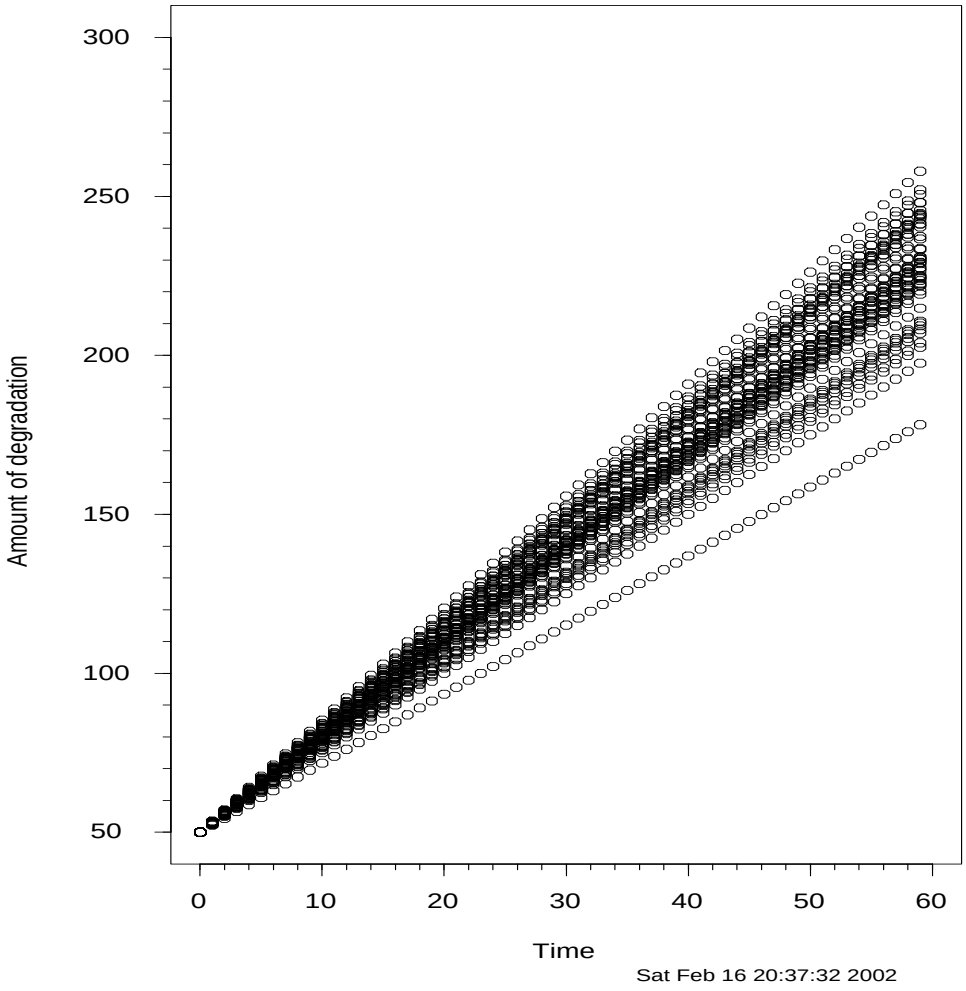

Figure 5: Plot of degradation model (4.1.1) with fix the initial level and random unit to unit variability from 50 degradation paths.

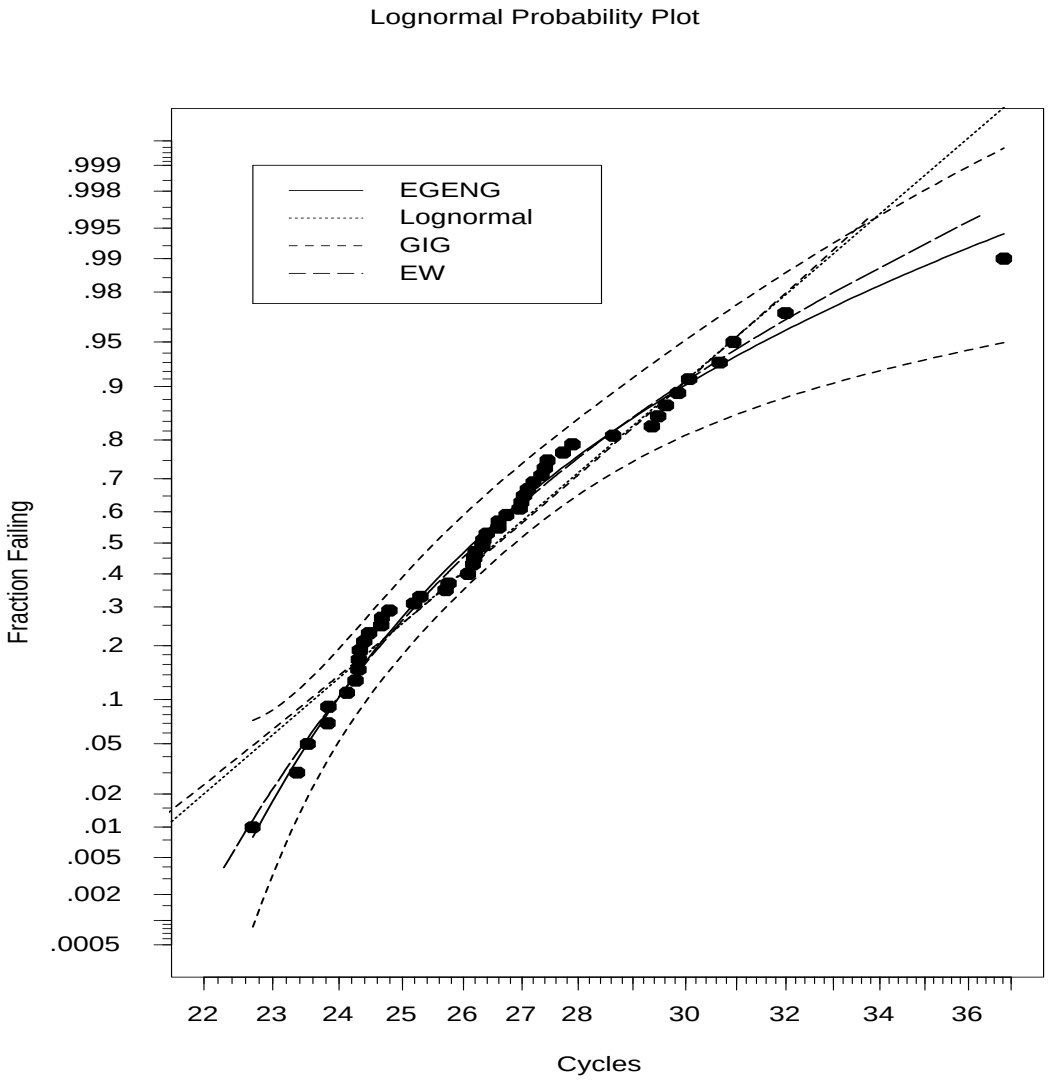

Figure 6: Lognormal probability plot of degradation model (4.1.1) with complete data, comparing EGENG, lognormal, generalized inverse Gaussian and exponential Weibull distributions. Approximate 95% pointwise confidence intervals for $F(t)$ is added to EGENG distribution. Fail level equal to 130.

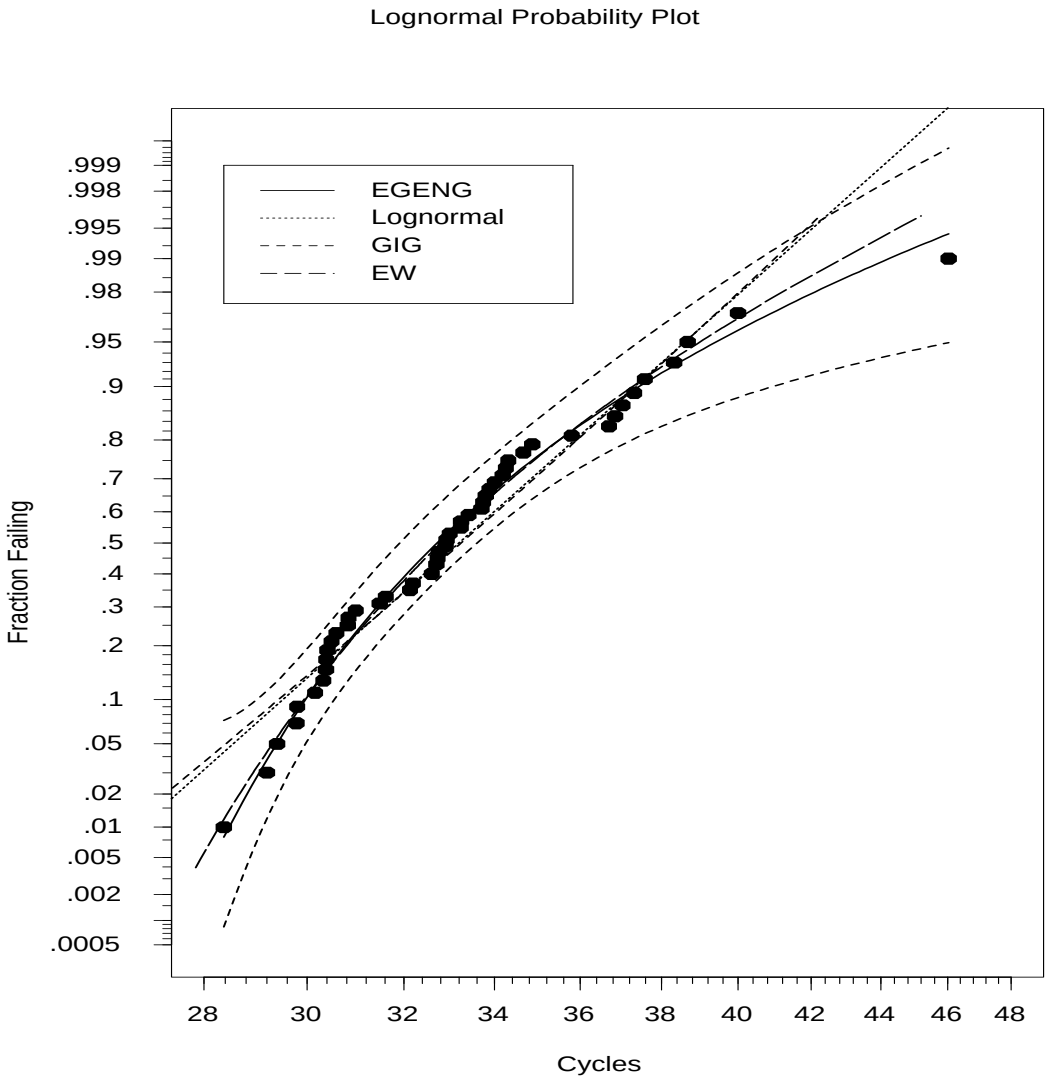

Figure 7: Lognormal probability plot of degradation model (4.1.1) with complete data, comparing EGENG, lognormal , generalized inverse Gaussian and exponential Weibull distributions. Approximate 95% pointwise confidence intervals for $F(t)$ is added to EGENG distribution. Fail level equal to 150.

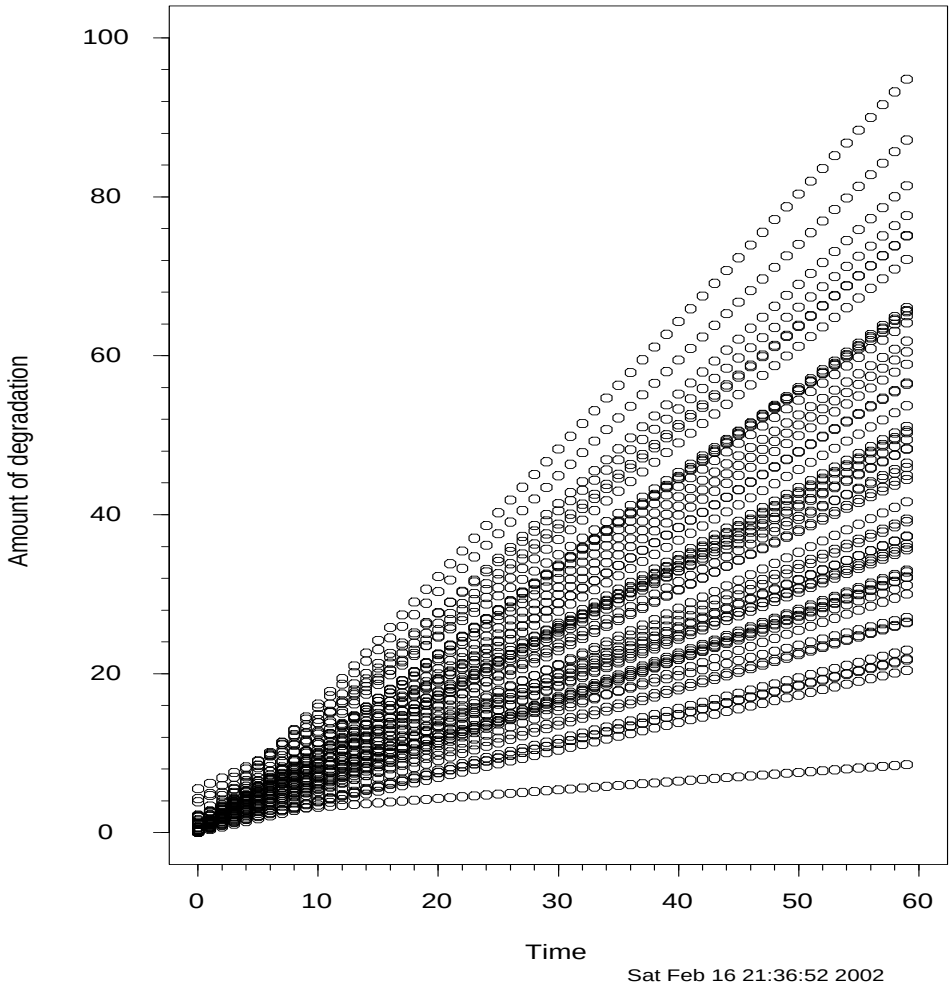

Figure 8: Plot of degradation model (4.1.2) with random initial level and unit to unit variability from 50 degradation paths.

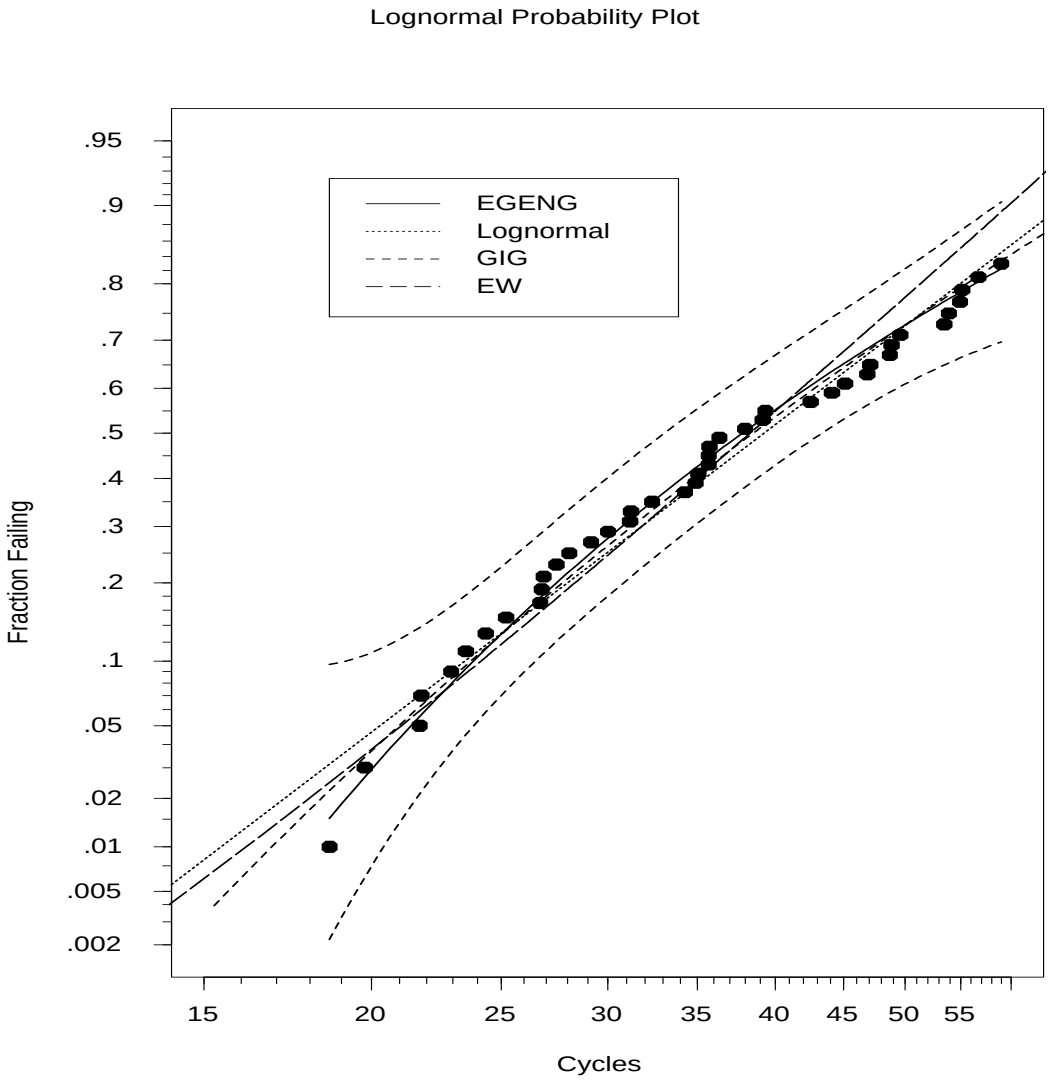

Figure 9: Lognormal probability plot of degradation model (4.1.2) with right censored data, comparingEGENG, lognormal, generalized inverse Gaussian and exponential Weibull distributions. Approximate 95% pointwise confidence intervals for $F(t)$ is added to EGENG distribution. Fail level equal to 30 and censored time equal to 59.

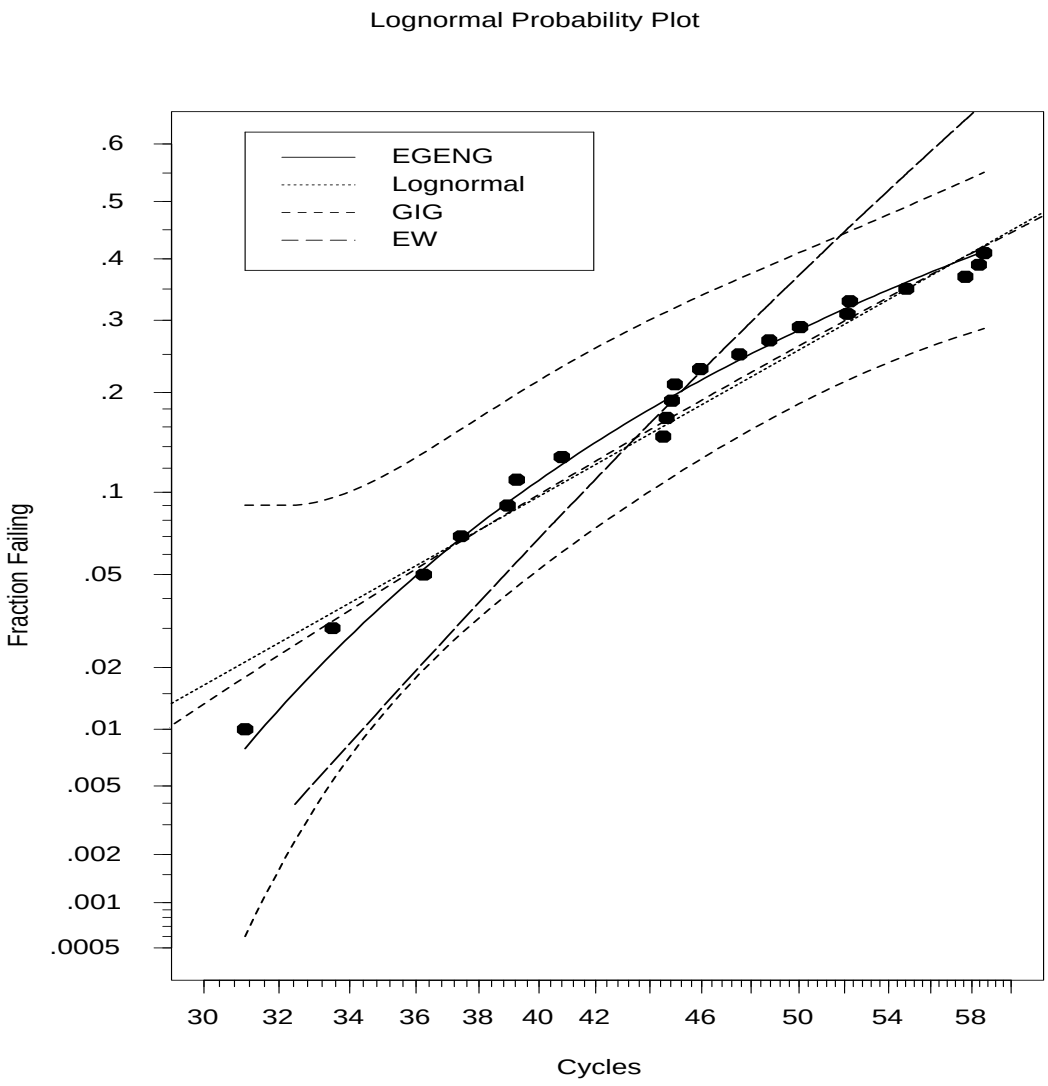

Figure 10: Lognormal probability plot of degradation model (4.1.2) with right censored data, comparing EGENG, lognormal, generalized inverse Gaussian and exponential Weibull distributions. Approximate 95% pointwise confidence intervals for $F(t)$ is added to EGENG distribution. Fail level equal to 50 and censored time equal to 59.

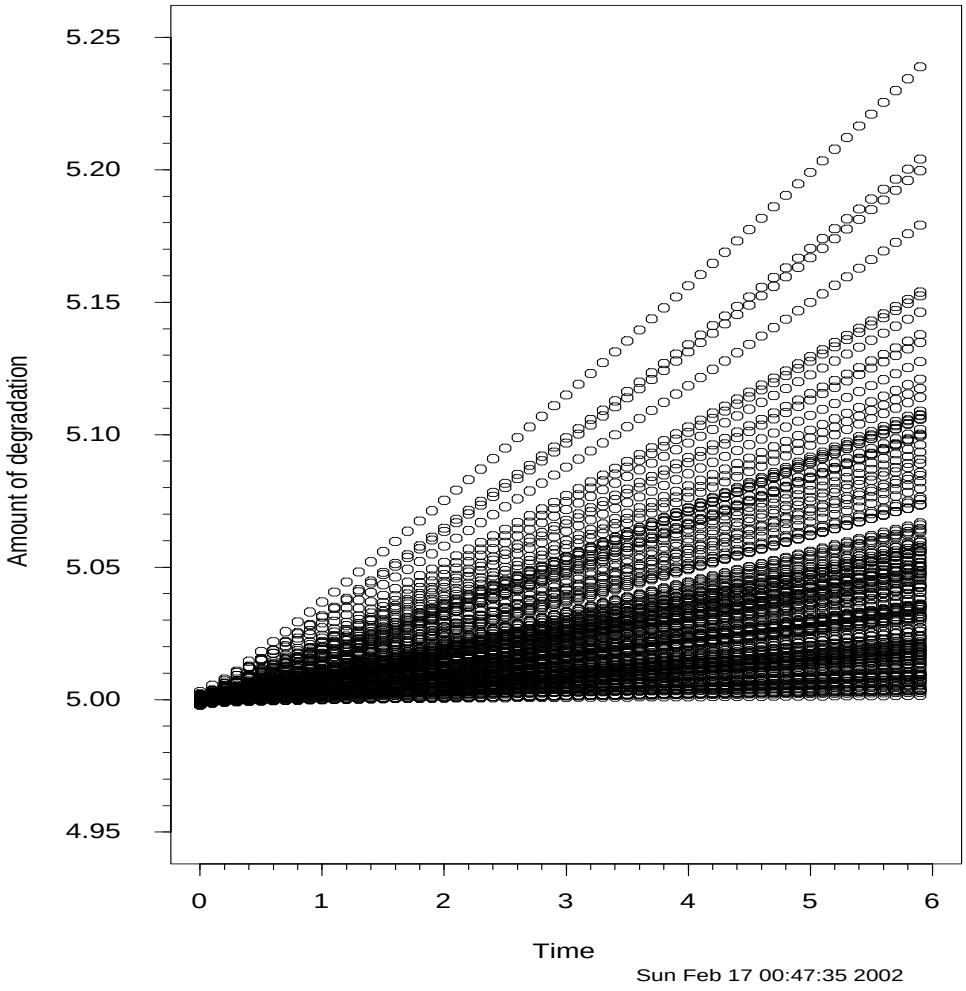

Figure 11: Plot of degradation model (4.1.3) with nonlinear degradation paths.

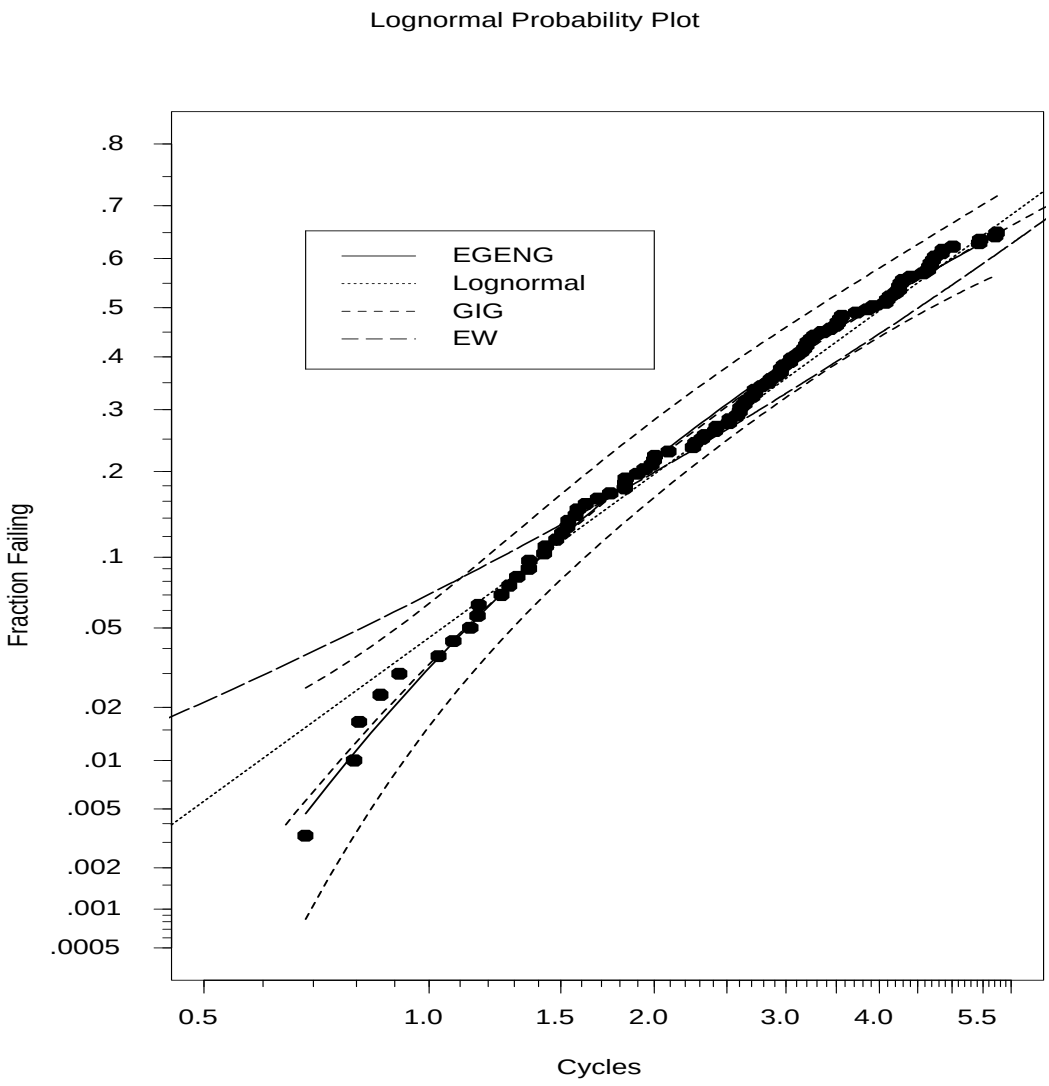

Figure 12: Lognormal probability plot of degradation model (4.1.3) with right censored, comparing EGENG, lognormal, generalized inverse Gaussian and exponential Weibull distributions. Approximate 95% pointwise confidence intervals for $F(t)$ is added to EGENG distribution.Fail level equal to 5.025 and censored time equal to 5.9.

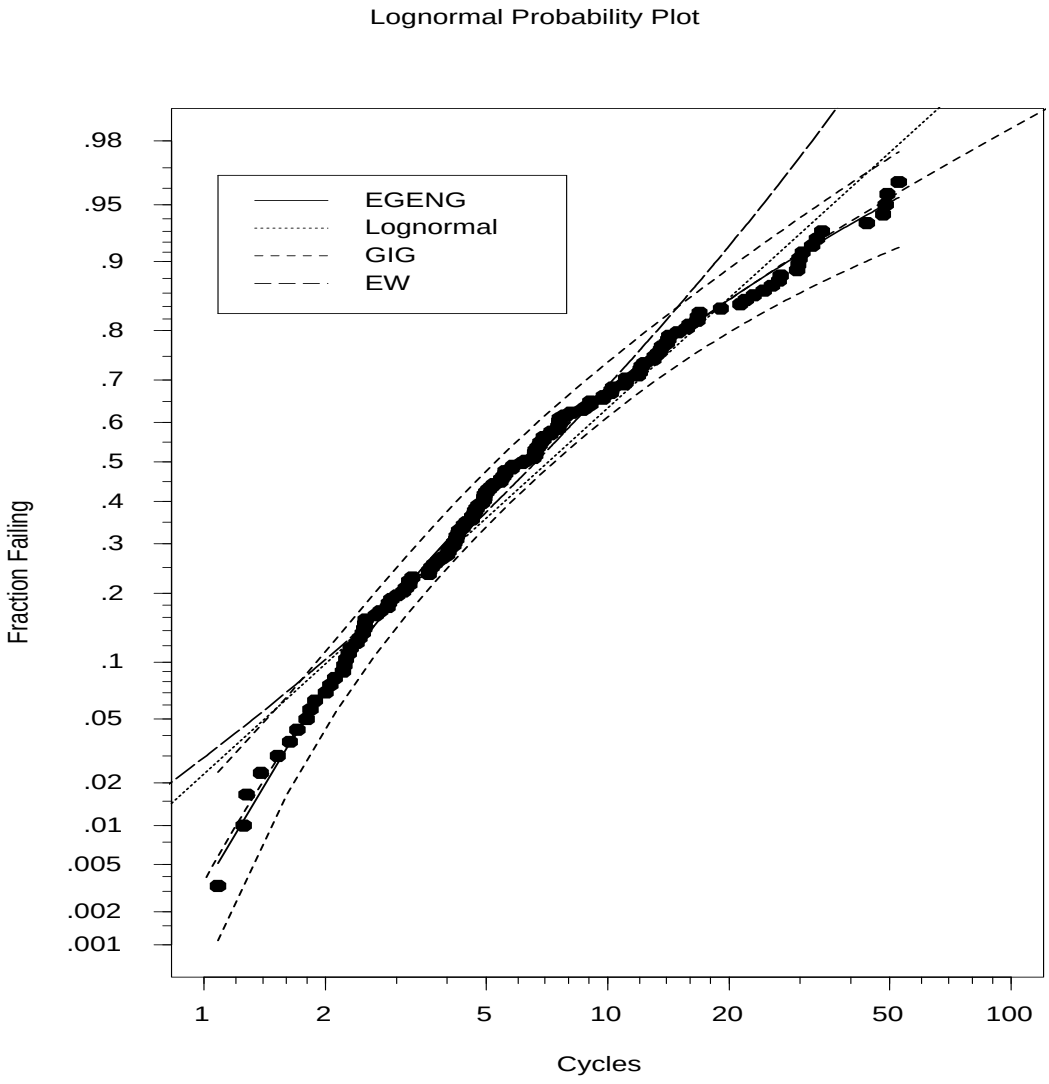

Figure 13: Lognormal probability plot of degradation model (4.1.3) with right censored, comparing EGENG, lognormal, generalized inverse Gaussian and exponential Weibull distributions. Approximate 95% pointwise confidence intervals for $F(t)$ is added to EGENG distribution.Fail level equal to 5.04 and censored time equal to 5.9.

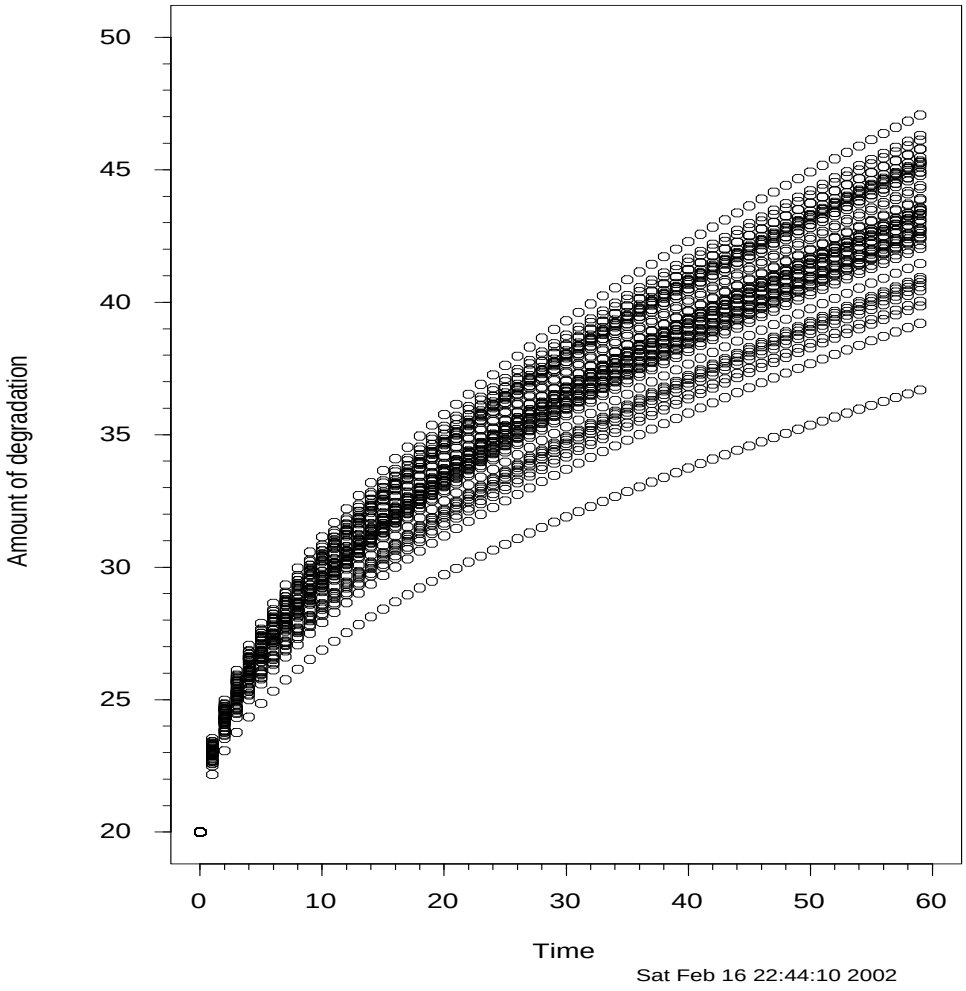

Figure 14: Plot of degradation model (4.1.4) with nonlinear degradation paths.

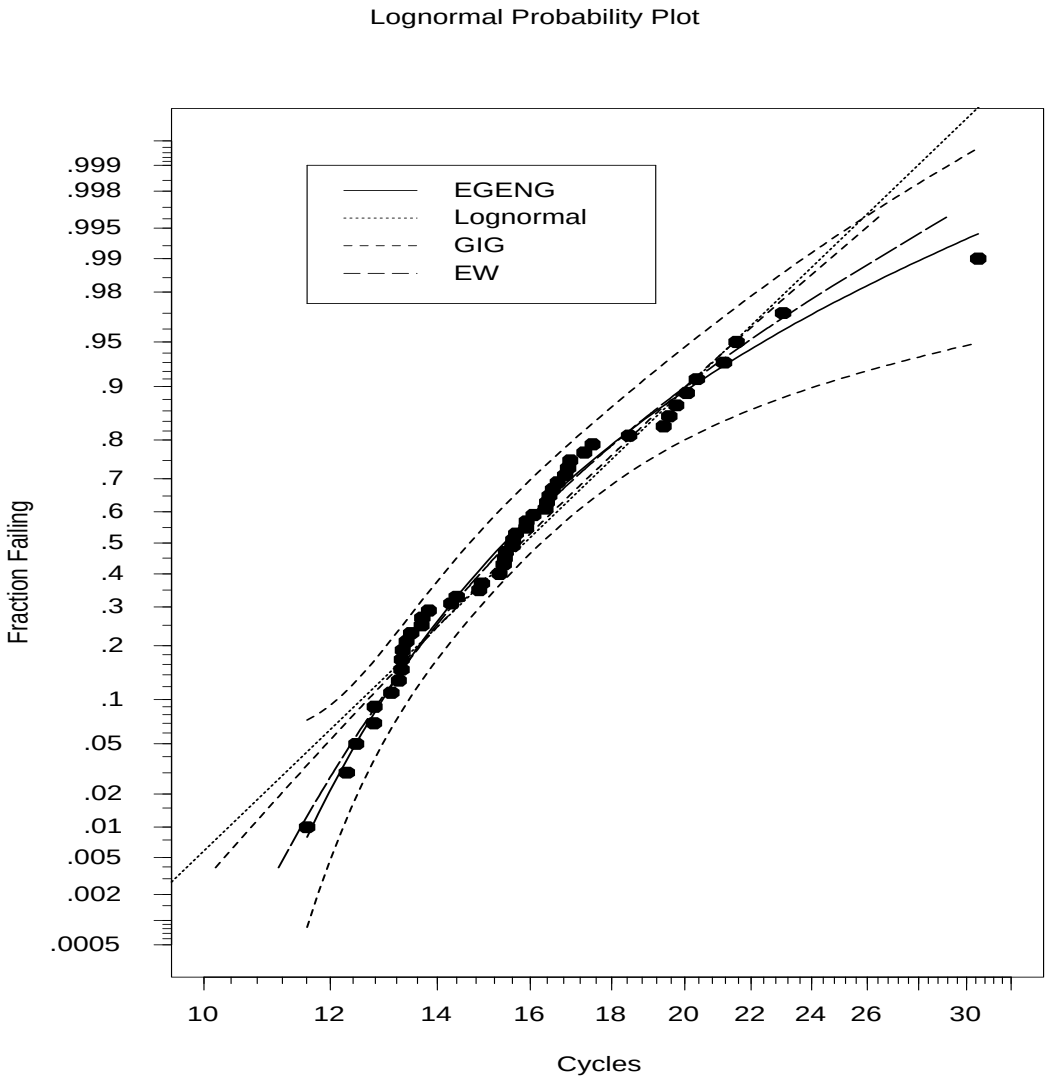

Figure 15: Lognormal probability plot of degradation model (4.1.4) with complete data, comparing EGENG, lognormal, generalized inverse Gaussian and exponential Weibull distributions. Approximate 95% pointwise confidence intervals for $F(t)$ is added to EGENG distribution. Fail level equal to 32.

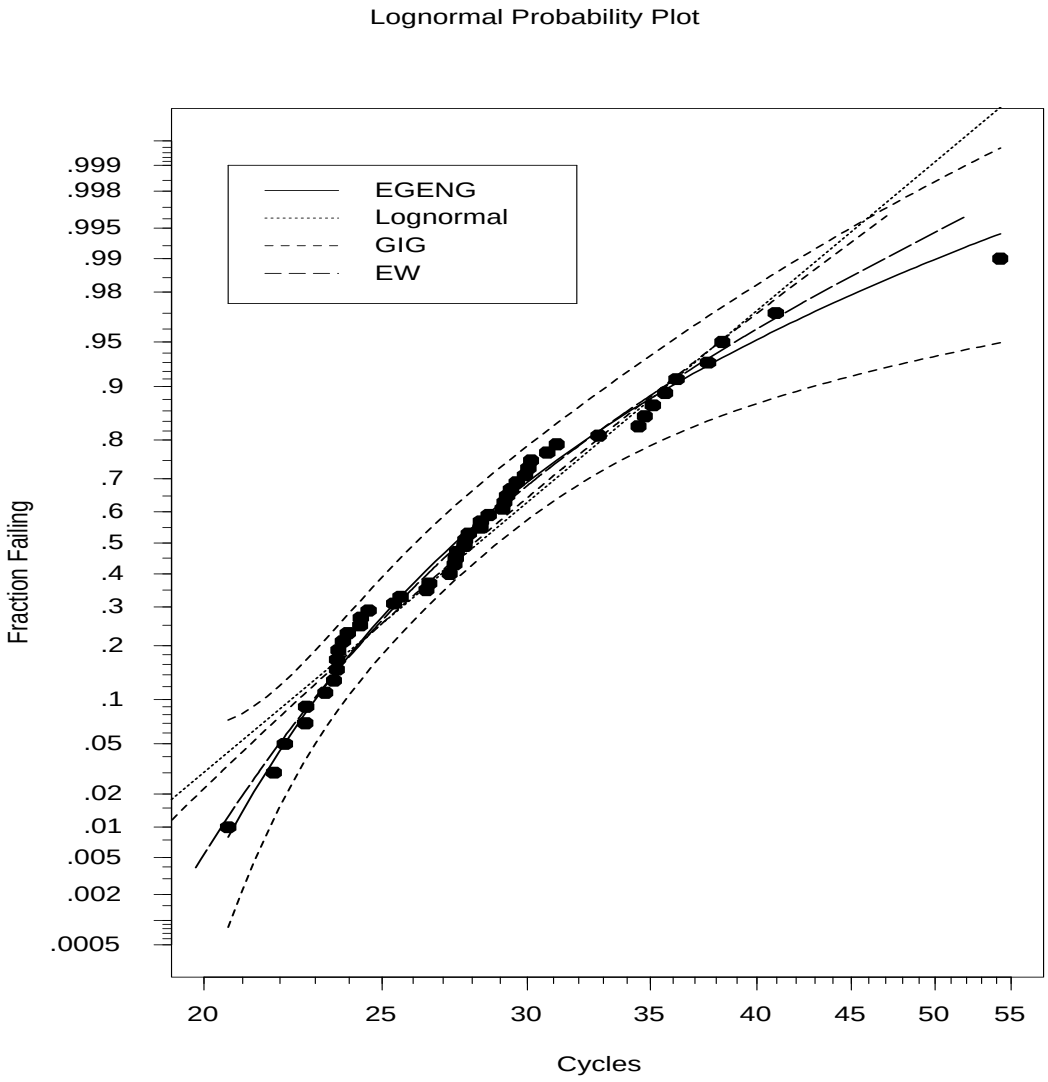

Figure 16: Lognormal probability plot of degradation model (4.1.4) with complete data, comparing EGENG, lognormal, generalized inverse Gaussian and exponential Weibull distributions. Approximate 95% pointwise confidence intervals for $F(t)$ is added to EGENG distribution. Fail level equal to 36.

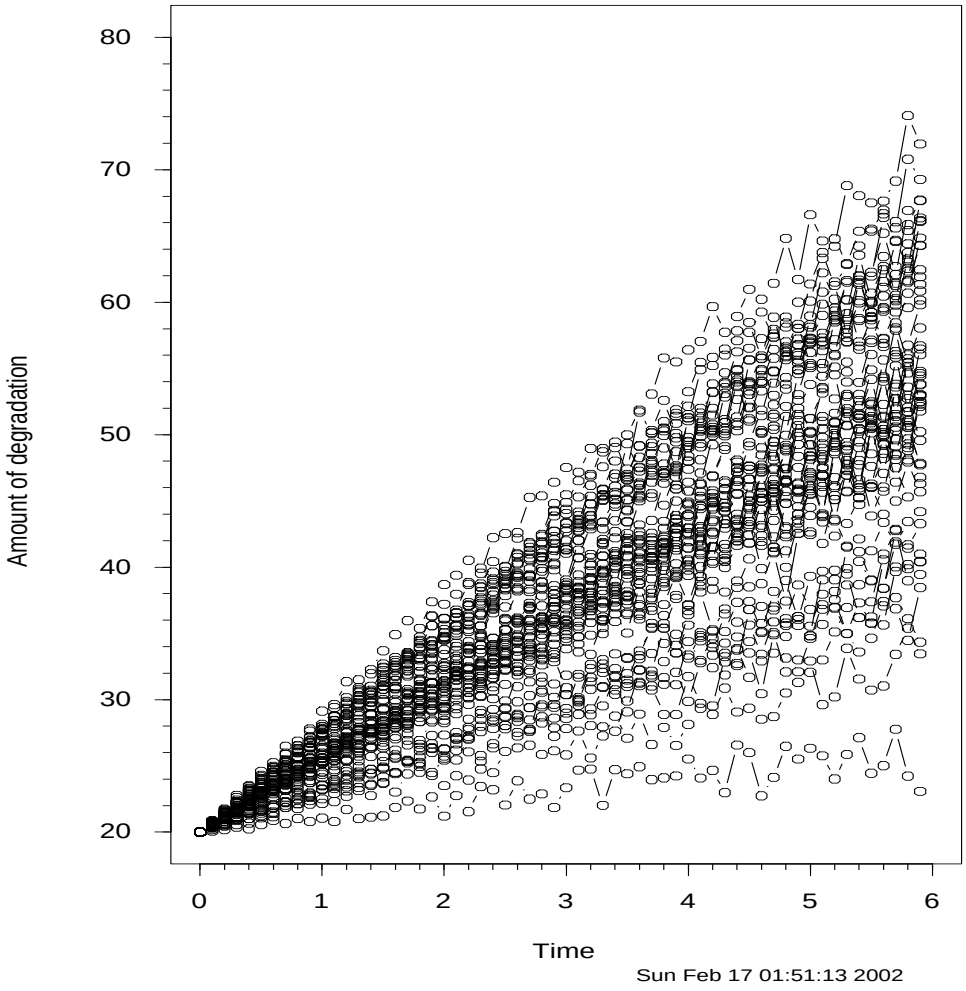

Figure 17: Plot the random error degradation model of (4.1.5).

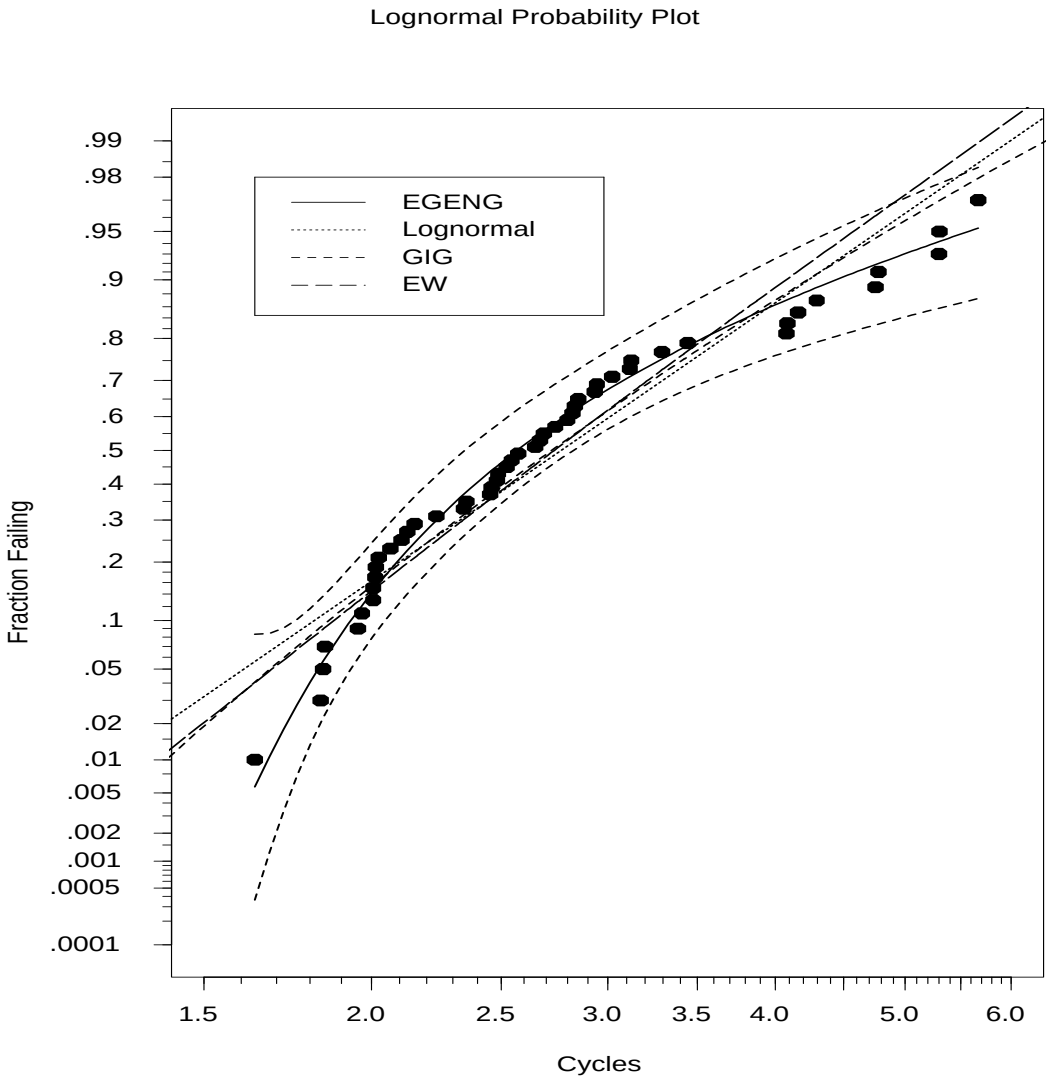

Figure 18: Lognormal probability plot of degradation model (4.1.5) with right censored, comparing EGENG, lognormal, generalized inverse Gaussian and exponential Weibull distributions. Approximate 95% pointwise confidence intervals for $F(t)$ is added to EGENG distribution. Fail level equal to 35 and censored time equal to 5.9.

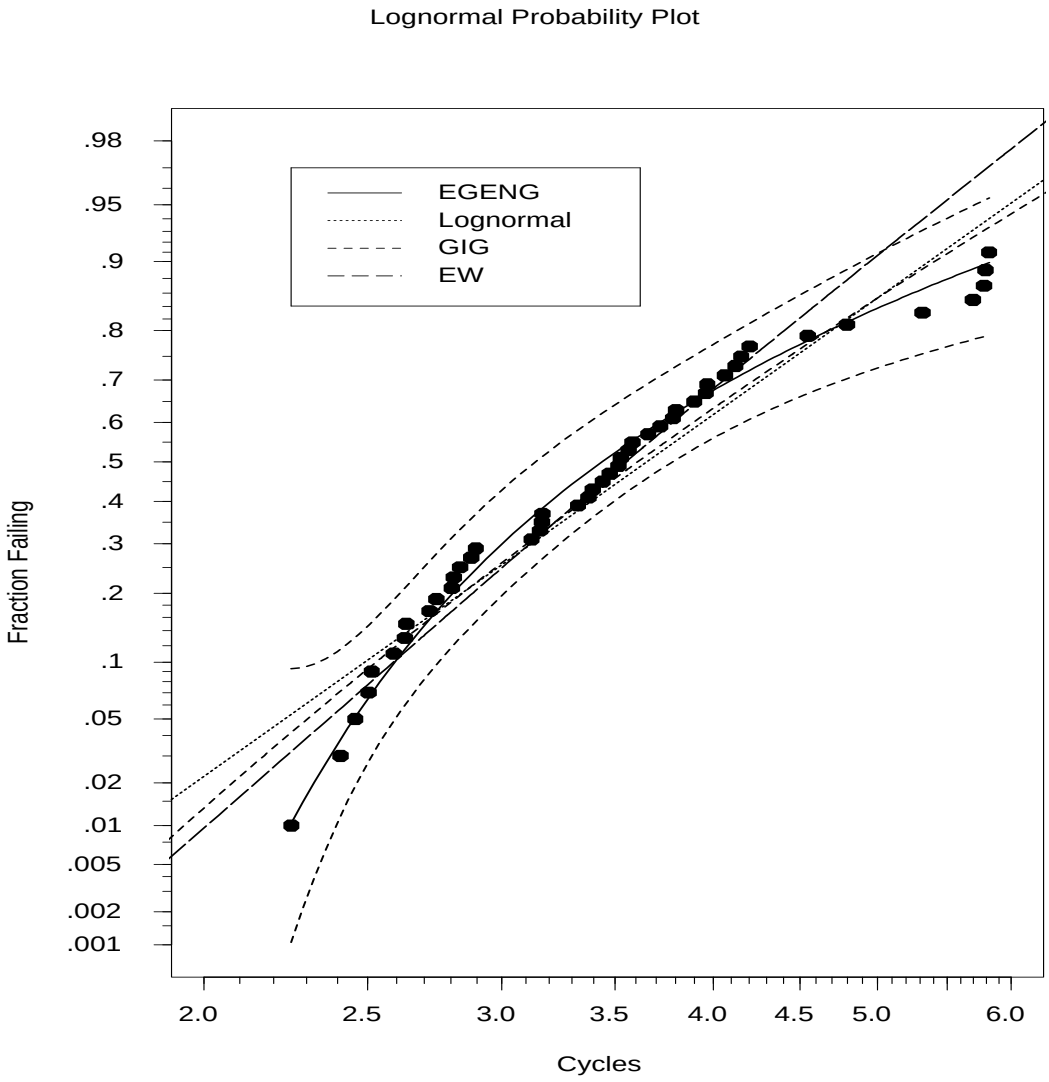

Figure 19: Lognormal probability plot of degradation model (4.1.5) with right censored, comparing EGENG, lognormal, generalized inverse Gaussian and exponential Weibull distributions. Approximate 95% pointwise confidence intervals for $F(t)$ is added to EGENG distribution. Fail level equal to 40 and censored time equal to 5.9.

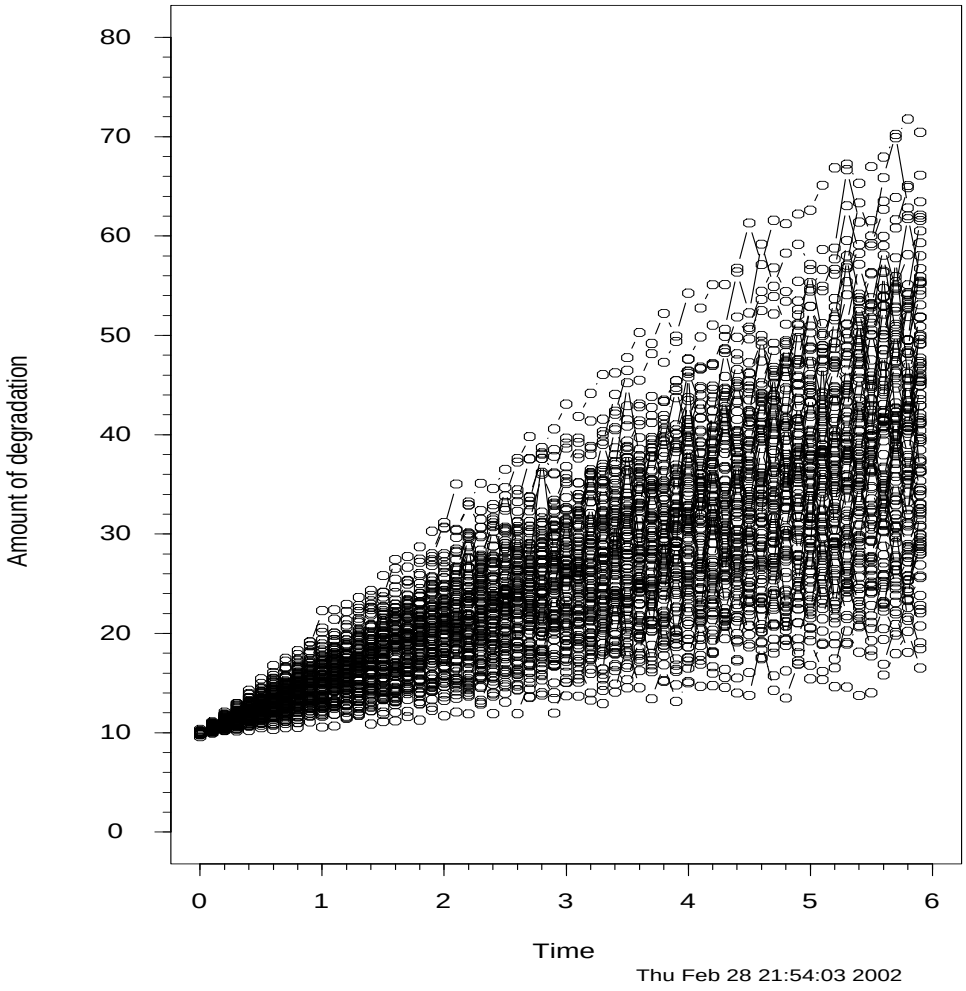

Figure 20: Plot of the random error degradation model of (4.1.6).

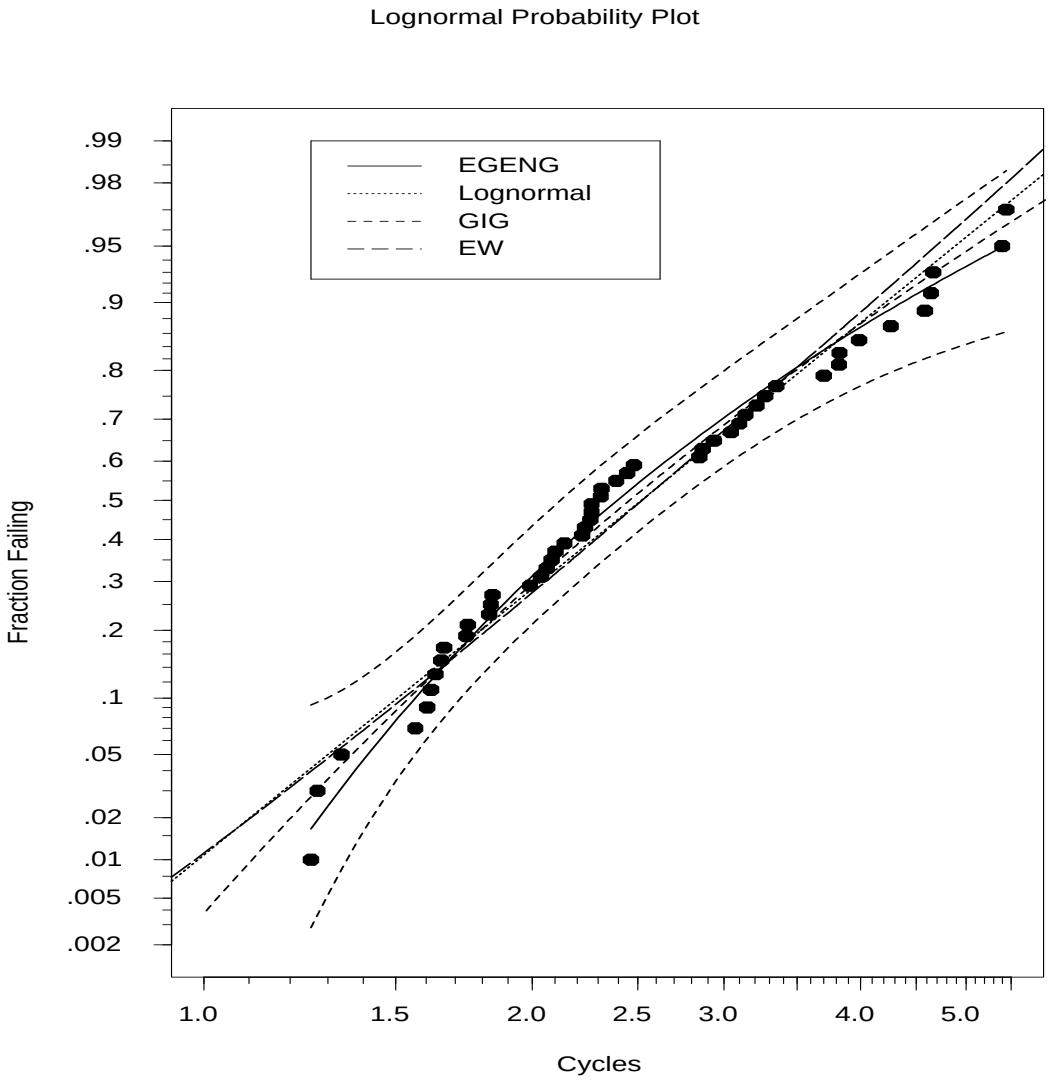

Figure 21: Lognormal probability plot of degradation model (4.1.6) with right censored, comparing EGENG, lognormal, generalized inverse Gaussian and exponential Weibull distributions. Approximate 95% pointwise confidence intervals for $F(t)$ is added to EGENG distribution. Fail level equal to 32 and censored time equal to 5.9.

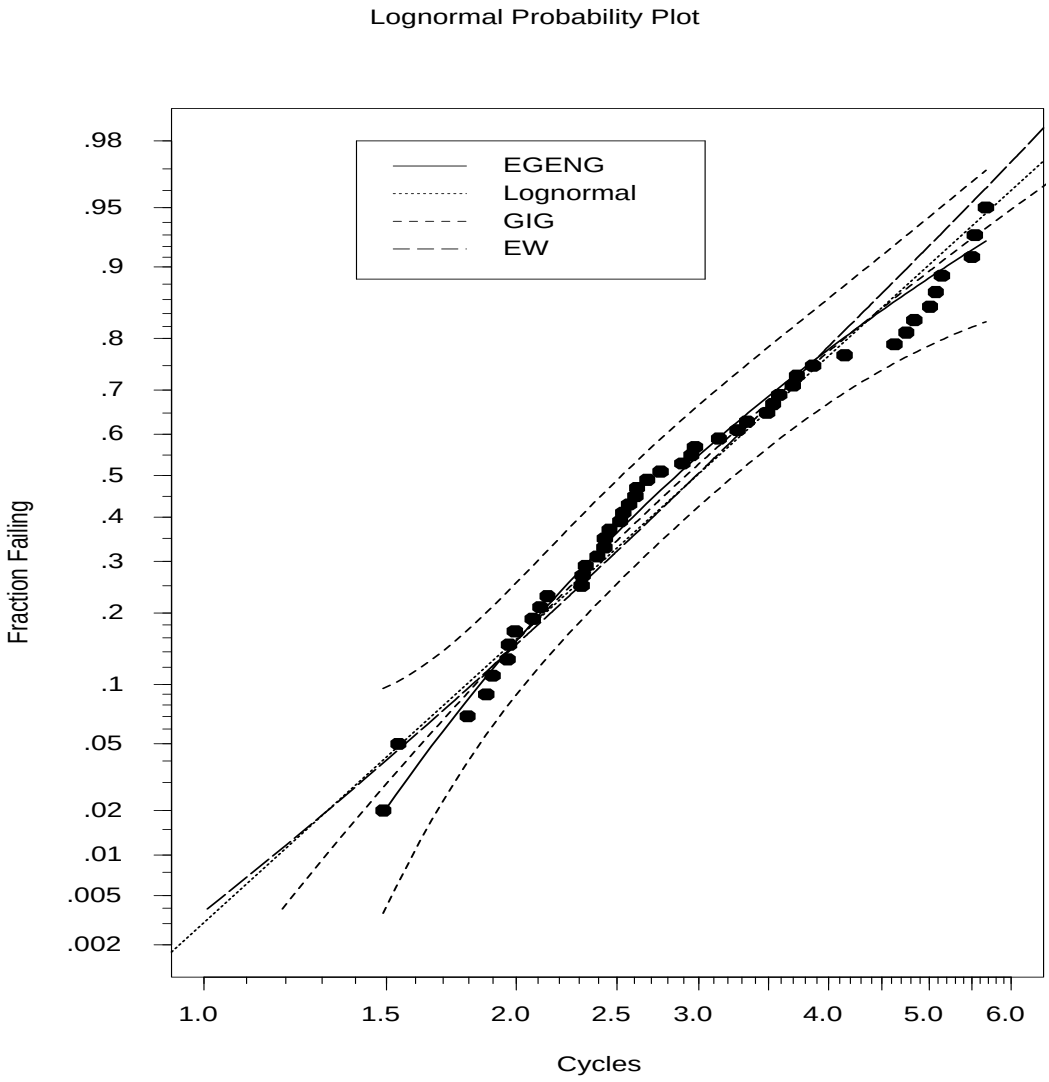

Figure 22: Lognormal probability plot of degradation model (4.1.6) with complete data, comparing EGENG, lognormal, generalized inverse Gaussian and exponential Weibull distributions. Approximate 95% pointwise confidence intervals for $F(t)$ is added to EGENG distribution. Fail level equal to 34 and censored time equal to 5.9.

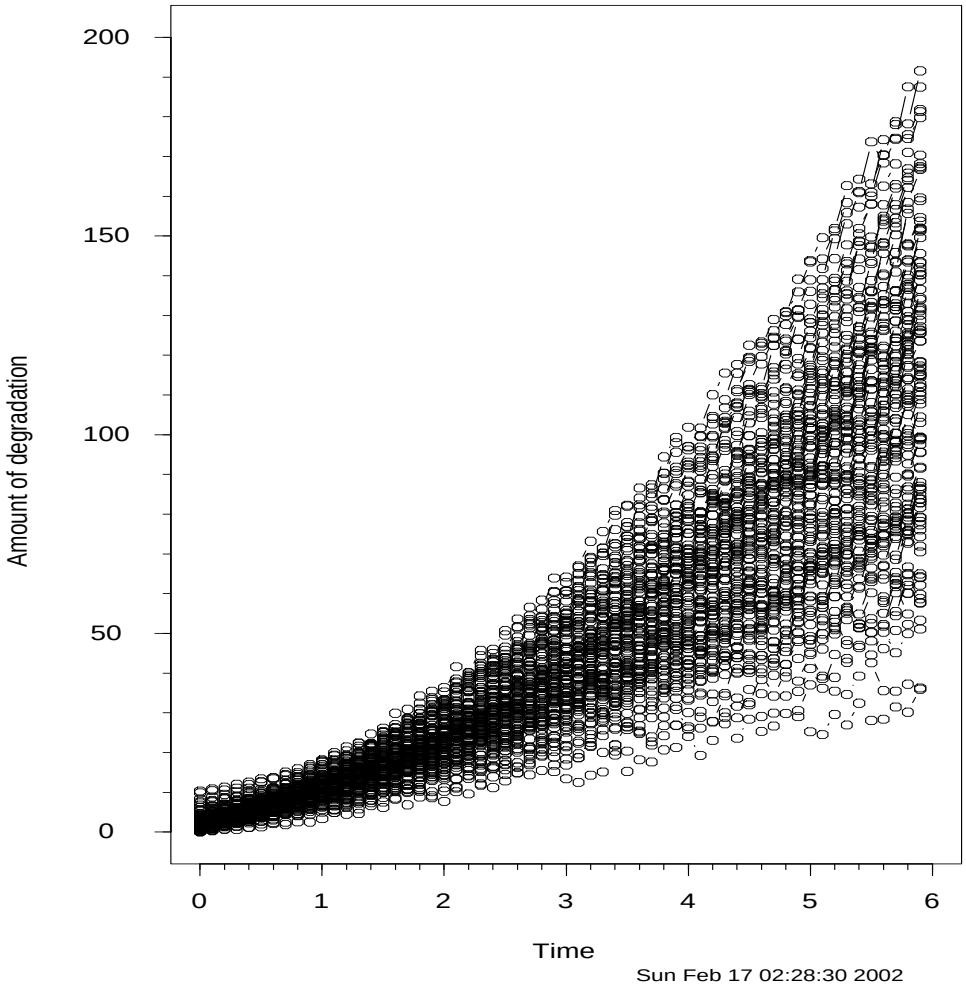

Figure 23: Plot of the random error degradation model of (4.1.7).

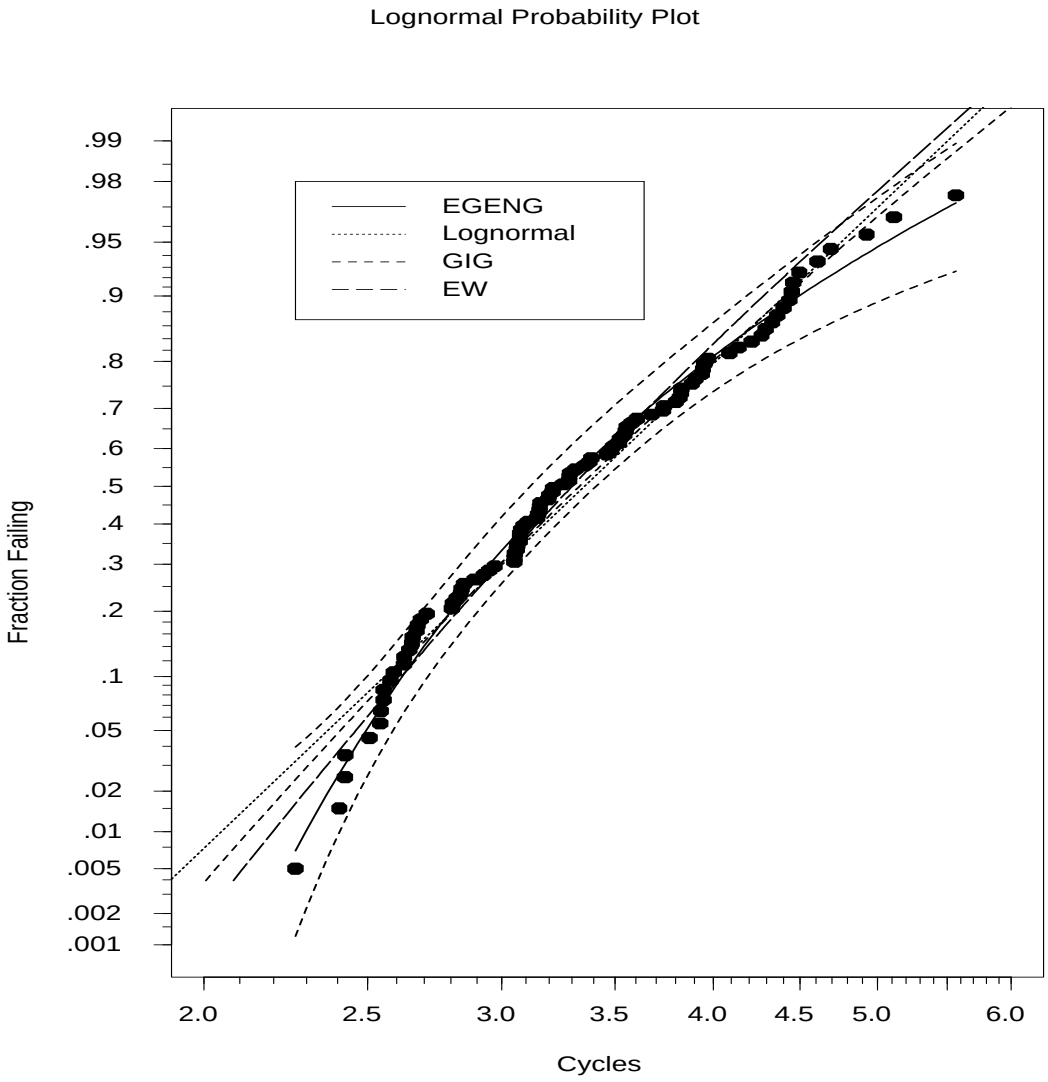

Figure 24: Lognormal probability plot of degradation model (4.1.7) with right censored, comparing EGENG, lognormal, generalized inverse Gaussian and exponential Weibull distributions. Approximate 95% pointwise confidence intervals for $F(t)$ is added to EGENG distribution. Fail level equal to 45 and censored time equal to 5.9.

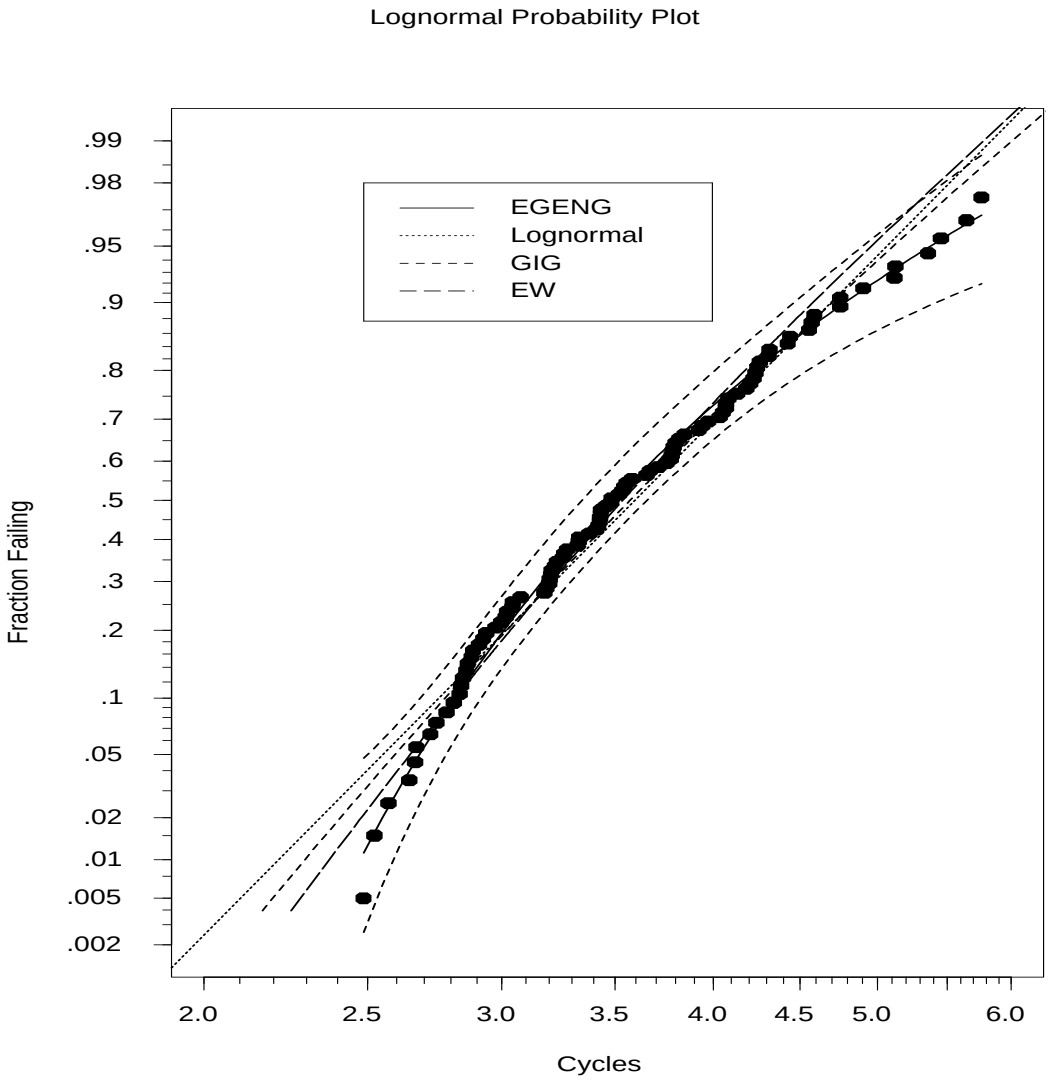

Figure 25: Lognormal probability plot of degradation model (4.1.7) with right censored, comparing EGENG, lognormal, generalized inverse Gaussian and exponential Weibull distributions. Approximate 95% pointwise confidence intervals for $F(t)$ is added to EGENG distribution. Fail level equal to 50 and censored time equal to 5.9.

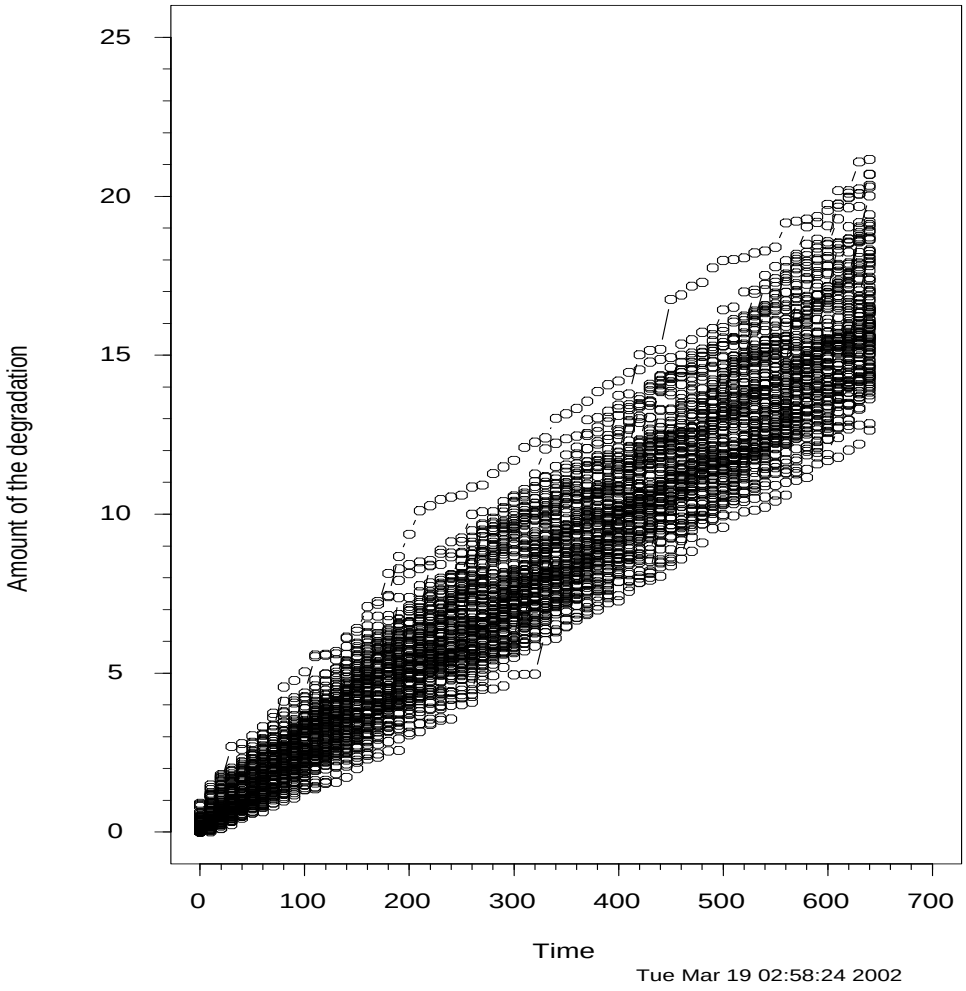

Figure 26: Plot of the First Order Autocorrelated degradation model of (4.1.8).

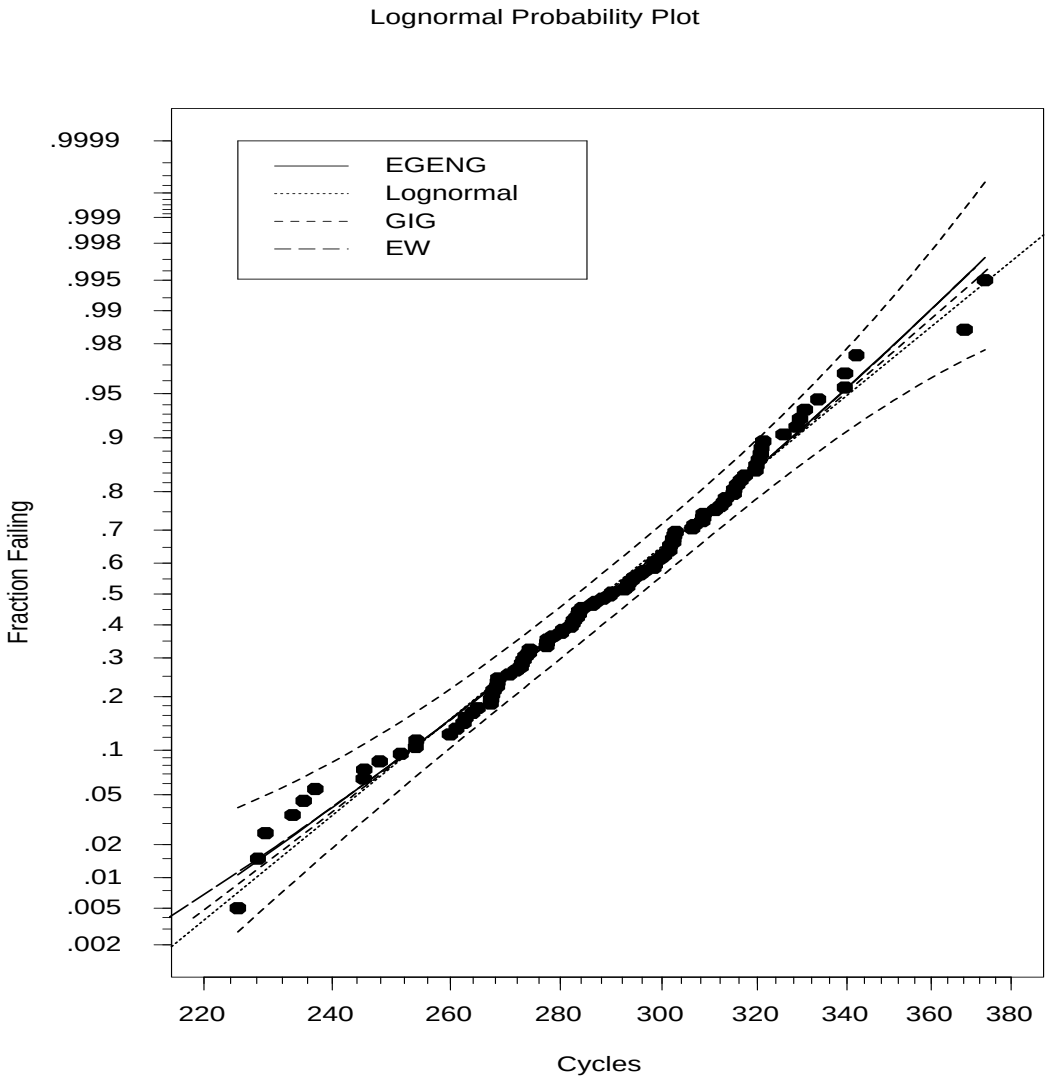

Figure 27: Lognormal probability plot of degradation model (4.1.8) with complete data, comparing EGENG, lognormal, generalized inverse Gaussian and exponential Weibull distributions. Approximate 95% pointwise confidence intervals for $F(t)$ is added to EGENG distribution. Fail level equal to 30 and censored time equal to 600.

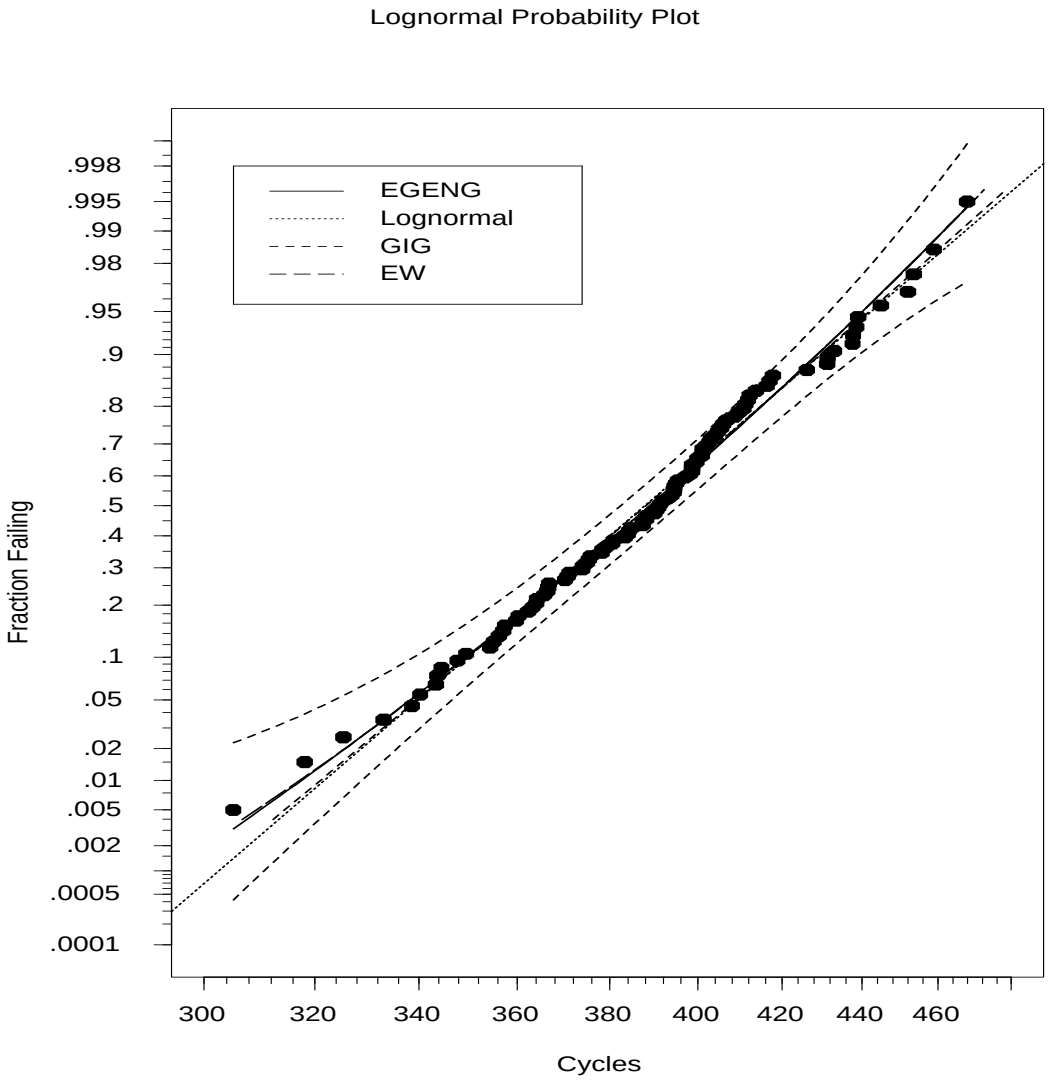

Figure 28: Lognormal probability plot of degradation model (4.1.8) with complete data, comparing EGENG, lognormal, generalized inverse Gaussian and exponential Weibull distributions. Approximate 95% pointwise confidence intervals for $F(t)$ is added to EGENG distribution. Fail level equal to 40 and censored time equal to 600.

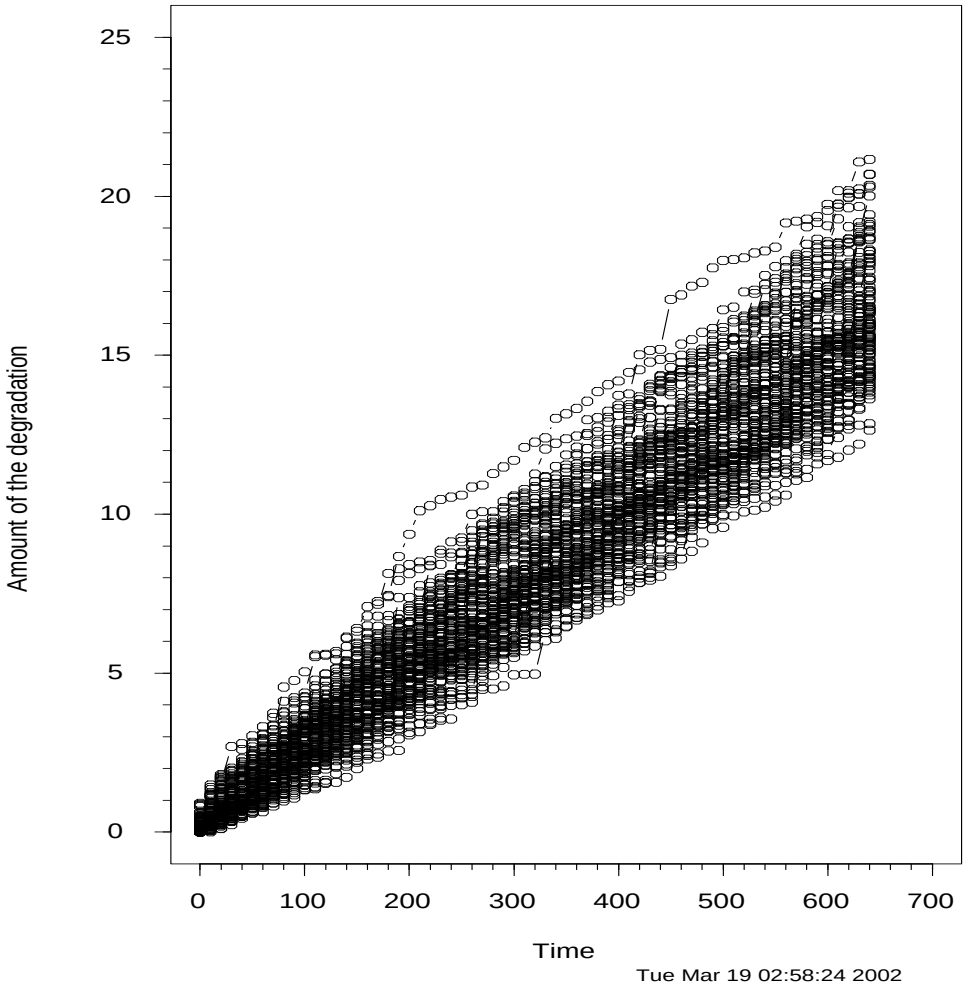

Figure 29: Plot of the First Order Autocorrelated degradation model of (4.1.9).

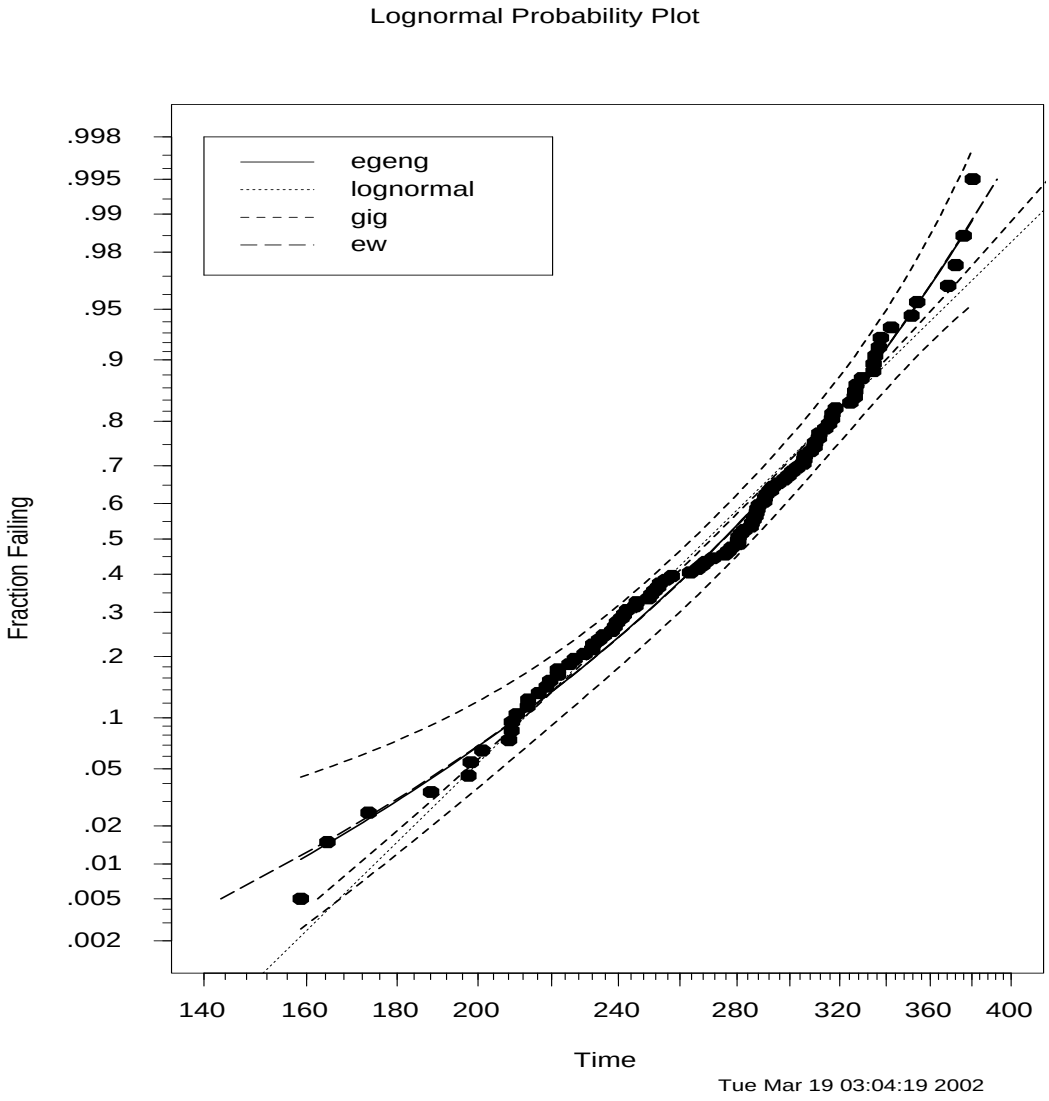

Figure 30: Lognormal probability plot of degradation model (4.1.9) with complete data, comparing EGENG, lognormal, generalized inverse Gaussian and exponential Weibull distributions. Approximate 95% pointwise confidence intervals for $F(t)$ is added to EGENG distribution. Fail level equal to 7 and censored time equal to 600.

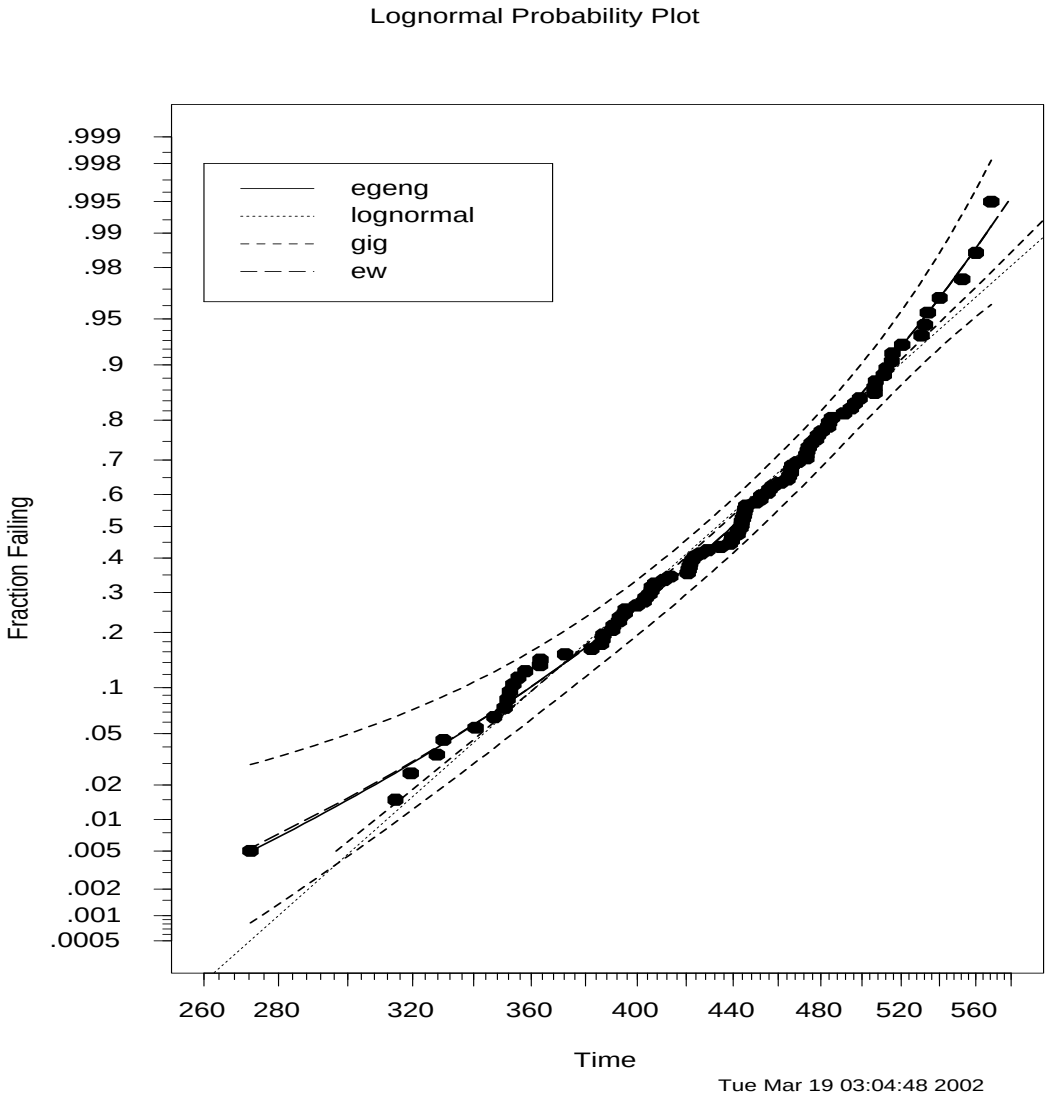

Figure 31: Lognormal probability plot of degradation model (4.1.9) with complete data, comparing EGENG, lognormal, generalized inverse Gaussian and exponential Weibull distributions. Approximate 95% pointwise confidence intervals for $F(t)$ is added to EGENG distribution. Fail level equal to 11 and censored time equal to 600.

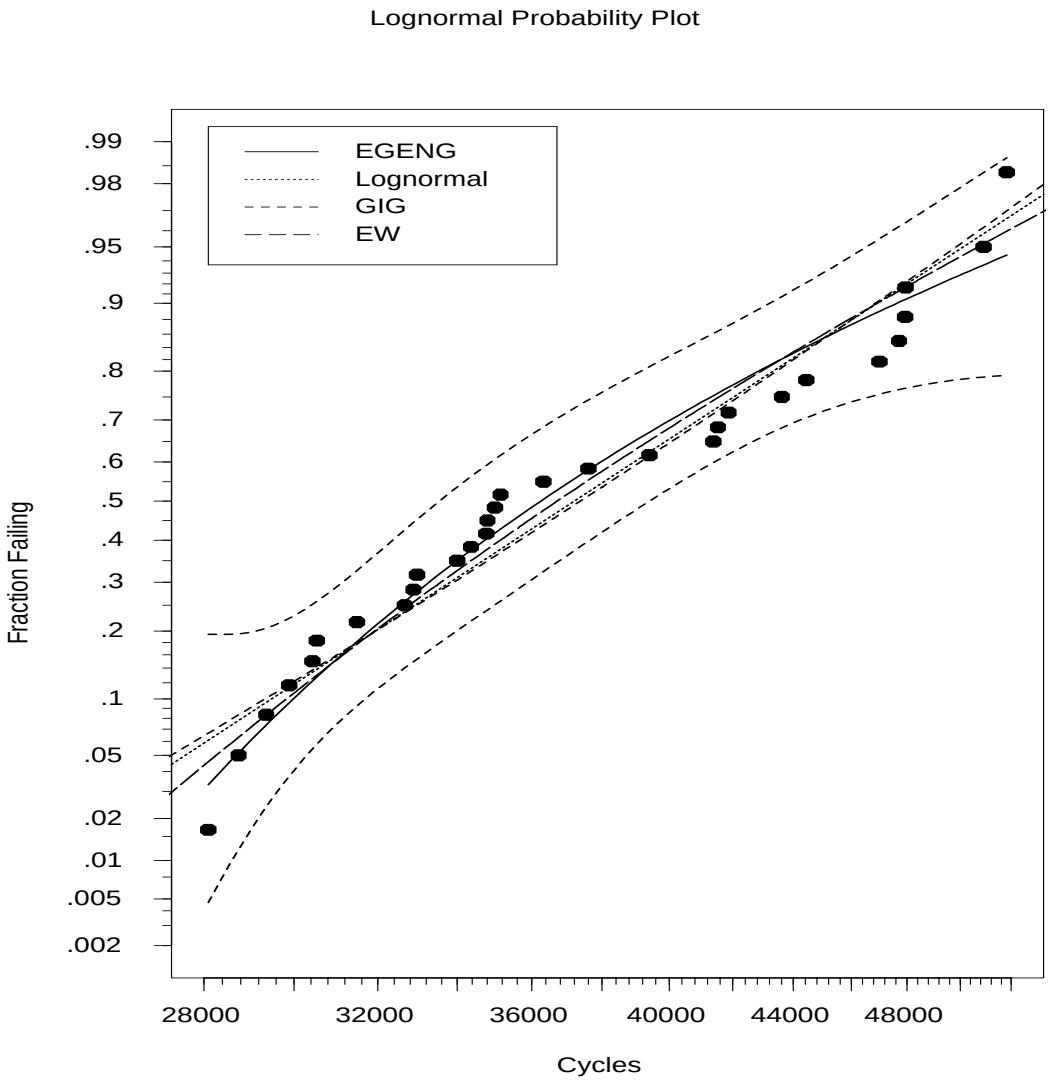

Figure 32: Lognormal probability plot of the 2024-T351 aluminum data, comparing EGENG, lognormal, exponential Weibull and generalize inverse Gaussian distributions with fail level equal to 23mm.

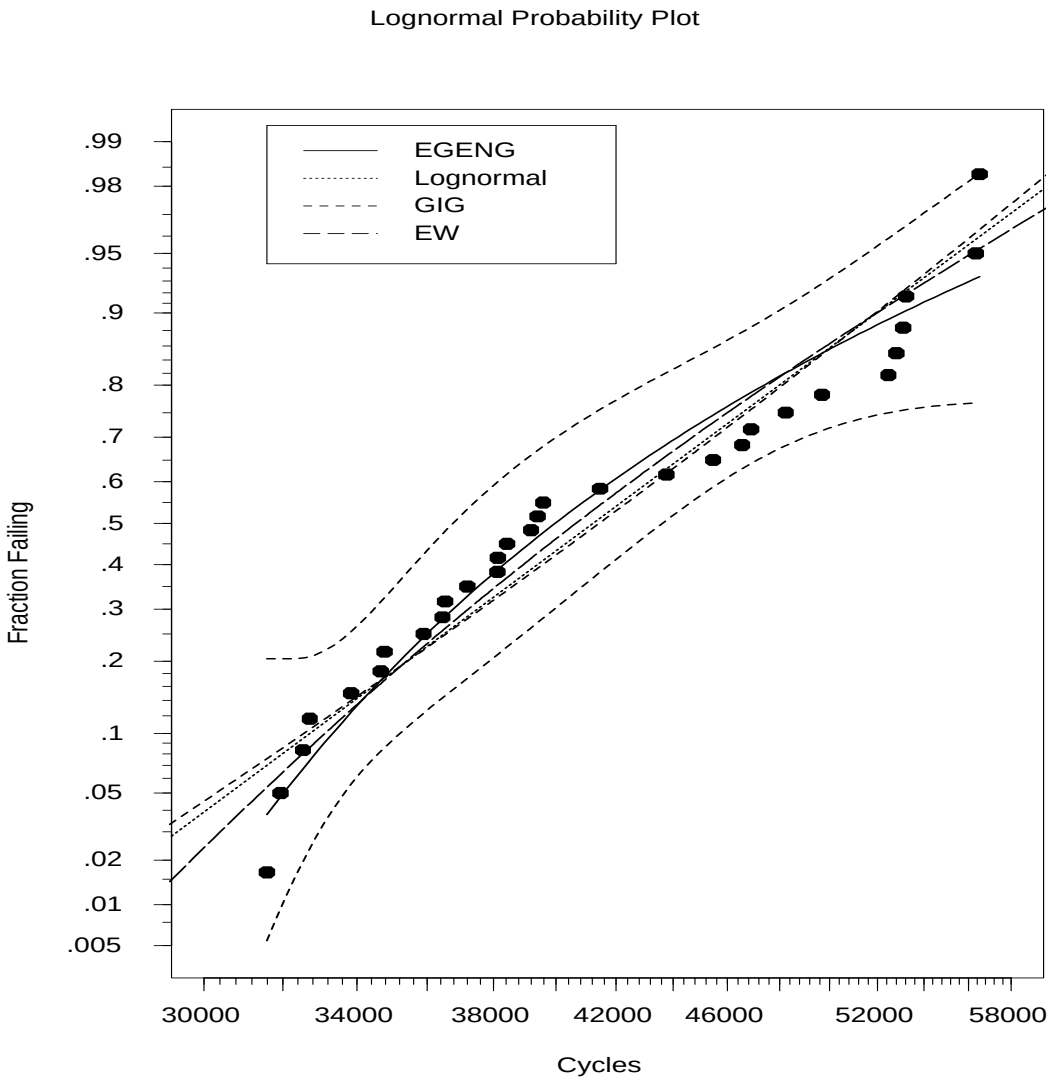

Figure 33: Lognormal probability plot of the 2024-T351 aluminum data, comparing EGENG, lognormal, exponential Weibull family and generalize inverse Gaussian distributions with fail level equal to 24mm.

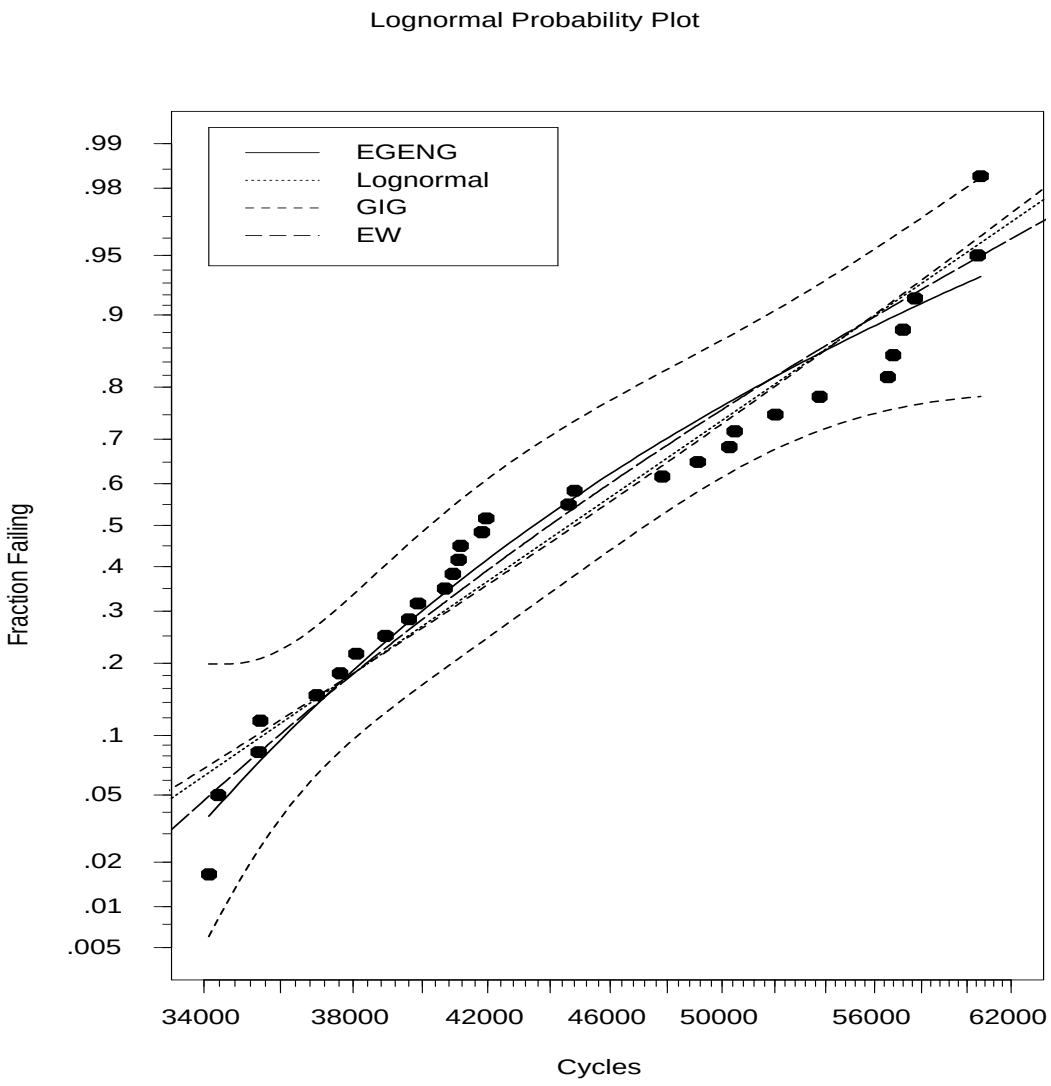

Figure 34: Lognormal probability plot of the 2024-T351 aluminum data, comparing EGENG, lognormal, exponential Weibull and generalize inverse Gaussian distributions with fail level equal to 25mm.

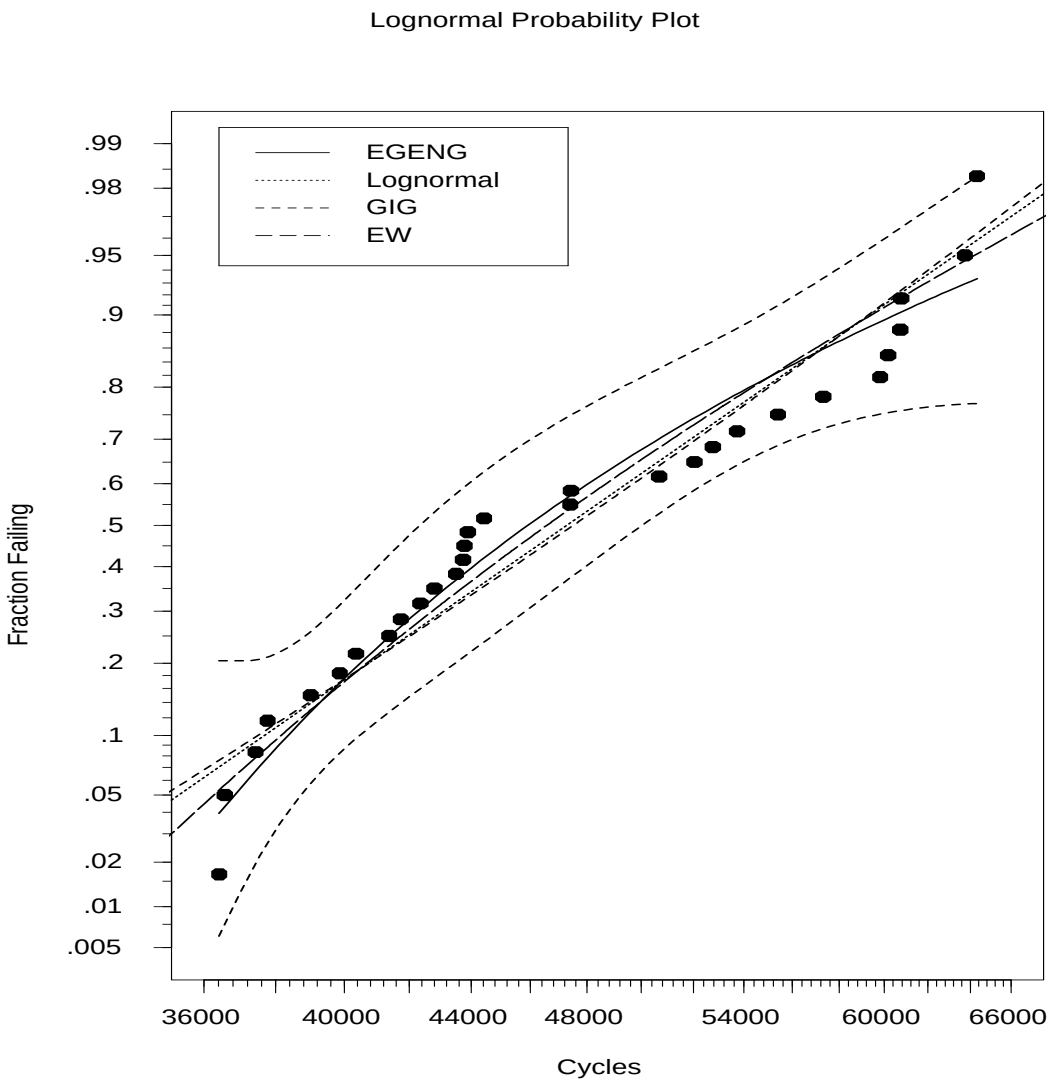

Figure 35: Lognormal probability plot of the 2024-T351 aluminum data, comparing EGENG, lognormal, exponential Weibull and generalize inverse Gaussian distributions with fail level equal to 26mm.

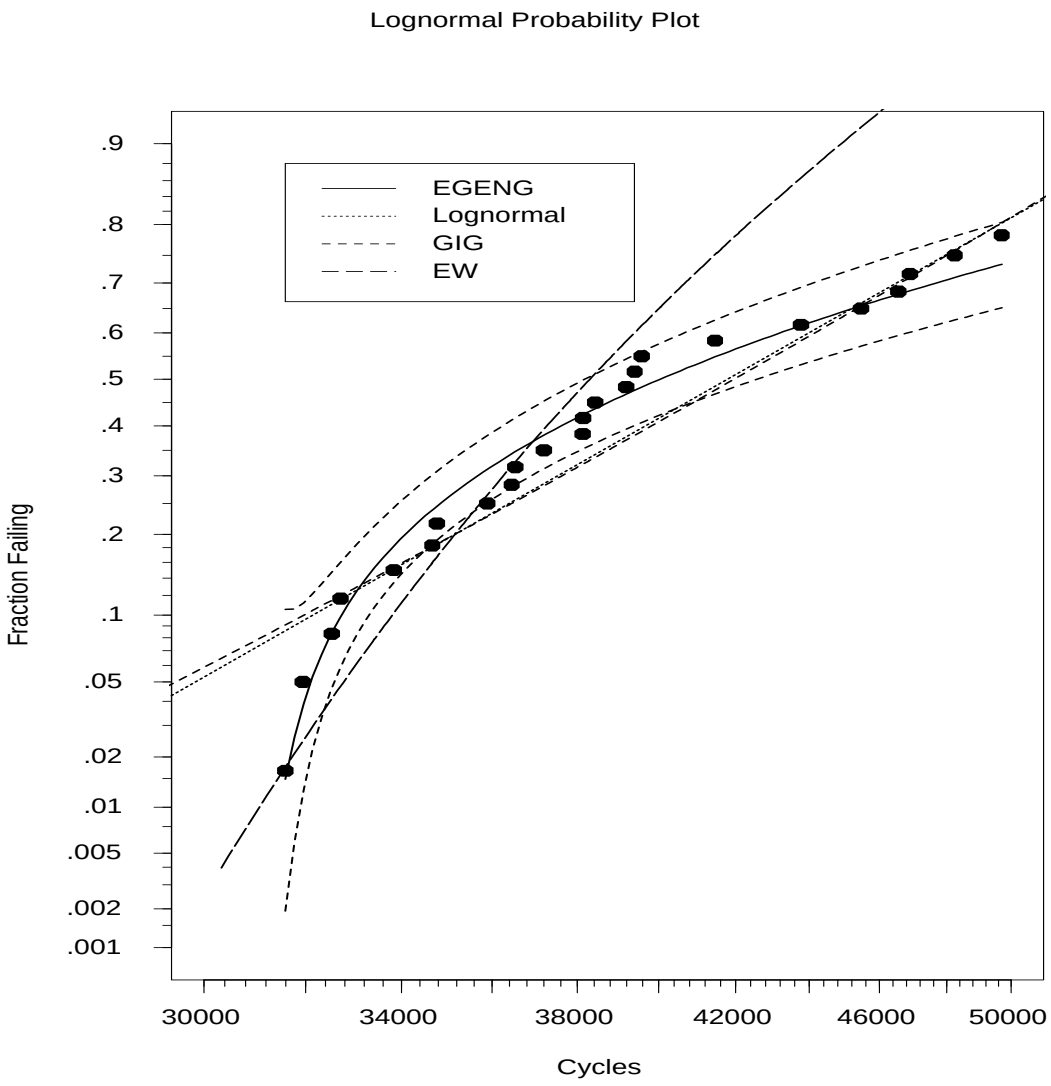

Figure 36: Lognormal probability plot of the 2024-T351 aluminum data, comparing EGENG, lognormal, exponential Weibull and generalize inverse Gaussian distributions with fail level equal to 24mm and censored after 52000 cycles.

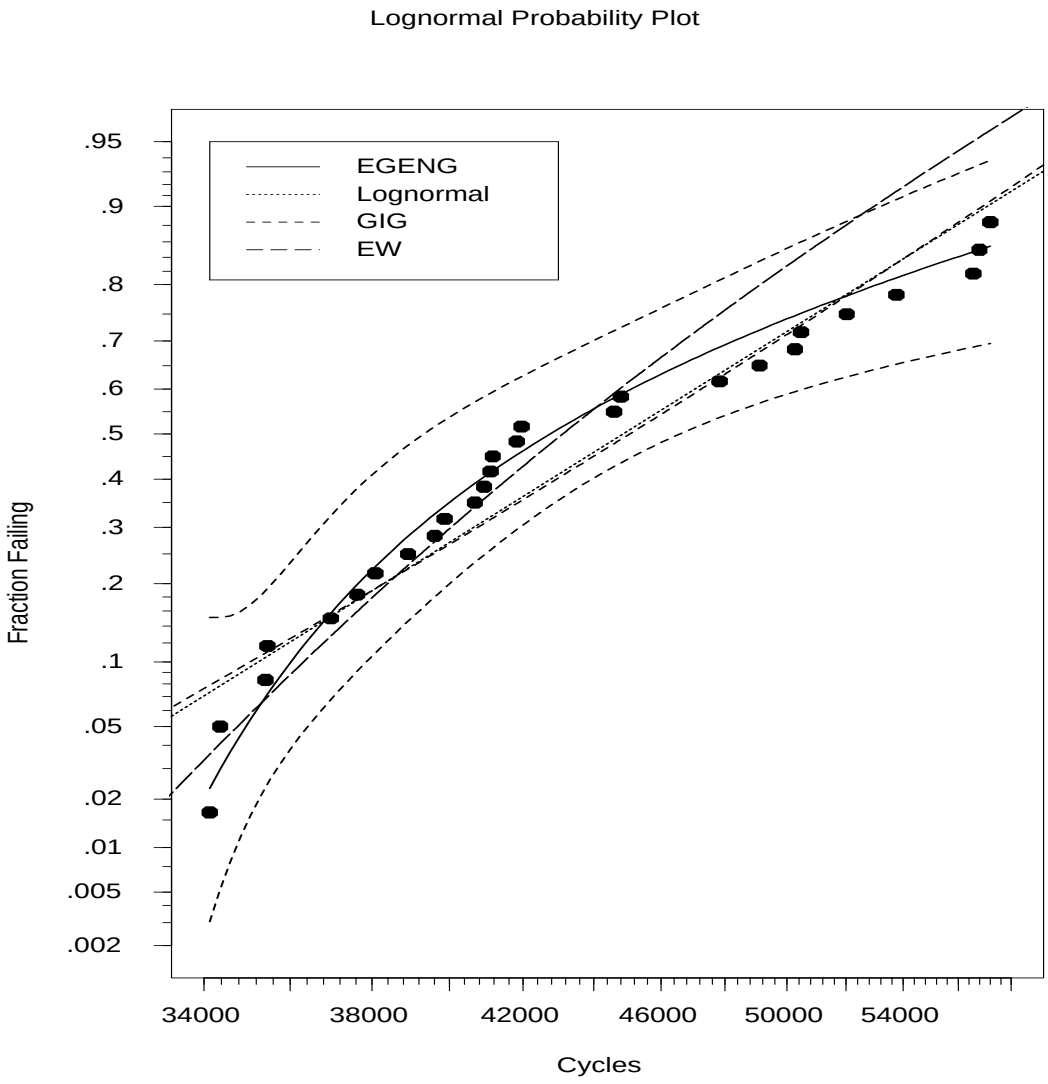

Figure 37: Lognormal probability plot of the 2024-T351 aluminum data, comparing EGENG, lognormal, exponential Weibull and generalize inverse Gaussian distributions with fail level equal to 25mm and censored after 57500 cycles.

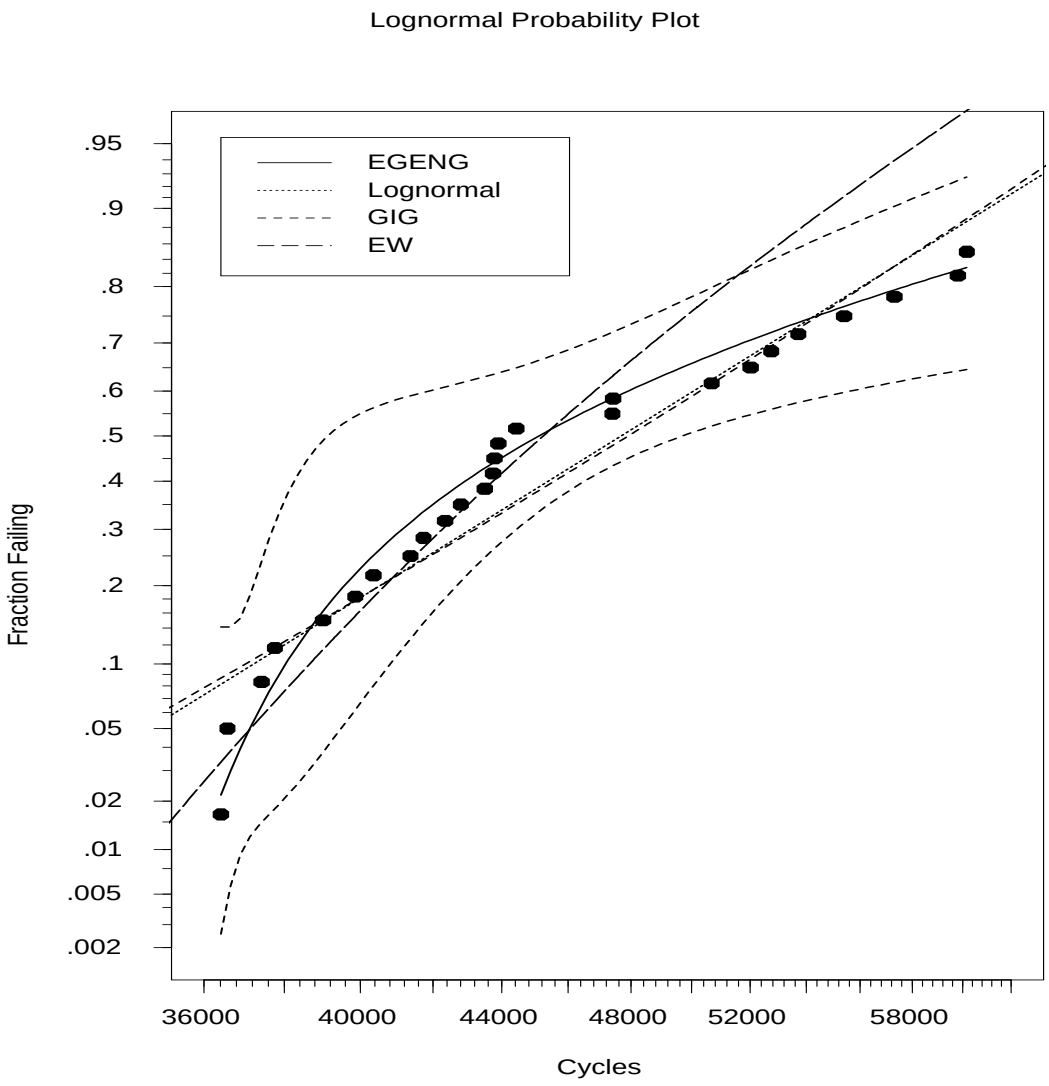

Figure 38: Lognormal probability plot of the 2024-T351 aluminum data, comparing EGENG, lognormal, exponential Weibull and generalize inverse Gaussian distributions with fail level equal to 26mm and censored after 60500 cycles.